Addis Ababa University
School of Graduate Studies
Addis Ababa Institute of Technology
School of Electrical & Computer Engineering

Application of Smart Antennas to Cognitive Radio Systems

A PhD Dissertation submitted to the School of Graduate Studies of Addis Ababa University in partial fulfillment of the requirements for the Degree of Doctor of Philosophy in Communication Engineering

By:

Murad Ridwan Hassen
School of Electrical & Computer Engineering
Addis Ababa Institute of Technology
Addis Ababa University.

Advisors:

Dr.-Ing. Mohammed Abdo
School of Electrical & Computer Engineering,
Addis Ababa Institute of Technology,
Addis Ababa University,
Ethiopia.

Prof. Dr.-Ing. Eduard Jorswieck
Chair of Communications Theory,
Faculty of Electrical and Computer Engineering,
Dresden University of Technology,
Germany.

February, 2013

Addis Ababa University
School of Graduate Studies

"Application of Smart Antennas to Cognitive Radio Systems"

A PhD Dissertation submitted to the School of Graduate Studies of Addis Ababa University in partial fulfillment of the requirements for the Degree of Doctor of Philosophy in Communication Engineering

By:
Murad Ridwan Hassen
School of Electrical & Computer Engineering
Addis Ababa Institute of Technology
Addis Ababa University.

Approved by Board of Examiners:

Chairman, Department of Graduate Committee	*Signature*
Advisor	*Signature*
Internal Examiner	*Signature*
Internal Examiner	*Signature*
External Examiner	*Signature*

Abstract

This dissertation studies three interrelated topics: design of non-uniform antenna arrays using genetic algorithm (GA), application of smart antennas to cognitive radio (CR) and determination of the distributions of signal-to-interference ratio (SIR) in Rayleigh fading.

The performance of a single-element antenna is limited. To obtain high directivity, narrow beamwidth, low sidelobes, point-to-point and preferred-coverage pattern characteristics, etc., antenna arrays are used. Nowadays, antenna arrays appear in wireless terminals and smart antennas, so robust and efficient array design is increasingly becoming necessary. In array design, it is frequently desirable to achieve both a narrow beamwidth and a low sidelobe level. A uniform array yields the smallest beamwidth and hence the highest directivity. It is followed, in order, by the Dolph-Chebyshev and Binomial arrays. In contrast, Binomial arrays usually possess the smallest sidelobes followed, in order, by the Dolph-Chebyshev and uniform arrays. In the dissertation, GA is used to design a non-uniform linear array that approximates the beamwidth of a uniform array and having smaller sidelobe level than the Dolph-Chebyshev array. The designed array generally exhibits the largest directivity as compared to the uniform, Binomial and Dolph-Chebyshev arrays. The result can be used in applications where narrow beamwidth and low sidelobes levels are preferred such as in switched-beam smart antennas.

The second topic addressed by the dissertation is application of smart antennas to cognitive radios. Conventional CRs exploit the licensed spectrum by opportunistically seeking the underutilized radio resource in time, frequency and space (geographic) domains. However, there are other dimensions that need to be explored further for spectrum opportunity. The angle dimension is a typical example. The literatures surveyed point to the fact that little work has been done in this dimension. The dissertation particulary investigates the performance of CRs equipped with smart antennas in exploiting the angle opportunity in Rayleigh fading channel. The proposed cognitive transmitter keeps the interference to the primary receiver below a given threshold while at the same time ensuring high enough signal-to-interference-plus-noise ratio (SINR) at the cognitive receiver. It was shown that the angle spectrum can be significantly exploited for spectrum opportunity using smart antennas. It was also shown that the angle spectral efficiency for Rayleigh channel is lower as compared to a non-fading channel with the same power levels and radio terminal locations. Moreover it has been shown that increasing the cognitive transmitter power beyond a certain level has negligible effect on the angle spectral efficiency.

The third topic of the dissertation extends the determination of the distribution of SIN in Rayleigh fading channel when N interferers are present. In fading channels the SINR and SIR are random variables and their distributions have to be known for a correct description of the receiver. The distributions of SIR in Rayleigh fading have been described by deriving a closed form expression for the probability density function, cumulative distribution and outage probabilities.

Keywords: *Antenna Arrays, Uniform Arrays, Non-Uniform Arrays, Binomial Arrays, Dolph-Chebyshev Arrays, Genetic Algorithm, Cognitive Radio, Smart Antenna, Angle Spectrum, Rayleigh Fading, SINR, SIR.*

Acknowledgements

In the name of Allah, the Most Gracious, the Most Merciful.

This dissertation would not have been possible without the support of many people who in one way or another contributed and extended their valuable assistance.

First and foremost, my utmost gratitude goes to my teacher and dissertation advisor Dr.-Ing. Mohammad Abdo. He was abundantly helpful and offered invaluable comments, assistance, support and guidance. Moreover, I will never forget his sincerity and encouragement.

Deepest gratitude and respect goes to my dissertation co-advisor Prof. Dr.-Ing. Eduard Jorswieck, Chair of Communications Theory, Dresden University of Technology (TUD), Germany. His constant support, invaluable help of constructive comments and suggestions throughout the work have contributed to the success of this research. Not forgetting his kind willingness and assistance to let me and my friend Yalemzewd Negash stay in Dresden for finalizing our dissertations.

Appreciation and deep respect goes to my teachers Prof. Woldegiorgis Woldemariam and the late Dr.-Ing. Hailu Ayele for their support and encouragement. I wish to express my special thanks to Dr.-Ing. Getahum Mekuria and Dr.-Ing. Dereje H. Woldegebreal for their support and encouragement to complete this study.

Special thanks also to Dr. Waltenegus Dargie of TUD. He was kind and helpful in providing us the opportunity to participate in the International Conference on Communications (ICC) 2009 held in Dresden. It was through him that I was introduced to my dissertation co-advisor.

I would also like to convey thanks to the members of our department staff. I am also indebted to my friends for their moral support.

Last but not the least, I wish to express my love and gratitude to my dad Ridwan and mom Safiya, my wife Maria and our children Sumeya, Ilham, Kedija and Muhammad for their endless love and understanding.

To my parents:

Ridwan Hassen
&
Safiya Adus.

Contents

List of Figures

List of Tables

Acronym

AoA	Angle-of-Arrival
ARQ	Automatic Repeat Request
AWGN	Additive White Gaussian Noise
BER	Bit Error Rate
BPSK	Binary Phase Shift Keying
CDMA	Code Division Multiple Access
CMA	Constant Modulus Algorithm
CR	Cognitive Radio
CR	Cognitive Receiver
CT	Cognitive Transmitter
DFT	Discrete Fourier Transform
DoA	Direction-of-Arrival
DPC	Dirty Paper Coding
EIRP	Equivalent Isotropically Radiated Power
ESPRIT	Estimation of Signal Parameters via Rotational Invariance Techniques
FCC	Federal Communications Commission of USA
FDMA	Frequency Division Multiple Access
FEC	Forward Error Correction
FM	Frequency Modulation
GA	Genetic Algorithm
GMSK	Gaussian Minimum-Shift Keying
GPS	Global Positioning System
GSM	Global System for Mobile Communications
HOS	Higher Order Statistics
i.i.d	Independent and identically distributed
IFC	Interference Channel
IR-UBS	Impulse Radio UWB
ITC	Interference Temperature Constraints
I-TCP	Indirect-TCP
ITS	Intelligent Transportation Systems
LMS	Least Mean Squares
MAC	Media Access Control
MEM	Maximum Entropy Method
MISO	Multiple-Input Single-Output
MUSIC	Multiple Signal Classification
MVDR	Minimum Variance Distortionless Response
NTSC	National Television System Committee
OBU	Onboard Unit
OFDM	Frequency Division Multiplexing
pdf	Probability distribution function

PR	Primary Transmitter
PSD	Power Spectral Density
PT	Primary Transmitter
QoS	Quality of Service
QPSK	Quadrature Phase Shift Keying
RBF	Radial Basis Function
RLS	Recursive Least Squares
RSU	Roadside Unit
RTT	Round-Trip-Time
SDMA	Spatial-Division Multiple Access
SDR	Software-Defined Radio
SINR	Signal-to-Interference-plus-Noise Ratio
SIR	Signal-to-Interference Ratio
SISO	Single-Input Single-Output
SMI	Sample Matrix Inversion
TCP	Transmission Control Protocol
TDMA	Time Division Multiple Access
UDP	User Datagram Protocol
UWB	Ultra Wide Band
V2R	Vehicle-to-Roadside
V2V	Vehicle-to-Vehicle
VANET	Vehicular ad hoc Network
VLSI	Very Large Scale Integration
WCDMA	Wideband CDMA
WiMAX	Worldwide Inter-operability for Microwave Access
WLAN	Wireless Local Area Network
WSS	Wide-Sense Stationary.

Outline of the Dissertation

This dissertation is arranged as follows:

- **Chapter 1** Gives a quick revision of antenna arrays with more emphasis on non-uniform arrays, discusses smart antennas at length, covers adaptive beamforming techniques and concludes with a discussion on Direction-of-Arrival algorithms.

- **Chapter 2** Looks at cognitive radios. The motivations behind the emergence of cognitive radio concept is discussed. The traditional spectrum sensing dimensions are described in depth and the angle spectrum opportunity is emphasised for further research. Potential applications of cognitive radio are listed and the major research challenges in cognitive radio system are discussed at length.

- **Chapter 3** Presents new results on the design of non-uniform linear array using genetic algorithm. The results have been peer reviewed and presented at the 13th International Conference on Advanced Communication Technology (ICACT 2011) [224] and subsequently published in the Journal of Wireless Networking and Communications [225].

- **Chapter 4** Addresses the issue of exploiting the angle dimension in cognitive radio using smart antennas. The results achieved show that the angle dimension can be greatly exploited to increase the efficiency of spectrum utilization in the already congested radio spectrum. The results have been peer reviewed and accepted at the 2012 International Conference on Computer, Information, and Telecommunication Systems, CITS 2012.

- **Chapter 5** Addresses the classical problem of finding the sum of random variables. The result obtained on the sum of N exponential random variables is used to derive a new closed form expression for the distribution of SIN in Rayleigh fading channel.

- **Chapter 6** Summarizes the findings of the dissertation and recommendations for future work.

- **Appendix A** Presents an overview of the Monte Carlo simulation method. The method is used in Chapter 4 to simulate the region where cognitive radios are to be successfully deployed.

Chapter 1

Smart Antennas

1.1 Introduction

Over the last two decades, there has been a considerable interest in using smart antennas for improving the performance of wireless radio systems. A smart antenna is basically an antenna array with a smart signal processing algorithm. Smart antenna systems include, in general, collection of techniques and algorithms that attempt to improve the received signal, suppress co-channel interference, and increase capacity.

This chapter is organized as follows. Section 1.2 gives a quick revision of antenna arrays. More emphasis is given to non-uniform arrays since, basically, smart antennas are non-uniform in their excitation current. It also shades more light to Chapter 3. In Section 1.3 smart antennas are described in depth, their types and advantages are discussed. The signal model basic to array processing is presented in Section 1.4. Adaptive beamforming techniques and algorithms are dealt in Section 1.5. A brief description of Direction-of-Arrival algorithms are described in Section 1.6. Throughout the chapter, extended references are provided to give us an overview of smart antenna research and applications.

1.2 Antenna Arrays

Smart antennas are composed of a collection of two or more antennas, called an *antenna array*, working in concert to establish a unique radiation pattern for the electromagnetic environment at hand. The antenna elements are allowed to work in concert by means of array element phasing, which is accomplished with hardware or is performed digitally [1]. Some very useful texts on array phasing include Haykin [2], Johnson and Dudgeon [3], and Van Trees [4]. Extensive material can be found in the phased array text by Brookner [5] or in the article by Dudgeon [6]. Arrays of antennas can assume any geometric form. A thorough treatment of linear arrays is found in the texts by Balanis [7] and Kraus and Marhefka [8].

1.2.1 Pattern of a Generalized Array

An antenna array consists of two or more antenna elements that are spatially arranged and electrically interconnected to produce a directional radiation pattern. The interconnection between elements, called the feed network, can provide fixed phase to each element or can form a phased array. The geometry of an array and the patterns, and orientations

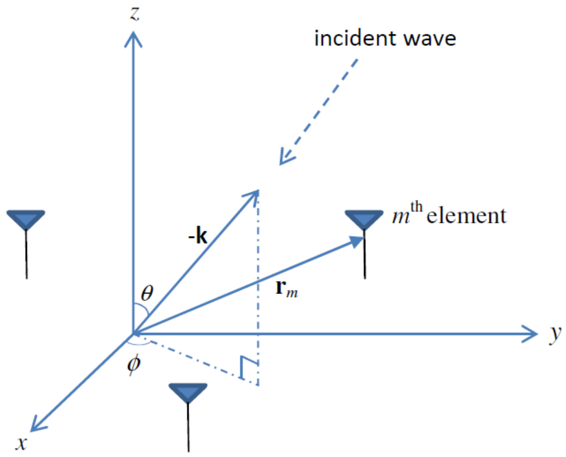

Figure 1.1: An arbitrary three dimensional array

of the elements influence the performance of the array.

Consider a three dimensional array with an arbitrary geometry shown in Figure 1.1. In spherical coordinates, the position vector $\mathbf{r}_m$ of the mth element of the array is given by

$$\mathbf{r}_m = (\rho_m, \theta_m, \phi_m) \tag{1.1}$$

where ρ_m is the magnitude of $\mathbf{r}_m$ while θ_m and ϕ_m are, respectively, the elevation and azimuth angles. The propagation (or wave) vector in the direction of the source of an incident wave is given by

$$\mathbf{k} = -k\, \mathbf{a}_r \tag{1.2}$$

where $k = \frac{2\pi}{\lambda}$ is the phase constant, λ is the operating wavelength and $\mathbf{a}_r$ is the unit vector in the direction of the position vector.

Throughout this discussion it is assumed that the source of the wave is in the far-field of the array and the incident wave can be treated as a plane wave. To find the array factor, it is necessary to find the relative phase of the received plane wave at each element. The phase is referred to the phase of the plane wave at the origin. Thus, the phase of the received plane wave at the mth element is obtained by the projection of the element position $\mathbf{r}_m$ on to the plane wave arrival vector $-\mathbf{k}$. This is given by $-\mathbf{r}_m \cdot \mathbf{k}$ with the dot product taken in rectangular coordinates. In rectangular coordinates,

$$-\mathbf{k} = k(\sin\theta\cos\phi\, \mathbf{a}_x + \sin\theta\sin\phi\, \mathbf{a}_y + \cos\theta\, \mathbf{a}_z), \qquad \text{and} \tag{1.3}$$

$$\mathbf{r}_m = \rho_m \sin\theta_m \cos\phi_m\, \mathbf{a}_x + \rho_m \sin\theta_m \sin\phi_m\, \mathbf{a}_y + \rho_m \cos\theta_m\, \mathbf{a}_z \tag{1.4}$$

where $\mathbf{a}_x, \mathbf{a}_y$, and $\mathbf{a}_z$ are the cartesian unit vectors.

The relative phase ξ_m of the incident wave at the mth element is

$$\begin{aligned}
\xi_m &= -\mathbf{k} \cdot \mathbf{r}_m \\
&= k\rho_m(\sin\theta\cos\phi\sin\theta_m\cos\phi_m + \sin\theta\sin\phi\sin\theta_m\sin\phi_m + \cos\theta\cos\theta_m) \\
&= k(x_m \sin\theta\cos\phi + y_m \sin\theta\sin\phi + z_m\cos\theta)
\end{aligned} \tag{1.5}$$

where (x_m, y_m, z_m) are the cartesian coordinates of the mth element.

1.2.2 Array Factor

For an array of M elements, the array factor is given by

$$AF(\theta, \phi) = \sum_{m=1}^{M} a_m e^{j(\xi_m + \delta_m)} \tag{1.6}$$

where a_m and δ_m are, respectively, the amplitude and phase of the weighting of the mth element.

The normalized array factor is given by

$$f(\theta, \phi) = \frac{AF(\theta, \phi)}{\max |AF(\theta, \phi)|} \tag{1.7}$$

This would be the same as the array pattern if the array consisted of ideal isotropic elements.

1.2.3 Array Pattern

If each element of the array has a pattern $g_m(\theta, \phi)$, which may be different for each element, the normalized array patter is given by

$$F(\theta, \phi) = \frac{\sum_{m=1}^{M} a_m g_m(\theta, \phi) e^{j(\xi_m + \delta_m)}}{\max \left| \sum_{m=1}^{M} a_m g_m(\theta, \phi) e^{j(\xi_m + \delta_m)} \right|} \tag{1.8}$$

In (1.8), the element patterns must be represented such that the pattern maxima are equal to the element gains relative to a common reference.

1.2.4 Equally Spaced Linear Arrays

Consider a linear array equally spaced along the $x-$axis with inter-element separation distance d. If the first element is located at the origin (Figure 1.2), the position vector (1.4) and relative phase (1.5) of the mth element become

$$\begin{aligned} \mathbf{r}_m &= \rho_m \, \mathbf{a}_x = (m-1)d \, \mathbf{a}_x \qquad \because \theta_m = 90^\circ, \phi_m = 0^\circ, \phi = 0^\circ & (1.9) \\ \xi_m &= k\rho_m \sin\theta = (m-1)kd\sin\theta & (1.10) \end{aligned}$$

Thus the array factor becomes

$$AF(\theta) = \sum_{m=1}^{M} a_m e^{j((m-1)kd\sin\theta + \delta_m)} \tag{1.11}$$

Uniform and non-uniform arrays are examples of equally spaced arrays.

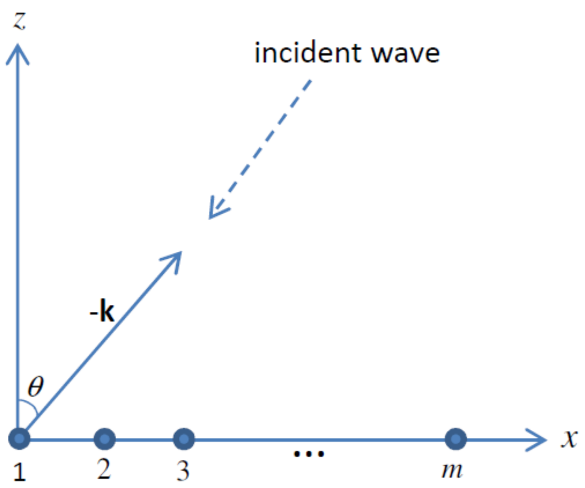

Figure 1.2: A linear array with m elements

1.2.5 Uniform Arrays

A uniform array is an equally spaced array with equal weighing magnitude and a progressive phase shift. Thus, for uniform equally spaced linear arrays,

$$a_m = 1 \qquad \text{(it can be any constant value)} \tag{1.12}$$

$$\delta_m = (m-1)\delta \tag{1.13}$$

where δ represents the phase by which the current in each element leads the current of the preceding element.

The array factor becomes

$$\boxed{AF(\theta) = \sum_{m=1}^{M} e^{j(m-1)(kd\sin\theta+\delta)}} \tag{1.14}$$

In many applications it is desirable to have the maximum radiation of an array directed normal to the axis of the array (i.e., $\theta = 0°$). This occurs when $\delta = 0$. This array is called a *broadside array* because the maximum radiation is broadside to the array geometry. Two major lobes are seen because the broadside array is symmetric about the $\theta = \pm\pi/2$ line. As the array element spacing increases, the array physically is longer, thereby decreasing the mainlobe width. The general rule for array radiation is that the mainlobe width is inversely proportional to the array length.

Figure 1.3 shows plot of the normalized array factor for uniform broadside array with 8 elements and $d = 0.25\lambda$ and 0.50λ.

1.2.6 Non-Uniform Arrays

Non-uniform linear arrays have uniform inter-element spacing and non-uniform amplitude distribution. In the simplest case, they are used to control sidelobe levels and beamwidth. In beamforming, the non-uniform array weights can be chosen to meet any specific criteria, such as, steering the main lobe towards direction of interest, placing nulls at certain

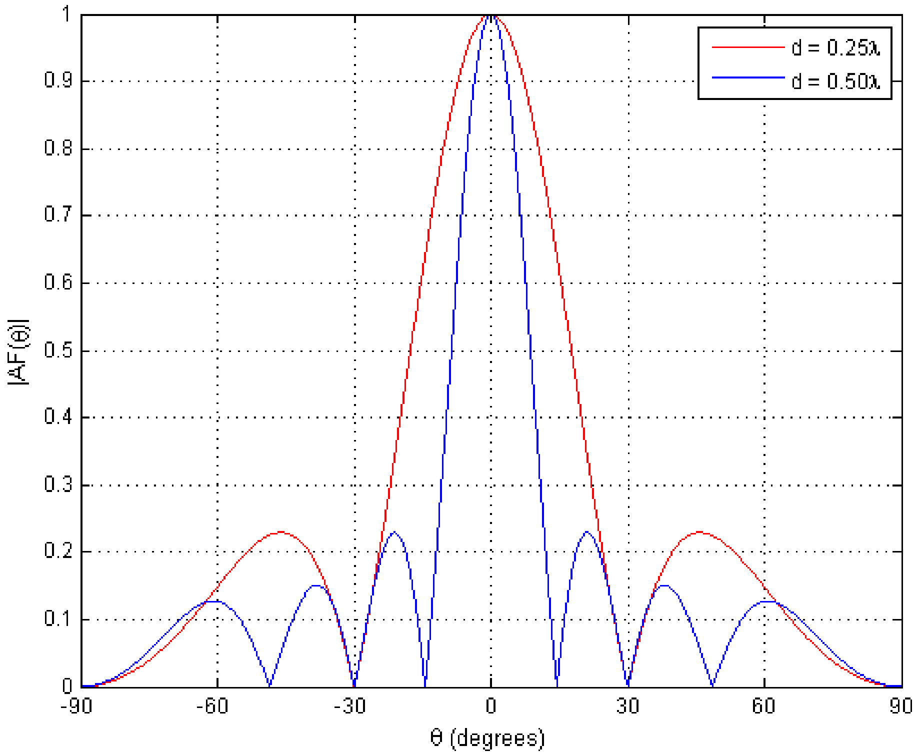

Figure 1.3: Uniform broadside arrays with $m = 8, d = 0.25\lambda$ and $d = 0.50\lambda$.

angles and shaping sidelobes.

Two of the most common non-uniform arrays, viz. Binomial and Dolph-Chebyshev arrays, will be considered next.

1.2.6 Binomial Arrays

Binomial weights create an array factor with no sidelobes, provided that the element spacing $d \leq \lambda/2$. The binomial weights are chosen from the rows of Pascal triangle. The first ten rows are shown in Table 1.1.

Table 1.1: Pascal's triangle

$N = 1$	1
$N = 2$	1 1
$N = 3$	1 2 1
$N = 4$	1 3 3 1
$N = 5$	1 4 6 4 1
$N = 6$	1 5 10 10 5 1
$N = 7$	1 6 15 20 15 6 1
$N = 8$	1 7 21 35 35 21 7 1
$N = 9$	1 8 28 56 70 56 28 8 1
$N = 10$	1 9 36 84 126 126 84 36 9 1

Figure 1.4 shows binomial arrays with $N = 8$ and inter-element spacing $d = 0.25\lambda, 0.5\lambda$.

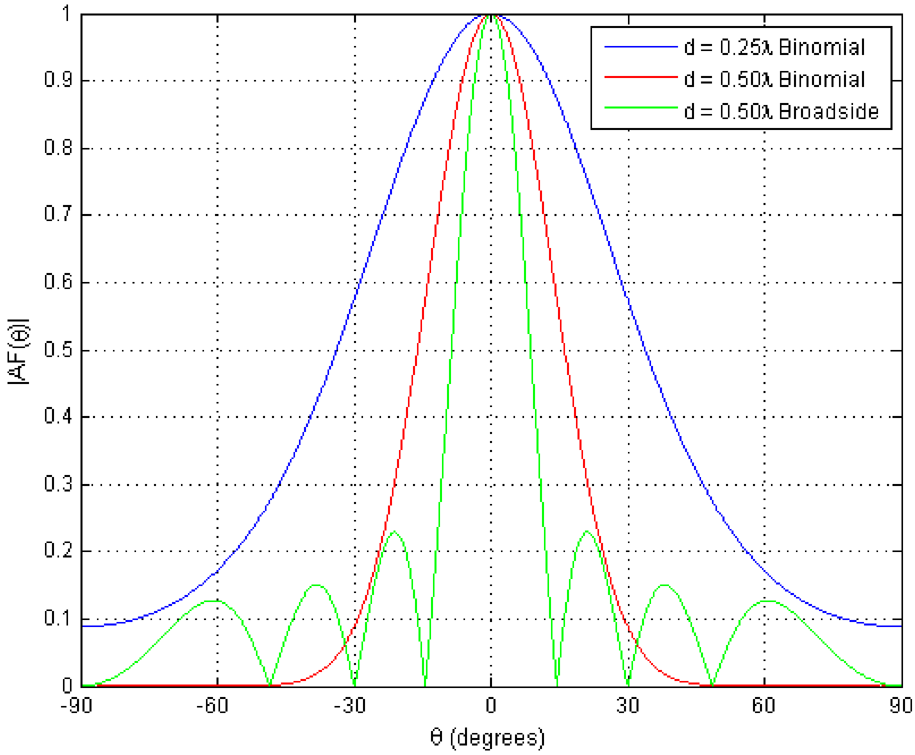

Figure 1.4: Binomial arrays with $m = 8, d = 0.25\lambda$ and $d = 0.50\lambda$ compared with a uniform broadside with $m = 8, d = 0.50\lambda$

1.2.6 Dolph-Chebyshev Array

The excitation coefficients of a Dolph-Chebyshev array are related to Chebyshev's polynomials. It is primarily a compromise between uniform and binomial arrays. A Dolph-Chebyshev array with no side lobes (or side lobes of $-\infty$ dB) reduces to the binomial array.

Chebyshev's polynomials can be given by the recursive formula

$$\begin{aligned} T_0(x) &= 1 \\ T_1(x) &= x \\ T_{n+1}(x) &= 2xT_n(x) - T_{n-1}(x) \end{aligned} \tag{1.15}$$

The main goal in Dolph-Chebyshev array design is to approximate the desired AF with a Chebyshev polynomial such that

- the sidelobe level meets a desired level, and
- the main beamwidth is as small as possible.

Figure 1.5 shows an example of Dolph-Chebyshev array with major-to-minor lobe ratio of 26 dB compared with a uniform and binomial arrays with the same number of elements and spacing.

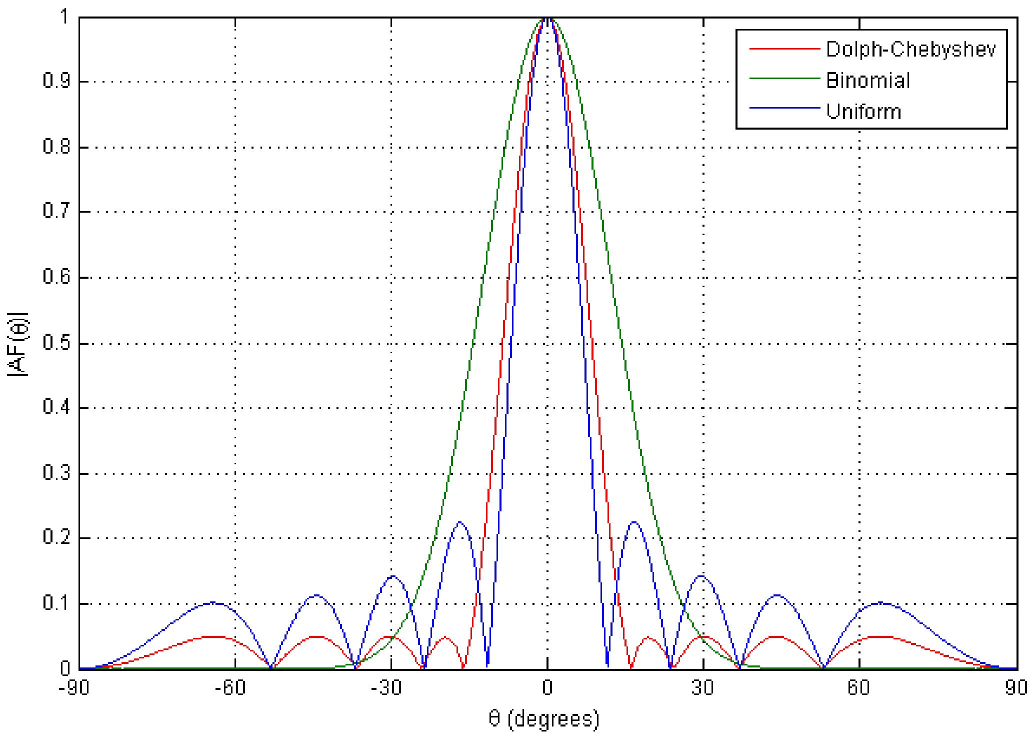

Figure 1.5: Dolph-Chebyshev array with major-to-minor lobe ratio of 26 dB and $N = 10, d = 0.5\lambda$ compared with Uniform and Binomial arrays with the same number of elements and spacing.

1.3 Smart Antennas

A smart antenna system combines multiple antenna elements with a signal-processing capability to optimize its radiation and/or reception pattern automatically in response to the signal environment. Spatial processing leads to more degrees of freedom in the system design, which can help improve the overall performance of the system.

Widespread interest in smart antennas has continued for several decades due to their use in numerous applications [9]. The first issue of IEEE Transactions of Antennas and Propagation, published in 1964 [10], was followed by special issues of various journals [11], [12], [13], [14], [15], books [16], [17], [2], [19], [20], [21], [1], a selected bibliography [22], and a vast number of specialized research papers. Tutorials are also presented in [23] and [24]. Some of the general papers in which various issues are discussed include [25], [26], [27], [28], [29], [30], [31], [32], [33], [34], [18],[35], [36].

Although phased arrays had been widely used to synthesize directive beams in radar and satellite communications, it was only in the 1990s that antenna arrays drew the attention of terrestrial wireless system designers. This attention was due, largely, to the enormous success of cellular systems and the need for higher capacities resulting from that success. The success was also partly due to the advent of very fast and low-cost digital signal processors that has made smart antennas cost effective and practical.

1.3.1 Advantages of Smart Antennas

In mobile-communication systems, smart antennas are used to overcome the problem of limited channel bandwidth, satisfying a growing demand for a large number of mobiles on communications channels. Smart antennas, when used appropriately, help in improving the system performance by increasing channel capacity and spectrum efficiency, extending range coverage, steering multiple beams to track many mobiles, and compensating electronically for aperture distortion. They reduce *delay spread, multipath fading, co-channel interference, system complexity, bit error rate (BER),* and *outage probability.* Smart antennas also provide *space diversity.*

Delay spread occurs in multipath propagation environments when a desired signal, arriving from different directions, becomes delayed due to different travel distances. Delay spread and multipath fading can be reduced with an antenna array that is capable of forming beams in certain directions and nulls in others, thereby canceling some of the delayed arrivals. Usually, in the transmitting mode, the array focuss energy in the required direction, which helps to reduce multipath reflections and the delay spread. In the receiving mode, however, the array provides compensation in multipath fading by adding the signals emanating from other clusters after compensating for delays, as well as by canceling delayed signals emanating from directions other than that of the desired signal.

System complexity and cost is decreased by the use of a smaller number of base stations.

The increase in the spectrum efficiency- which is defined as the amount of traffic a given system with certain spectrum allocation could manage is a result of the capability of the antenna array to provide virtual channels in an angle domain. This is referred to as Spatial-Division Multiple Access (SDMA), which means that it is possible to multiplex channels in the spatial dimension, just as in the frequency and time dimensions [37]. The increase is achieved by using spatially selective reception and spatially selective transmission.

Perhaps the most important feature of a smart-antenna system is its capability to cancel co-channel interference. Co-channel interference is caused by radiation from cells that use the same set of channel frequencies. Thus, co-channel interference in the transmitting mode is reduced by focusing a directive beam in the direction of a desired signal, and nulls in the directions of other receivers. In the receiving mode, co-channel interference can be reduced by knowing the directional location of the signals source, and utilizing interference cancelation.

The reduction in outage probability, which is the probability that a mobile user would lose the ability to communicate, is achieved from the increase in the available channels.

Smart antennas can provide space diversity to alleviate the effects of channel fading. Space diversity is used extensively in wireless networks. The basic idea of space diversity is as follows: if several replicas of the same information carrying signal are received over multiple branches with comparable strengths and which exhibit independent fading, then there is a high probability that at least one (or more) branch will not be in a fade at any given instant of time. When a receiver is equipped with two or more antennas that are sufficiently separated (typically several wavelengths) they offer useful diversity branches. Diversity branches tend to fade independently, therefore, a proper selection or combination of the branches increases link reliability. Without diversity, the protection against deep channel fades requires higher transmit power to ensure the link margins. Therefore, diversity at the base can be traded for reduced power consumption and longer battery life at the user terminal. Also, lower transmit power decreases the amount of co-channel interference and increases the system capacity [24].

The smart antenna system needs to differentiate the desired signal from the co-channel interference, and normally requires either 'a priori' knowledge of a reference signal, or the direction of the desired signal source, to achieve its desired objectives. There exist a variety of methods to estimate the direction of sources, with conflicting demands of accuracy and processing power. Similarly, there are many algorithms to update the array weights, each with its speed of convergence and required processing time [2], [38]. Algorithms also exist that exploit properties of signals to eliminate the need of training signals, in some circumstances.

1.3.2 Types of Smart Antennas

Today, several terms are used to refer to the various aspects of smart-antenna system technology, including intelligent antennas, phased arrays, SDMA, spatial processing, digital beamforming, adaptive antenna systems, and others [39]. Smart-antenna systems, however, are usually categorized as either *switched-beam* or *adaptive-array* systems. Although both systems attempt to increase gain in the direction of the user, only the adaptive-array system offers optimal gain, while simultaneously identifying, tracking, and minimizing interfering signals. It is the adaptive system's active interference capability that offers substantial performance advantages and flexibility over the more-passive switched-beam approach. Smart antennas communicate directionally by forming specific antenna-beam patterns. They direct their main lobe, with increased gain, in the direction of the user, and they direct nulls in directions away from the main lobe. Different switched-beam and adaptive smart antennas control the lobes and the nulls with varying degrees of accuracy and flexibility.

Figure 1.6 illustrates the beam patterns that each system might choose, in a scenario involving one desired signal and two co-channel interferers. The switched-beam system is depicted on the left, while the adaptive system is on the right. Both systems direct their major lobe in the general direction of the signal of interest, but the adaptive system chooses a more-accurate placement, providing greater signal enhancement. Similarly, the interfering signals arrive at places of lower gain outside the main lobe, but, again, in the adaptive system, the interfering signals receive maximum suppression.

The traditional switched-beam method is considered as an extension of the current cellular sectorization scheme, in which a typical sectorized cell site is composed of three 120-degree macro-sectors. The switched-beam approach further subdivides the macro-sectors into several micro-sectors. Each micro-sector contains a predetermined fixed beam pattern, with the greatest gain placed in the center of the beam. Typically, the switched-beam system establishes certain choices of beam patterns before deployment, and selects from one of several choices during operation. When a mobile user is in the vicinity of a macro-sector, the switched-beam system selects the micro-sector containing the strongest signal. During the call, the system monitors the signal strength, and switches to other fixed micro-sectors, if required. All switched-beam systems offer similar benefits, even though the different systems utilize different hardware and software designs. Compared

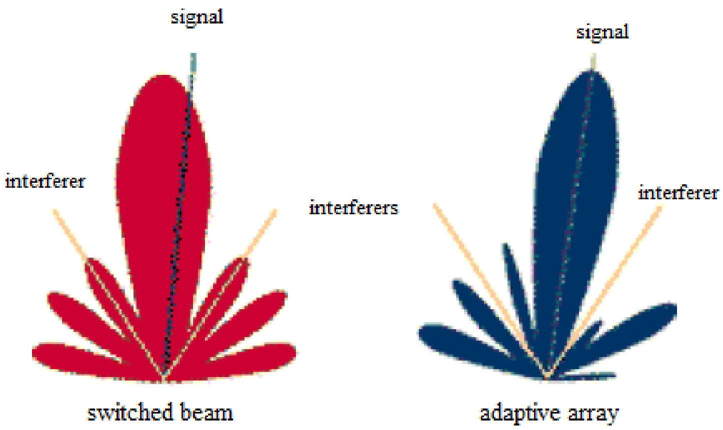

Figure 1.6: Beamforming lobes and nulls that switched beam (left) and adaptive array (right) systems might choose for identical user signals (green line) and co-channel interferers (yellow lines)

to conventional sectored cells, switched-beam systems can increase the range of a base station from 20% to 200%, depending on the circumstances of operation [23]. The additional coverage means that an operator can achieve a substantial reduction in infrastructure costs.

There are, however, limitations to switched-beam systems. Since the beams are predetermined, the signal strength varies as the user moves through the sector. As a mobile unit approaches the far azimuth edges of a beam, the signal strength degrades rapidly before the user is switched to another micro-sector. Moreover, a switched-beam system does not distinguish between a desired signal and interfering signals. If the interfering signal is around the center of a selected beam and the user is away from the center, the quality of the signal is degraded for the mobile user.

Adaptive antennas take a very different approach. By adjusting to an RF environment as it changes, adaptive-antenna technology can dynamically alter the signal patterns to optimize the performance of the wireless system. The adaptive antenna utilizes sophisticated signal-processing algorithms to continuously distinguish among desired signals, multipath, and interfering signals, as well as to calculate their directions of arrival. The adaptive approach continuously updates its beam pattern, based on changes in both the desired and interfering signal locations. The ability to smoothly track users with main lobes, and interferers with nulls, insures that the link budget is constantly maximized. This effect is similar to a persons hearing. When one person listens to another, the brain of the listener collects the sound in both ears, combines it to hear better, and determines the direction from which the speaker is talking. If the speaker is moving, the listener, even if his eyes are closed, can continue to update the angular position, based solely on what he hears. The listener also has the ability to tune out unwanted noise and interference, and to focus on the conversation at hand.

Figure 1.7 shows a comparison, in terms of relative coverage area, of conventional sectorized, switched-beam, and adaptive antennas. In the presence a low level of interference (Figure 1.7a), both types of smart antennas provide significant gains over the conventional sectored systems. When a high level of interference is present (Figure 1.7b), the interference-rejection capability of the adaptive system provides significantly more coverage than either the conventional or switched-beam system.

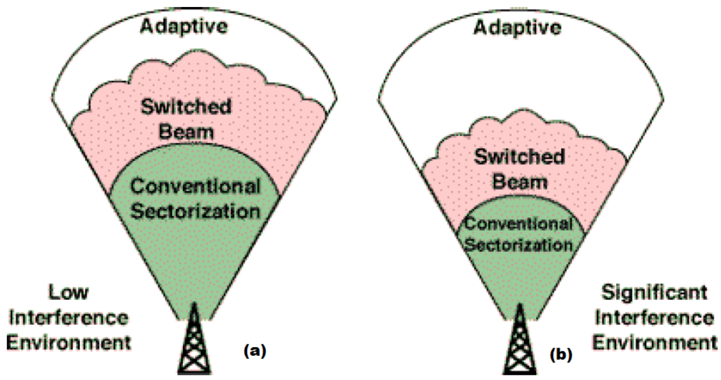

Figure 1.7: Coverage patterns for switched beam and adaptive array antennas

Another important advantage of adaptive-antenna systems is its capability to 'create' spectrum. Because of the accurate tracking and robust interference-rejection capabilities, multiple users can share the same conventional channel within the same cell as shown in Figure 1.8. This enables us to use SDMA. In this case, users may use the same frequency, time, or code allocations over the air interface and only be separated spatially. This enables SDMA to be a complementary scheme to FDMA, TDMA, and CDMA. Thus SDMA provides increased capacity within congested areas.

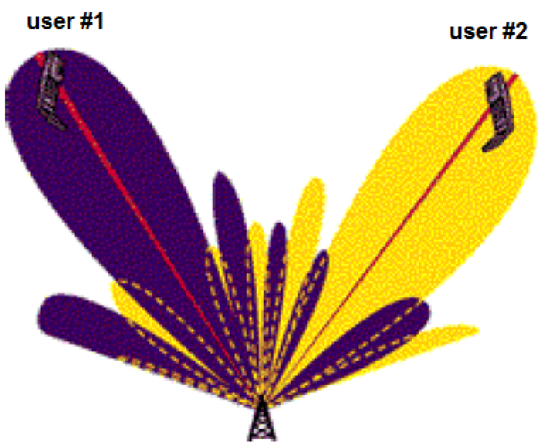

Figure 1.8: Fully adaptive spatial processing, supporting two users on the same conventional channel simultaneously in the same cell.

1.4 Signal Model

Array signal processing involves the manipulation of signals induced onto the elements of an array. A signal model useful for array processing is presented here. Detailed information can be found in [9], [38].

Consider an array antenna of L, isotropic elements, shown in Figure 1.9. Assume the array to be receiving M uncorrelated sinusoidal point sources, of frequency f_0. A plane wave, radiated from the ith source in direction (ϕ_i, θ_i) arriving at the lth element of the array after time

$$\tau_l(\phi_i, \theta_i) = \frac{\mathbf{r}_l \cdot \mathbf{a}(\phi_i, \theta_i)}{c} \tag{1.16}$$

where $\mathbf{r}_l$ is the position vector of the lth element, $\mathbf{a}(\phi_i, \theta_i)$ is the unit vector in direction (ϕ_i, θ_i), and c is the speed of propagation of the plane wavefront.

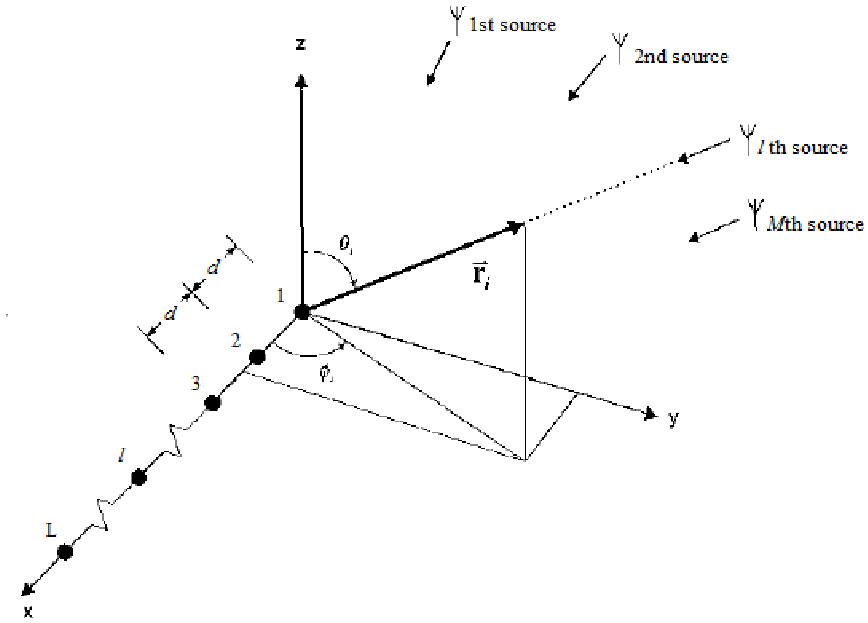

Figure 1.9: The coordinate system for the signal model [23].

For a linear equally spaced array, aligned with the x-axis such that the first element is situated at the origin (Figure 1.9), this becomes

$$\tau_l(\theta_i) = \frac{d}{c}(l-1)\sin\theta_i \cos\phi_i \tag{1.17}$$

where d is the inter-element distance. The signal induced on the reference element due to the ith source is normally expressed in complex notation as

$$m_i(t)\exp(j2\pi f_0 t), \tag{1.18}$$

where $m_i(t)$ denotes the complex modulating function.

Assuming that the plane wave on the lth element arrives $\tau_l(\phi_i, \theta_i)$ seconds before it arrives at the reference element, the signal induced on the lth element due to the ith source can he expressed as

$$m_i(t)\exp\{j2\pi f_0[t + \tau_l(\phi_i, \theta_i)]\}, \tag{1.19}$$

This expression is based upon the narrow-band assumption for array signal processing, which assumes that the bandwidth of the signal is narrow enough for the modulating function to stay almost constant during $\tau_l(\phi_i, \theta_i)$ seconds, that is, the approximation

$$m_l(t) \cong m_l[t + \tau_l(\phi_i, \theta_i)] \quad \text{holds.} \tag{1.20}$$

Let x_l denote the total signal induced due to all M directional sources and background noise on the lth element. Then, it is given by

$$x_l = \sum_{i=1}^{M} m_i(t) \exp\{j2\pi f_0[t + \tau_l(\phi_i, \theta_i)]\} + n_l(t) \tag{1.21}$$

where $n_l(t)$ is a random-noise component on the lth element, which includes background noise and electronic noise generated in the lth channel. It is assumed to be temporally white, with zero mean and variance equal to σ_n^2.

Consider a narrow-band beamformer, shown in Figure 1.10a, where signals from each element are multiplied by a complex weight, and summed to form the array output. It follows from the figure that an expression for the array output can be given by

$$y(t) = \sum_{l=1}^{L} w_l^* x_l(t), \tag{1.22}$$

where $*$ denotes the complex conjugate.

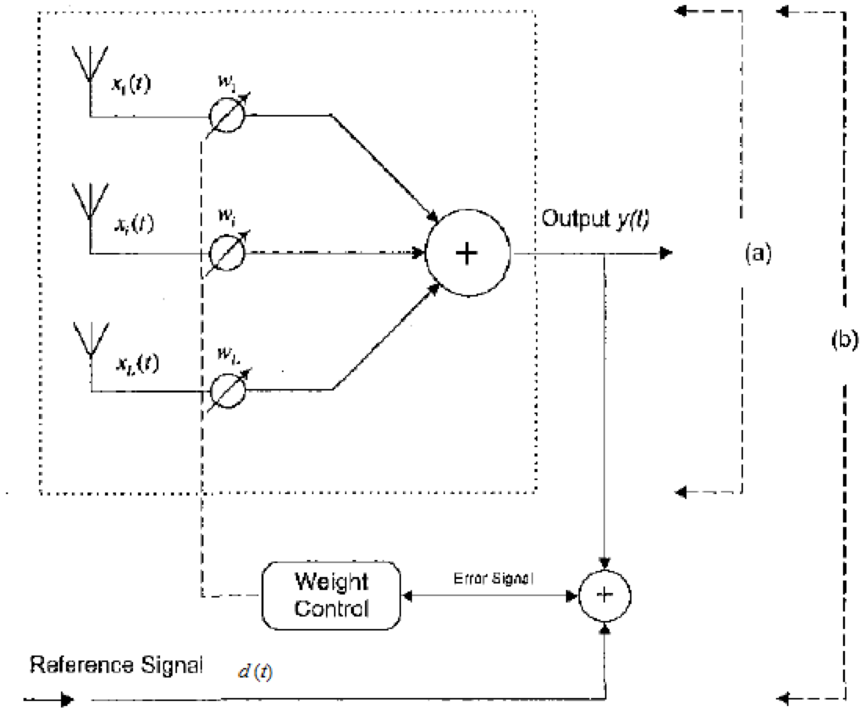

Figure 1.10: The structure of a narrow-band beamformer (a) without and (b) with a reference signal [23].

Denoting the weights of the beamformer as

$$\bar{w} = [w_1, w_2, \ldots, w_L]^T \tag{1.23}$$

and the signals induced on all elements as

$$\bar{x}(t) = [x_1(t), x_2(t), \ldots, x_L(t)]^T \tag{1.24}$$

the output of the beamformer becomes

$$y(t) = \bar{w}^H \bar{x}(t) \tag{1.25}$$

where superscripts T and H, respectively, denote the transpose and complex-conjugate transpose of a vector or matrix. $\bar{w}$ and $\bar{x}(t)$ are referred to as the *array weight vector* and the *array signal vector*, respectively.

If the components of $\bar{x}(t)$ can be modeled as zero-mean stationary processes, then for a given $\bar{w}$, the mean output power of the processor is given by

$$P(\bar{w}) = \mathbb{E}\left[y(t)y^*(t)\right] = \bar{w}^H R_{xx} \bar{w} \tag{1.26}$$

where $\mathbb{E}[\cdot]$ denotes the expectation operator, and R_{xx} is the array correlation matrix, defined by

$$R_{xx} = \mathbb{E}\left[\bar{x}(t)\bar{x}^H(t)\right] \tag{1.27}$$

Elements of this matrix denote the correlation between various elements. For example, $R_{xx}(i,j)$, denotes the correlation between the ith and the jth elements of the array.

Denote the steering vector, associated with the direction (ϕ_i, θ_i) or the ith source by an L-dimensional complex vector $\bar{s}_i$, by

$$\bar{s}_i = \{\exp[j2\pi f_0 \tau_1(\phi_i, \theta_i), \ldots, j2\pi f_0 \tau_L(\phi_i, \theta_i)]\}^T \tag{1.28}$$

From the above equations, it follows that

$$R_{xx} = \sum_{i=1}^{M} p_i \bar{s}_i \bar{s}_i^H + \sigma_n^2 I, \tag{1.29}$$

where I is an identity matrix and p_i denotes the power of the ith source, measured at one of the elements of the array. Using matrix notation, the correlation matrix, R_{xx}, may be expressed in the following compact form

$$R_{xx} = \Lambda S \Lambda^H + \sigma_n^2 I \tag{1.30}$$

where columns of the L by M matrix Λ are made up of steering vectors, i.e.,

$$\Lambda = [\bar{s}_1, \bar{s}_2, \ldots, \bar{s}_M] \tag{1.31}$$

and the M by M matrix S denotes the source correlation. For uncorrelated sources, it is a diagonal matrix with

$$S_{ij} = \begin{cases} p_i, & i = j; \\ 0, & i \neq j. \end{cases} \tag{1.32}$$

Sometimes, it is useful to express R_{xx} in terms of its eigenvalues and their associated eigenvectors. The eigenvalues of R_{xx} can be divided into two sets, when the environment consists of uncorrelated directional sources and uncorrelated white noise. Thus, the R_{xx} matrix of an array of L elements immersed in M directional sources and white noise has M signal eigenvalues and $L - M$ noise eigenvalues.

Denoting the L eigenvalues of R_{xx} in descending order by $\lambda_l, l = 1, \ldots, L$, and their corresponding unit-norm eigenvectors by $\bar{U}_l, l = 1, \ldots, L,$, the matrix takes the following form:

$$R_{xx} = \Sigma \Lambda \Sigma^H, \tag{1.33}$$

with a diagonal matrix

$$\Lambda = \begin{bmatrix} \lambda_1 & & & & \\ & \cdot & & 0 & \\ & & \lambda_l & & \\ & 0 & & \cdot & \\ & & & & \lambda_L \end{bmatrix} \tag{1.34}$$

and

$$\Sigma = [\bar{U}_1 \cdots \bar{U}_L] \tag{1.35}$$

This representation sometimes is referred to as the spectral decomposition of R_{xx}. Using the fact that the eigenvectors form an orthonormal set, this leads to the following expression for R:

$$R_{xx} = \sum_{l=1}^{M} \lambda_l \bar{U}_l \bar{U}_l^H + \sigma_n^2 I \tag{1.36}$$

There are many schemes that can be used to select the weights of the beamformer, as depicted in Figure 1.10a. Some of these schemes are discussed in the next section.

1.5 Adaptive Beamforming Algorithms

Adaptive beamforming algorithms iteratively adjust the weights until a certain performance criterion is met. The most common performance criteria are the minimum mean-squared error (MMSE) and maximum signal-to-interference-plus-noise ratio (MSINR).

Let's consider the MMSE. It is required to minimize the mean squared error (MSE) between the array output and the reference signal $d(t)$ (see Figure 1.10). The reference signal is preferably either identical to the desired signal or is highly correlated with desired signal and uncorrelated with the interfering signals.

The error $e(n)$ between the desired signal, $d(n)$, and the output signal of the array, $y(n)$, at time index n is

$$e(n) = d(n) - \bar{w}^H \bar{x}(n) \tag{1.37}$$

The MMSE based cost function can be written as

$$\begin{aligned} J(\bar{w}) &= \mathbb{E}[|e(n)|^2] && (1.38)\\ &= \mathbb{E}[|d(n) - \bar{w}^H \bar{x}(n)|^2] && (1.39)\\ &= \mathbb{E}[|d(n)|^2 - 2d(n)\bar{w}^H \bar{x}(n) + \bar{w}^H \bar{x}(n)\bar{x}(n)^H \bar{w}] && (1.40)\\ &= \mathbb{E}[|d(n)|^2] - 2\bar{w}^H \mathbb{E}[d^*(n)\bar{x}(n)] + \bar{w}^H \mathbb{E}[\bar{x}(n)\bar{x}(n)^H]\bar{w} && (1.41)\\ &= \mathbb{E}[|d(n)|^2] - 2\bar{w}^H r_{xd} + \bar{w}^H R_{xx}\bar{w} && (1.42) \end{aligned}$$

where $\mathbb{E}[\cdot]$ is the expectation operator, $R_{xx} = \mathbb{E}[\bar{x}(n)\bar{x}^H(n)]$ is the signal covariance matrix and $r_{xd} = \mathbb{E}[d^*(n)\bar{x}(n)]$ is the signal correlation matrix. The quantities R_{xx} and r_{xd} are functions of the angles of arrival of the signals.

To minimize the cost function, its gradient is set to zero

$$\min_{\bar{w}} J(\bar{w}) \Rightarrow \nabla_{\bar{w}} \{J(\bar{w})\} = 0 \tag{1.43}$$

but

$$\nabla_{\bar{w}} \{J(\bar{w})\} = \nabla_{\bar{w}} \left\{\mathbb{E}[|d(n)|^2] - 2\bar{w}^H r_{xd} + \bar{w}^H R_{xx}\bar{w}\right\} = 2R_{xx}\bar{w} - 2r_{xd} \tag{1.44}$$

hence, the solution for the optimum weights becomes

$$\boxed{\bar{w}_{opt} = R_{xx}^{-1} r_{xd}} \qquad \text{(Wiener solution)} \tag{1.45}$$

In general, the signal statistics is not known and thus one must resort to estimating the array correlation matrix, R_{xx}, and the signal correlation vector, r_{xd}, over a range of snapshots or for each instant in time. The instantaneous estimates of these values are given as

$$\hat{R}_{xx}(n) \approx \bar{x}(n)\bar{x}^H(n) \tag{1.46}$$

$$\hat{r}_{xd}(n) \approx d^*(n)\bar{x}(n) \tag{1.47}$$

Adaptive beamforming algorithms iteratively approximate the optimum weights (1.45). Adaptive beamforming began with the work of Howells and Applebaum [9]. Since then many beamforming algorithms have been developed. Some of the most commonly used adaptive algorithms are briefly described below.

1.5.1 Least Mean Squares (LMS)

Application of least mean squares algorithm to estimate optimal weights of an array is widespread and its study has been of considerable interest for some time. This algorithm uses a steepest-descent method and computes the weight vector recursively using the method advocated by Widrow [18]

$$\bar{w}(n+1) = \bar{w}(n) - \frac{1}{2}\mu\nabla_{\bar{w}} J(\bar{w}(n)) \tag{1.48}$$

where $\bar{w}(n+1)$ denotes the new weights computed at the $(n+1)$th iteration and μ is the *step size* which controls the rate of adaptation.
Upon substituting (1.44), we have

$$\bar{w}(n+1) = \bar{w}(n) - \mu[R_{xx}\bar{w} - r_{xd}] \tag{1.49}$$

If the instantaneous correlation approximations is substituted in (1.46) and (1.47), the LMS solution becomes

$$\bar{w}(n+1) = \bar{w}(n) + \mu\bar{x}(n)[d^*(n) - \bar{x}^H(n)\bar{w}(n)] \tag{1.50}$$

In order to assure convergence of the weights, $\bar{w}(n)$, the step size μ is bounded by the condition [17]

$$0 < \mu < \frac{1}{2\lambda_{\max}} \tag{1.51}$$

where $\lambda_{\max}$ is the maximum eigenvalue of the covariance matrix, R_{xx}.

Since the correlation matrix is positive definite, all eigenvalues are positive. If all the interfering signals are noise and there is only one signal of interest, one can approximate the condition in (1.51) as [1]

$$0 < \mu < \frac{1}{2\text{trace}(\hat{R}_{xx})} \tag{1.52}$$

The LMS algorithm updates the weights at each iteration by estimating the gradient of the quadratic MSE surface, and then moving the weights in the negative direction of the gradient by a small amount. The step size μ is the constant that determines this amount. The convergence and transient behavior of these weights along with their covariance characterize the LMS algorithm, and the way the step size and the process of gradient estimation affect these parameters are of great practical importance.

The LMS algorithm requires knowledge of the desired signal. This can be done in a digital system by periodically transmitting a training sequence that is known to the receiver, or using the spreading code in the case of a direct-sequence CDMA system. This algorithm converges slowly if the eigenvector spread of R_{xx} is large.

The LMS has been studied by many authors [18], [38], [40]- [52].

1.5.2 Sample Matrix Inversion (SMI)

One of the drawbacks of the LMS adaptive scheme is that the algorithm must go through many iterations before satisfactory convergence is achieved. If the signal characteristics are rapidly changing, the LMS adaptive algorithm may not allow tracking of the desired signal in a satisfactory manner. One possible approach to circumventing the relatively slow convergence of the LMS scheme is by use of sample matrix inversion (SMI) method. The sample matrix is a time average estimate of the array correlation matrix using K-time samples.

In this algorithm (1.45) is used to obtain the weights, but with R_{xx} and r_{xd} estimated from data sampled over a finite interval. The estimates are given by

$$\hat{R}_{xx}(N) = \frac{1}{N}\sum_{n=0}^{N-1} \bar{x}(n)\bar{x}^H(n) \tag{1.53}$$

$$\hat{r}_{xd}(N) = \frac{1}{N}\sum_{n=0}^{N-1} d^*(n)\bar{x}(n) \tag{1.54}$$

where N is the observation interval, $\hat{R}_{xx}(N)$ and $\hat{r}_{xd}(N)$ denote, respectively, the estimated array correlation matrix and signal correlation matrix using N samples, and $\bar{x}(n)$ denotes the array signal sample also known as the array snapshot at the nth instant of time with t replaced by nT and T denoting the sampling time. The sampling time T has been omitted for ease of notation.

Let $\hat{R}_{xx}(n)$ denote the estimate of array correlation matrix and $\bar{w}(n)$ denote the array weights at the nth instant of time. The estimate of R_{xx} may be updated when the new samples arrive using [9]

$$\hat{R}_{xx}(n+1) = \frac{n\hat{R}(n) + \bar{x}(n+1)\bar{x}^H(n+1)}{n+1} \tag{1.55}$$

and a new estimate of the weights $\bar{w}(n+1)$ at time instant $n+1$ may be made.

Let $P(n)$ denote the output power at the nth instant of time given by

$$P(n) = \bar{w}^H(n)\bar{x}(n)\bar{x}^H(n)\bar{w}(n) \tag{1.56}$$

When N samples are used to estimate the array correlation matrix and the processor has K degree of freedom (due to K-time samples) the mean output power is given by [9][54]

$$\mathbb{E}[P(n)] = \frac{N-K}{N}\hat{P} \tag{1.57}$$

where $\hat{P}$ denotes the mean output power of the processor with the optimal weights, that is,

$$\hat{P} = \bar{w}_{opt}^H R_{xx} \bar{w}_{opt} \tag{1.58}$$

The factor $(N - K)/N$ represents the loss due to estimate of R_{xx} and determines the convergence behavior of the mean output power.

It should be noted that as the number of samples grows, the matrix update approaches its true value and thus the estimated weights approaches optimal weights, that is, as $n \to \infty, R_{xx}(n) \to R_{xx}$ and $\bar{w}(n) \to \bar{w}_{opt}$, as the case may be [9].

The SMI algorithm converges more rapidly than the LMS algorithm but it is more computationally complex. The SMI algorithm also requires a reference signal. More discussion on the SMI algorithm is found in [53], [54], [55].

Application of SMI to estimate the weights of an array to operate in mobile communication systems has been considered in many studies [37], [58], [59], [60], [61], [62]. One of these studies [59] considers beamforming for GSM signals using a variable reference signal as available during the symbol interval of the time-division multiple access (TDMA) system. Applications discussed include vehicular mobile communications [60], reducing delay spread in indoor radio channels [62], and mobile satellite communication systems [58].

1.5.3 Recursive Least Squares Algorithm (RLS)

As was mentioned in the previous section, the SMI technique has several drawbacks. Even though the SMI method is faster than the LMS algorithm, the computational burden and potential singularities can cause problems. However, one can recursively calculate the required correlation matrix and the required correlation vector [1], [32], [26], [38].

The RLS algorithm estimates R_{xx} and r_{xd} using weighted sums as

$$\hat{R}_{xx}(n) = \sum_{k=0}^{n} \gamma^{n-k} \bar{x}(k) \bar{x}^H(k) \tag{1.59}$$

$$\hat{r}_{xd}(n) = \sum_{k=0}^{n} \gamma^{n-k} d^*(k) \bar{x}(k) \tag{1.60}$$

where γ called the *forgetting factor* is a positive constant close to 1 such that $0 \leq \gamma \leq 1$.

The γ is used for exponential weighting of past data and it tends to de-emphasize the old samples. When $\gamma = 1$, the ordinary least squares algorithm is restored. $\gamma = 1$ also indicates infinite memory. Let us break up the summation in (1.59) and (1.60) into two terms: the summation for values up to $k = n - 1$ and last term for $k = n$.

$$
\begin{aligned}
\hat{R}_{xx}(n) &= \gamma \sum_{k=0}^{n-1} \gamma^{n-1-k} \bar{x}(k)\bar{x}^H(k) + \bar{x}(n)\bar{x}^H(n) \\
&= \gamma \hat{R}_{xx}(n-1) + \bar{x}(n)\bar{x}^H(n) \qquad (1.61) \\
\hat{r}_{xd}(n) &= \gamma \sum_{k=0}^{n-1} \gamma^{n-1-k} d^*(k)\bar{x}(k) + d^*(n)\bar{x}(n) \\
&= \gamma \hat{r}_{xd}(n-1) + d^*(n)\bar{x}(n) \qquad (1.62)
\end{aligned}
$$

Thus, future values for the array correlation estimate and the vector correlation estimate can be found using previous values.

One can use (1.61) to derive a recursion relationship for the inverse of the correlation matrix. Invoking the Sherman Morrison-Woodbury theorem [57] for matrix $\bar{A}$ and vector $\bar{z}$

$$
(\bar{A} + \bar{z}\bar{z}^H)^{-1} = \bar{A}^{-1} - \frac{\bar{A}^{-1}\bar{z}\bar{z}^H\bar{A}^{-1}}{1 + \bar{z}^H\bar{A}^{-1}\bar{z}} \qquad (1.63)
$$

then

$$
\hat{R}_{xx}^{-1}(n) = \gamma^{-1}\hat{R}_{xx}^{-1}(n-1) - \frac{\gamma^{-2}\hat{R}_{xx}^{-1}(n-1)\bar{x}(n)\bar{x}^H(n)\hat{R}_{xx}^{-1}(n-1)}{1 + \gamma^{-1}\bar{x}^H(n)\hat{R}_{xx}^{-1}(n-1)\bar{x}(n)} \qquad (1.64)
$$

The matrix initializes as [9]

$$
\hat{R}_{xx}^{-1}(0) = \frac{1}{\varepsilon_0} I, \quad \varepsilon_0 > 0 \qquad (1.65)
$$

where I is the identity matrix.

One can simplify (1.64) by defining the gain vector $\bar{g}(n)$

$$
\bar{g}(n) = \frac{\gamma^{-1}\hat{R}_{xx}^{-1}(n-1)\bar{x}(n)}{1 + \gamma^{-1}\bar{x}^H(n)\hat{R}_{xx}^{-1}(n-1)\bar{x}(n)} \qquad (1.66)
$$

Thus

$$
\hat{R}_{xx}^{-1}(n) = \gamma^{-1}\hat{R}_{xx}^{-1}(n-1) - \gamma^{-1}\bar{g}(n)\bar{x}^H(n)\hat{R}_{xx}^{-1}(n-1) \qquad (1.67)
$$

Equation (1.67) is known as the *Riccati equation* for the recursive least squares method.

Rearrange (1.66) by multiplying the denominator times both sides of the equation to yield

$$
\bar{g}(n) = [\gamma^{-1}\hat{R}_{xx}^{-1}(n-1) - \gamma^{-1}\bar{g}(n)\bar{x}^H(n)\hat{R}_{xx}^{-1}(n-1)]\bar{x}(n) \qquad (1.68)
$$

One can observe that the term inside of the brackets of (1.68) is equal to (1.67). Thus

$$
\bar{g}(n) = \hat{R}_{xx}^{-1}(n)\bar{x}(n) \qquad (1.69)
$$

Now a recursion relationship can be derived to update the weight vectors. Substitute (1.62) in the optimum Wiener solution, then

$$
\begin{aligned}
\bar{w}(n) &= \hat{R}_{xx}^{-1}(n)\hat{r}_{xd}(n) \\
&= \gamma\hat{R}_{xx}^{-1}(n)\hat{r}_{xd}(n-1) + \hat{R}_{xx}^{-1}(n)\bar{x}(n)d^*(n) \qquad (1.70)
\end{aligned}
$$

Substituting the Riccati equation (1.67) into the first correlation matrix inverse seen in (1.70), one can have

$$\begin{aligned}\bar{w}(n) &= \hat{R}_{xx}^{-1}(n-1)\hat{r}_{xd}(n-1) - \bar{g}(n)\bar{x}^H(n)\hat{R}_{xx}^{-1}(n-1)\hat{r}_{xd}(n-1) + \hat{R}_{xx}^{-1}(n)\bar{x}(n)d^*(n) \\ &= \bar{w}(n-1) - \bar{g}(n)\bar{x}^H(n)\bar{w}(n-1) + \hat{R}_{xx}^{-1}(n)\bar{x}(n)d^*(n) \qquad (1.71)\end{aligned}$$

Finally (1.69) can be substituted into (1.71) to yield

$$\begin{aligned}\bar{w}(n) &= \bar{w}(n-1) - \bar{g}(n)\bar{x}^H(n)\bar{w}(n-1) + \bar{g}(n)d^*(n) \\ &= \bar{w}(n-1) + \bar{g}(n)[d^*(n) - \bar{x}^H(n)\bar{w}(n-1)] \qquad (1.72)\end{aligned}$$

Note that from (1.65), $\bar{w}$ initializes as $\bar{w}(0) = \hat{R}_{xx}^{-1}(0)\hat{r}_{xd}(0) = \frac{1}{\varepsilon_0}I\hat{r}_{xd}(0)$.

The RLS algorithm converges about an order of magnitude faster than the LMS algorithm if $SINR$ is high. It requires a reference signal. More discussion on the RLS algorithm can be found in [83], [86], [84] and [9]. Computer simulation study of RLS, LMS, and SMI algorithms in mobile communication situations suggests that the former outperforms the latter two in flat fading channels [85]. An application of the RLS algorithm for the reverse link of a cellular communication using the CDMA system is considered in [71] to show an increase in channel capacity by an adaptive array.

1.5.4 Constant Modulus Algorithm (CMA)

Many adaptive beamforming algorithms are based on minimizing the error between a reference signal and the array output. The reference signal is typically a training sequence used to *train* the adaptive array or a desired signal based upon an a priori knowledge of nature of the arriving signals. In the case where a reference signal is not available one must resort to an assortment of optimization techniques that are *blind* to the exact content of the incoming signals [1].

Many wireless communication and radar signals are frequency-or phase-modulated signals. Some examples of phase and frequency modulated signals are FM, PSK, FSK, QAM, and polyphase. This being the case, the amplitude of the signal should ideally be a constant. Thus the signal is said to have a constant magnitude or *modulus*. However, in fading channels, where multipath terms exist, the received signal is the composite of all multipath terms. Thus, the channel introduces an amplitude variation on the signal magnitude. Frequency selective channels by definition destroy the constant modulus property of the signal. If it is known that the arriving signals of interest should have a constant modulus, then an algorithms can be devised to restore or equalize the amplitude of the original signal [1].

The CMA is a blind adaptive algorithm proposed by Dominique Goddard [63] and by Treichler and Agee [64]. It requires no previous knowledge of the desired signal. Instead it exploits the constant or nearly constant amplitude properties of most modulation formats used in wireless communication. By forcing the received signal to have a constant amplitude, CMA recovers the desired signal.

Goddard used a cost function called a dispersion function of order p and, after minimization, the optimum weights are found. The Goddard cost function is given by [1]

$$J(n) = \mathbb{E}[(|y(n)|^p - R_p)^q] \qquad (1.73)$$

where p and q are positive integer and $q = 2$. Goddard showed that the gradient of the cost function is zero when R_p is defined by

$$R_p = \frac{\mathbb{E}[|s(n)|^{2p}]}{\mathbb{E}[|s(n)|^p]} \tag{1.74}$$

where $s(n)$ is the zero-memory estimate of $y(n)$.

The resulting error signal is given by

$$e(n) = y(n)|y(n)|^{p-2}(R_p - |y(n)|^p) \tag{1.75}$$

The weight update equation is given by

$$\bar{w}(n+1) = \bar{w}(n) + \mu e^*(n)\bar{x}(n) \tag{1.76}$$

where

$$e(n) = y(n) - \frac{y(n)}{|y(n)|} \tag{1.77}$$

This error signal can replace the traditional error signal in the LMS algorithm to yield

$$\bar{w}(n+1) = \bar{w}(n) + \mu e^*(n)\bar{x}(n) \tag{1.78}$$

The $p = 1$ case reduces the cost function to the form

$$J(n) = \mathbb{E}[(|y(n)| - R_1)^2] \tag{1.79}$$

where

$$R_1 = \frac{\mathbb{E}[|s(n)|^2]}{\mathbb{E}[|s(n)|]} \tag{1.80}$$

If the output estimate $s(n)$ is scaled to unity, one can write the error signal in (1.75) as

$$e(n) = \left(y(n) - \frac{y(n)}{|y(n)|}\right) \tag{1.81}$$

Thus the weight vector, in the $p = 1$ case, becomes

$$\bar{w}(n+1) = \bar{w}(n) + \mu\left(1 - \frac{1}{|y(n)|}\right) y^*(n)\bar{x}(n) \tag{1.82}$$

The $p = 2$ case reduces the cost function to the form

$$J(n) = \mathbb{E}[(|y(n)|^2 - R_2)^2] \tag{1.83}$$

where

$$R_2 = \frac{\mathbb{E}[|s(n)|^4]}{\mathbb{E}[|s(n)|^2]} \tag{1.84}$$

If the output estimate $s(n)$ is scaled to unity, one can write the error signal in (1.75) as

$$e(n) = y(n)(1 - |y(n)|^2) \tag{1.85}$$

Thus the weight vector, in the $p = 2$ case, becomes

$$\bar{w}(n+1) = \bar{w}(n) + \mu\left(1 - |y(n)|^2\right) y^*(n)\bar{x}(n) \tag{1.86}$$

The $p = 1$ case has been proven to converge much more rapidly than the $p = 2$ case [72]. A similar algorithm was developed by Treichler and Agee [64] and is identical to the Godard case for $p = 2$.

When the CMA algorithm converges, it converges to the optimal solution, but convergence of this algorithm is not guaranteed because the cost function $e(k)$ is not convex and may have false minima [65]. Another potential problem is that if there is more than one strong signal, the algorithm may acquire an undesired signal. This problem can be overcome if additional information about the desired signal is available.

Its application to digital, land mobile radio communication systems using TDMA to compensate for selective fading is studied in [66]. Discussions of hardware implementation of a CMA adaptive array and its BER performance for high-speed transmission in mobile communications may be found in [68] and [67]. Development of CMA for beam-space array signal processing including its hardware realization has been reported in [69]. The results presented in [70] indicate that the beam space CMA is able to cancel interferences arriving from other than the look direction.

CMA is useful for eliminating correlated arrivals and is effective for constant modulated envelope signals such as GMSK and QPSK, which are used in digital communications. However, the algorithm is not appropriate for the CDMA system because of the required power control [71]. Use of CMA to blindly separate co-channel FM signals in mobile communications has been investigated in [73]. A variation referred to as differential CMA reported in [74] has inferior convergence characteristics compared to CMA but may be improved using direction of arrival information to make it operative in beam space [9].

1.6 Direction-of-Arrival Algorithms

As was shown for adaptive beamforming algorithms, the calculation of the direction-of-arrival (DoA) of a signal or interference is of great importance. DoA estimation has also been known as spectral estimation, Angle-of-arrival (AoA) estimation, or bearing estimation [1].

Some of the earliest references refer to spectral estimation as the ability to select various frequency components out of a collection of signals. This concept was expanded to include frequency-wave number problems and subsequently DoA estimation. Bearing estimation is a term more commonly used in the sonar community and is DoA estimation for acoustic problems. Much of the state-of-the-art in DoA estimation has its roots in time series analysis, spectrum analysis, periodograms, eigenstructure methods, parametric methods, linear prediction methods, beamforming, array processing, and adaptive array methods. Some of the more useful materials include a survey paper by Godara [38], spectrum analysis by Capon [75], a review of spectral estimation by Johnson [76], an exhaustive text by Van Trees [77] and a text by Stoica and Moses [78].

DoA algorithms estimate the directions using spectral estimation methods or eigenstructure methods. Spectral estimation methods estimate the DoA by computing the mean power spatial spectrum $P(\theta)$ received by an array as a function of angle of incident (θ) and then determine the local maxima of the computed spatial spectrum. For spatially sampled signals, the discrete Fourier transform (DFT) [79], or the Maximum

Entropy Method (MEM) [80] can be employed [23]. The weight coefficients are updated by the Wiener solution, derived from the estimated spatial spectrum. Examples of spectral estimation based DoA algorithms include: Bartlett, Minimum Variance Distortionless Response (MVDR), Linear Prediction and Maximum Likelihood methods.

Eigenstructure methods are based on partitioning the array correlation eigenvectors into signal and noise subspaces. Examples of eigenstructure methods include: MUltiple SIgnal Classification (MUSIC) and Estimation of Signal Parameters via Rotational Invariance Techniques (ESPRIT). The MUSIC algorithm estimates DoAs in the noise subspace [81], which is defied by the eigenvectors of a covariance matrix of spatially sampled signals. It exploits the orthogonality of the noise subspace with the array correlation matrix. MUSIC has better estimation performance than MEM if the noise subspace is larger for uncorrelated signals than is the signal subspace.
The ESPRIT technique was first proposed by Roy and Kailath [87] in 1989. The goal of ESPRIT is to exploit the rotational invariance in the signal subspace which is created by two arrays with a translational invariance structure.

These spatial-spectral estimation algorithms can be used to obtain optimum or suboptimum weights by using spatial samples at one time instant, i.e. one snapshot. Therefore, if the processing speed is fast enough to track the time variation of channels, these algorithms can be more attractive for a fast-fading channel than the temporal updating algorithms. Most recently, neural networks have also been employed to detect the direction of arrival. Once the neural network is trained offline, multiple signals can be tracked in real time [82][23].

Chapter 2

Cognitive Radio System

2.1 Introduction

This chapter discusses cognitive radios (CR) at length. The chapter is arranged as follows. Section 2.2 defines cognitive radios and discusses the motivations behind the emergence of cognitive radio concept. Section 2.3 briefly looks at software-defined radios, which are the foundations on which cognitive radios are built. Section 2.4 deals with spectrum sensing- which constitute the core component of a cognitive system. The traditional sensing dimensions are described at length. Section 2.5 emphasises the angle spectrum opportunity for further research. The present dissertation exploits this dimension using beamforming smart antenna. Section 2.6 discusses the underlay, overlay and interweave cognitive radio paradigms. Section 2.7 lists some of the potential applications of cognitive radio. Finally, Section 2.8 concludes the chapter by pointing at the major research challenges in cognitive radio system.

2.2 Cognitive Radio

Cognitive radio is an emerging innovative design paradigm of wireless communications systems which aims at exploiting the under-utilized radio frequency (RF) spectrum in dynamically changing environment.

The motivation behind cognitive radio is the scarcity of the available radio frequency spectrum mainly caused by the continuous demand for higher and higher data rates as a result of the evolution from purely voice-only communications to multimedia applications coupled with the exponential increase in wireless devices and users. Most of the available radio spectrum has already been allocated to existing wireless systems, however, and only small part of it can be licensed to new wireless applications. Nonetheless, surveys made by Regulatory bodies in different countries such as the Federal Communications Commission [88] of USA and Ofcom of UK [89] on spectrum utilization has indicated that the actual licensed spectrum is largely under-utilized in vast spatio-temporal dimensions (see Figure 2.1). Some measurements by FCC in the United States has even shown that more than 70% of the allocated spectrum is not utilized [90].

Fixed spectrum licensing is the major factor that leads to inefficient use of the radio spectrum. In the traditional spectrum allocation scheme, the radio spectrum allocated to licensed users cannot be utilized by unlicensed users and applications [91]. This static and inflexible allocation forces traditional wireless systems to operate only on a dedicated

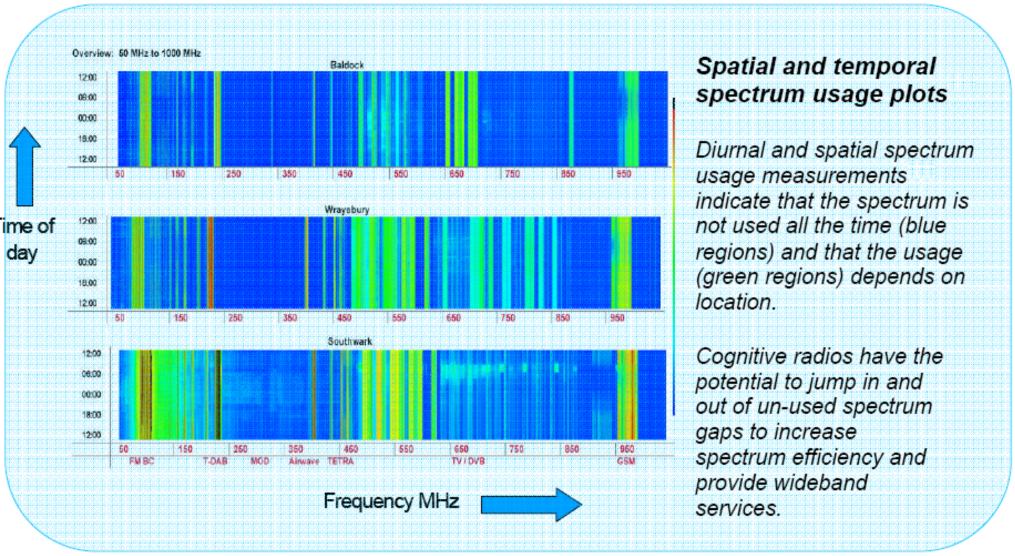

Figure 2.1: Spatial and temporal spectrum usage plot [89].

spectrum band, and cannot allow adaption to the transmission band according to the changing dynamic environment. For example, if a spectrum band is heavily used, the wireless system is not allowed to operate on another more lightly used band.

The licensee authority usually sets the right to access the spectrum. This right is generally defined by frequency, geographic space, transmit power, type of use, and the duration of license. Normally, a license is assigned to one licensee, and the use of spectrum by this licensee must conform to the specification in the license (e.g. maximum transmit power, location of base station). In the current spectrum licensing scheme, the license cannot change the type of use or transfer the right to other licensee. This limits the use of the frequency spectrum and results in low utilization of the frequency spectrum. Essentially, due to the current static spectrum licensing scheme, spectrum holes or spectrum opportunities arise. The limitations in spectrum access due to the static spectrum licensing scheme can be summarized as follows [92]:

- *Fixed type of spectrum usage*: In the current spectrum licensing scheme, the type of spectrum use cannot be changed. For example, a TV band which is allocated to National Television System Committee (NTSC)-based analog TV cannot be used by digital TV broadcast or broadband wireless access technologies. However, this TV band could remain largely unused in many locations due to cable TV systems.

- *Licensed for a large region*: When a spectrum is licensed, it is usually allocated to a particular user or wireless service provider in a large region (e.g. an entire city or state). However, the wireless service provider may use the spectrum only in areas with a good number of subscribers, to gain the highest return on investment. Consequently, the allocated frequency spectrum remains unused in other areas, and other users or service providers are prohibited from accessing this spectrum.

- *Large chunk of licensed spectrum*: A wireless service provider is generally licensed with a large chunk of radio spectrum (e.g. 50 MHz). For a service provider, it may not be possible to obtain license for a small spectrum band to use in a certain area for a short period of time to meet a temporary peak traffic load. For example, a cdma2000 cellular service provider may require a spectrum with bandwidth of 1.25MHz or 3.75MHz to provide temporary wireless access service in a hotspot area.

- *Prohibit spectrum access by unlicensed users*: In the current spectrum licensing scheme, only a licensed user can access the corresponding radio spectrum and unlicensed users are prohibited from accessing the spectrum even though it is unoccupied by the licensed users. For example, in a cellular system, there could be areas in a cell without any users. In such a case, unlicensed users with short-range wireless communications would not be able to access the spectrum, even though their transmission would not interfere with cellular users.

In order to improve the efficiency and utilization of the available spectrum, these limitations are being remedied by modifying the spectrum licensing scheme. The idea is to make spectrum access more flexible by allowing unlicensed users to access the radio spectrum under certain restrictions. Since the legacy wireless systems were designed to operate on a dedicated frequency band, they are not able to utilize the improved flexibility provided by this spectrum licensing scheme. Therefore, the concept of cognitive radio has been introduced. The main goal of cognitive radio is to provide adaptability to wireless transmission through dynamic spectrum access so that the performance of wireless transmission can be optimized, as well as enhancing the utilization of the frequency spectrum [92]. Thus cognitive radio improves the spectrum utilization by seeking and opportunistically utilizing radio resources in time, frequency and space domains on a real time basis [96][97][98].

In cognitive radio terminology, *primary users* can be defined as the users who have higher priority or legacy rights on the usage of a specific part of the spectrum. On the other hand, *secondary users*, which have lower priority, exploit this spectrum in such a way that they do not cause interference to primary users. Therefore, secondary users need to have cognitive radio capabilities, such as sensing the spectrum reliably to check whether it is being used by a primary user, and to change the radio parameters to exploit the unused part of the spectrum [95]. Secondary users and cognitive users are synonymously used.

The major functionalities of a cognitive radio system include *spectrum sensing*, *spectrum management*, and *spectrum mobility*. Through spectrum sensing, the information of the target radio spectrum (e.g. the type and current activity of the licensed user) has to be obtained so that it can be utilized by the cognitive radio user. The spectrum sensing information is exploited by the spectrum management function to analyze the spectrum opportunities and make decisions on spectrum access. If the status of the target spectrum changes, the spectrum mobility function will control the change of operational frequency bands for the cognitive radio users [92].

2.3 Software-Defined Radio

A software-defined radio (SDR) is a reconfigurable wireless communication system in which the properties of carrier frequency, signal bandwidth, modulation, protocol and network access are defined by software and can be controlled dynamically. This adjustability function is achieved by software-controlled signal-processing algorithms. Today's modern SDR also implements any necessary cryptography; forward error correction (FEC) coding;

and source coding of voice, video, or data in software as well [93]. SDR is a key component to implement cognitive radios. The main functions of SDR are as follows [92][94]:

- *Multiband operation*: SDR will support wireless data transmissions over a different frequency spectrum used by different wireless access systems (e.g. cellular band, ISM band, TV band).
- *Multistandard support*: SDR will support different standards (e.g. GSM, WCDMA, cdma2000, WiMAX, WiFi). Also, different air interfaces within the same standard (e.g. IEEE 802.11a, 802.11b, 802.11g, or 802.11n in WiFi standard) can be supported by SDR.
- *Multiservice support*: SDR will support multiple types of services, e.g. cellular telephony or broadband wireless Internet access.
- *Multichannel support*: SDR will be able to operate (i.e. transmit and receive) on multiple frequency bands simultaneously.

2.4 Spectrum Sensing

One of the most important components of the cognitive radio concept, which is implemented based on the SDR, is *spectrum sensing*. It is the essence upon which the entire operation of cognitive radio rests. Spectrum sensing is the task of finding *spectrum holes* by sensing the radio spectrum in the local neighborhood of the cognitive radio receiver in an unsupervised manner. The term 'spectrum holes' stands for those sub-bands of the radio spectrum that are under-utilized in part or full at a particular instant of time and specific geographical location [99].

Spectrum holes are *opportunities*. The definition of opportunity determines the ways of measuring and exploiting the spectrum space [100]. The conventional definition of spectrum opportunity, which is often defined as 'a band of frequencies that are not being used by the primary user of that band at a particular time in a particular geographic area' [101], only exploits three dimensions of the spectrum space: *frequency*, *time*, and *space*. Conventional sensing methods usually relate to sensing the spectrum in these three dimensions.

In the literature a number of different methods were proposed for identifying the presence of signal transmissions in these dimensions. The most common methods are discussed below [100].

2.4.1 Energy Detector Based Sensing

Also known as radiometry or periodogram, is the most common way of spectrum sensing because of its low computational and implementation complexities [102]-[106], [108], [111]-[117], [119]. In addition, it is more generic as receivers do not need any knowledge on the primary users' signal. The signal is detected by comparing the output of the energy detector with a threshold which depends on the noise floor [120]. Some of the challenges with energy detector based sensing include selection of the threshold for detecting primary users, inability to differentiate interference from primary users and noise, and poor performance under low SNR values [119]. Moreover, energy detectors do not work efficiently for detecting spread spectrum signals [121].

Let us assume that the received signal has the following simple form

$$y(n) = s(n) + w(n) \tag{2.1}$$

where $s(n)$ is the signal to be detected, $w(n)$ is the additive white Gaussian noise (AWGN) sample, and n is the sample index. Note that $s(n) = 0$ when there is no transmission by primary user. The decision metric for the energy detector can be written as

$$M = \sum_{n=1}^{N} |y(n)|^2 \tag{2.2}$$

where N is the size of the observation vector. The decision on the occupancy of a band can be obtained by comparing the decision metric M against a fixed threshold λ_E. This is equivalent to distinguishing between the following two hypotheses:

$$\mathcal{H}_0 \;:\; y(n) = w(n), \tag{2.3}$$
$$\mathcal{H}_1 \;:\; y(n) = s(n) + w(n). \tag{2.4}$$

The performance of the detection algorithm can be summarized with two probabilities: probability of detection P_D and probability of false alarm P_F. P_D is the probability of detecting a signal on the considered frequency when it truly is present. Thus, a large detection probability is desired. It can be formulated as

$$P_D = Pr(M > \lambda_E | \mathcal{H}_1) \tag{2.5}$$

P_F is the probability that the test incorrectly decides that the considered frequency is occupied when it actually is not, and it can be written as

$$P_F = Pr(M > \lambda_E | \mathcal{H}_0) \tag{2.6}$$

P_F should be kept as small as possible in order to prevent underutilization of transmission opportunities. The decision threshold λ_E can be selected for finding an optimum balance between P_D and P_F . However, this requires knowledge of noise and detected signal powers. The noise power can be estimated, but the signal power is difficult to estimate as it changes depending on ongoing transmission characteristics and the distance between the cognitive radio and primary user. In practice, the threshold is chosen to obtain a certain false alarm rate [105]. Hence, knowledge of noise variance is sufficient for selection of a threshold.

The threshold used in energy detector based sensing algorithms depends on the noise variance. Consequently, a small noise power estimation error causes significant performance loss [121]. As a solution to this problem, noise level is estimated dynamically by separating the noise and signal subspaces using multiple signal classification (MUSIC) algorithm [133]. Noise variance is obtained as the smallest eigenvalue of the incoming signal's autocorrelation. Then, the estimated value is used to choose the threshold for satisfying a constant false alarm rate. An iterative algorithm is proposed to find the decision threshold in [110]. The threshold is found iteratively to satisfy a given confidence level, i.e. probability of false alarm. Forward methods based on energy measurements are studied for unknown noise power scenarios in [104]. The proposed method adaptively estimates the noise level. Therefore, it is suitable for practical cases where noise variance is not known.

Measurement results are analyzed in [113], [135], [137] using energy detector to identify the idle and busy periods of WLAN channels. The energy level for each global system for mobile communications (GSM) slot is measured and compared in [117] for identifying the idle slots for exploitation. The sensing task in this work is different in the sense that cognitive radio has to be synchronized to the primary user network and the sensing time is limited to slot duration. A similar approach is used in [136] as well for opportunistic exploitation of unused cellular slots. The performance of energy detector based sensing over various fading channels is investigated in [114]. Closed-form expressions for probability of detection under AWGN and fading (Rayleigh, Nakagami, and Ricean) channels are derived. Average probability of detection for energy detector based sensing algorithms under Rayleigh fading channels is derived in [138]. The effect of log-normal shadowing is obtained via numerical evaluation in the same paper. It is observed that the performance of energy-detector degrades considerably under Rayleigh fading.

2.4.2 Waveform-Based Sensing

Known patterns are usually utilized in wireless systems to assist synchronization or for other purposes. Such patterns include preambles, midambles, regularly transmitted pilot patterns, spreading sequences etc. A preamble is a known sequence transmitted before each burst and a midamble is transmitted in the middle of a burst or slot. In the presence of a known pattern, sensing can be performed by correlating the received signal with a known copy of itself [119], [121], [122]. This method is only applicable to systems with known signal patterns, and it is termed as waveform-based sensing or coherent sensing. In [119], it is shown that waveform-based sensing outperforms energy detector based sensing in reliability and convergence time. Furthermore, it is shown that the performance of the sensing algorithm increases as the length of the known signal pattern increases.

Using the same model given in (2.1), the waveform-based sensing metric can be obtained as [119]

$$M = \mathcal{R}e\left[\sum_{n=1}^{N} y(n)s^*(n)\right] \tag{2.7}$$

where $*$ represents the conjugation operation. In the absence of the primary user, the metric value becomes

$$M = \mathcal{R}e\left[\sum_{n=1}^{N} w(n)s^*(n)\right] \tag{2.8}$$

Similarly, in the presence of a primary user's signal, the sensing metric becomes

$$M = \sum_{n=1}^{N} |s(n)|^2 + \mathcal{R}e\left[\sum_{n=1}^{N} w(n)s^*(n)\right] \tag{2.9}$$

The decision on the presence of a primary user signal can be made by comparing the decision metric M against a fixed threshold λ_W.

Measurement results presented in [108] show that waveform-based sensing requires short measurement time; however, it is susceptible to synchronization errors. Uplink packet preambles are exploited for detecting Worldwide Inter-operability for Microwave Access (WiMAX) signals in [122].

2.4.3 Cyclostationarity-Based Sensing

Cyclostationarity feature detection is a method for detecting primary user transmissions by exploiting the cyclostationarity features of the received signals [102], [123], [115]. Cyclostationary features are caused by the periodicity in the signal or in its statistics like mean and autocorrelation [139] or they can be intentionally induced to assist spectrum sensing [140], [141]. Instead of power spectral density (PSD), cyclic correlation function is used for detecting signals present in a given spectrum. The cyclostationarity based detection algorithms can differentiate noise from primary users' signals. This is a result of the fact that noise is wide-sense stationary (WSS) with no correlation while modulated signals are cyclostationary with spectral correlation due to the redundancy of signal periodicities [143]. Furthermore, cyclostationarity can be used for distinguishing among different types of transmissions and primary users [128].

The cyclic spectral density (CSD) function of a received signal (2.1) can be calculated as [139]

$$S(f,\alpha) = \sum_{\tau=-\infty}^{\infty} R_y^{\alpha}(\tau) e^{-j2\pi f \tau} \tag{2.10}$$

where

$$R_y^{\alpha}(\tau) = E[y(n+\tau)y^*(n-\tau)e^{j2\pi\alpha n}] \tag{2.11}$$

is the cyclic autocorrelation function (CAF) and α is the cyclic frequency. The CSD function outputs peak values when the cyclic frequency is equal to the fundamental frequencies of transmitted signal $x(n)$. Cyclic frequencies can be assumed to be known [124], [126] or they can be extracted and used as features for identifying transmitted signals [143].

The OFDM waveform is altered before transmission in [140], [141], [142] in order to generate system specific signatures or cycle-frequencies at certain frequencies. These signatures are then used to provide an effective signal classification mechanism. In [142], the number of features generated in the signal is increased in order to increase the robustness against multipath fading. However, this comes at the expense of increased overhead and bandwidth loss. Even though the methods given in [140] and [141] are OFDM specific, similar techniques can be developed for any type of signal [144]. Hardware implementation of a cyclostationary feature detector is presented in [145].

2.4.4 Radio Identification Based Sensing

A complete knowledge about the spectrum characteristics can be obtained by identifying the transmission technologies used by primary users. Such an identification enables cognitive radio with a higher dimensional knowledge as well as providing higher accuracy [118]. For example, assume that a primary user's technology is identified as a Bluetooth signal. Cognitive radio can use this information for extracting some useful information in space dimension as the range of Bluetooth signal is known to be around 10 meters.

In radio identification based sensing, several features are extracted from the received signal and they are used for selecting the most probable primary user technology by employing various classification methods. In [146], features obtained by energy detector based methods are used for classification. These features include amount of energy detected and its distribution across the spectrum. Channel bandwidth and its shape are used in [147] as reference features. Channel bandwidth is found to be the most discriminating parameter among others. For classification, radial basis function (RBF) neural network is employed. Operation bandwidth and center frequency of a received signal are extracted using energy detector based methods in [118]. These two features are fed to a Bayesian classifier for determining the active primary user and for identifying spectrum opportunities. The standard deviation of the instantaneous frequency and the maximum duration of a signal are extracted using time-frequency analysis in [130] and neural networks are used for identification of active transmissions using these features. Cycle frequencies of the incoming signal are used for detection and signal classification in [129]. Neural network are utilized for classification in [143] while statistical tests are used in [124].

2.4.5 Matched-Filtering

Matched-filtering is known as the optimum method for detection of primary users when the transmitted signal is known [148]. The main advantage of matched filtering is the short time to achieve a certain probability of false alarm or probability of missdetection [149] as compared to other methods that are discussed in this section. In fact, the required number of samples grows as $O(1/SNR)$ for a target probability of false alarm at low SNRs for matched-filtering [149]. However, matched-filtering requires cognitive radio to demodulate received signals. Hence, it requires perfect knowledge of the primary users signaling features such as bandwidth, operating frequency, modulation type and order, pulse shaping, and frame format. Moreover, since cognitive radio needs receivers for all signal types, the implementation complexity of sensing unit is impractically large. Another disadvantage of match filtering is large power consumption as various receiver algorithms need to be executed for detection.

2.4.6 Other Sensing Methods

Other alternative spectrum sensing methods include multitaper spectral estimation, wavelet transform based estimation, Hough transform, and time-frequency analysis.

Multitaper spectrum estimation is proposed in [97]. The proposed algorithm is shown to be an approximation to maximum likelihood PSD estimator, and for wideband signals, it is nearly optimal. Although the complexity of this method is smaller than the maximum likelihood estimator, it is still computationally demanding. Random Hough transform of received signal is used in [134] for identifying the presence of radar pulses in the operating channels of IEEE 802.11 systems. This method can be used to detect any type of signal with a periodic pattern as well. Statistical covariance of noise and signal are known to be different. This fact is used in [150] to develop algorithms for identifying the existence of a communication signal. Proposed methods are shown to be effective to detect digital television (DTV) signals.

In [131], wavelets are used for detecting edges in the PSD of a wideband channel. Once the edges, which correspond to transitions from an occupied band to an empty band or vice versa, are detected, the powers within bands between two edges are estimated. Using this information and edge positions, the frequency spectrum can be characterized as occupied or empty in a binary fashion. The assumptions made in [131], however, need to be relaxed for building a practical sensing algorithm. The method proposed in [131] is extended in [132] by using sub-Nyquist sampling. Assuming that the signal spectrum is sparse, sub-Nyquist sampling is used to obtain a coarse spectrum knowledge in an efficient way. Analog implementation of wavelet-transform based sensing is proposed in [151], [152], [153] for coarse sensing. Analog implementation yields low power consumption and enables realtime operation. Multi-resolution spectrum sensing is achieved by changing the basis functions without any modification to sensing circuitry in [151]. Basis function is changed by adjusting the wavelets pulse width and carrier frequency. Hence, fast sensing is possible by focusing on the frequencies with active transmissions after an initial rough scanning. A testbed implementation of this algorithm is explained in [153].

2.5 The Angle Opportunity

As pointed above, the conventional sensing methods only exploits the three dimensions of the spectrum space, viz., frequency, time, and space. They usually relate to sensing the spectrum in these three dimensions. But there are other dimensions that need to be explored further for spectrum opportunity [100]. For example, the *code* dimension of the spectrum space has not been explored well in the literature. Therefore, the conventional spectrum sensing algorithms do not know how to deal with signals that use spread spectrum, time or frequency hopping codes. Naturally, this brings about new challenges for detection and estimation of this new opportunity.

Similarly, the *angle* dimension has not been exploited well enough for spectrum opportunity. It is assumed that the primary users and/or the secondary users transmit in all directions using omnidirectional antennas. However, with the recent advances in multi-antenna beamforming technologies, multiple users can be multiplexed into the same channel at the same time in the same geographical area. In other words, an additional dimension of spectral space can be created as opportunity. This new dimension also creates new opportunities for spectral estimation. *It is to be noted that angle dimension is different than geographical space dimension. In angle dimension, a primary and a secondary user can be in the same geographical area and share the same channel. However, geographical space dimension refers to physical separation of radios in distance.* [100]

To exploit the angle dimension spectrum opportunity, the primary and/or secondary users must be equipped with a beamforming smart antenna. Figure 2.2 summarizes the various spectrum opportunities.

The present dissertation is aimed at further exploring the angle spectrum opportunity using beamforming smart antenna in a fading environment.

2.6 Cognitive Radio Paradigms

A cognitive radio is an intelligent wireless communication device that exploits side information about its environment to improve spectrum utilization. This side information typically comprises knowledge about the activity, channels, codebooks, and/or messages of other nodes with which the cognitive node shares the spectrum. Based on the nature of the available side information as well as *a priori* rules about spectrum usage, cognitive radio systems seek to *underlay*, *overlay*, or *interweave* the cognitive radios' signals with the transmissions of noncognitive nodes [154].

The underlay paradigm allows cognitive users to operate if the interference caused to noncognitive users is below a given threshold. In overlay systems, the cognitive radios use sophisticated signal processing and coding to maintain or improve the communication of

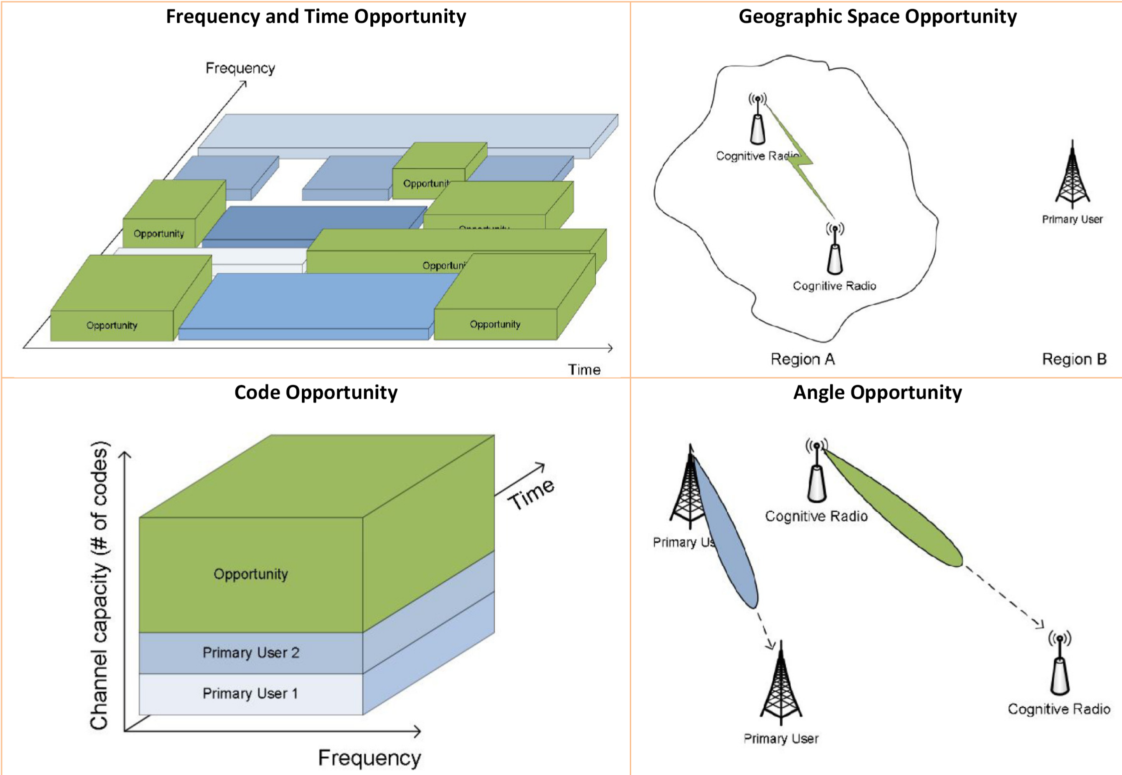

Figure 2.2: Radio Spectrum Space Opportunities [100].

noncognitive radios while also obtaining some additional bandwidth for their own communication. In interweave systems, the cognitive radios opportunistically exploit spectral holes to communicate without disrupting other transmissions [154]. Each of these three paradigms is discussed below in more detail [155].

2.6.1 Underlay Paradigm

The underlay paradigm mandates that concurrent noncognitive and cognitive transmissions may occur only if the interference generated by the cognitive devices at the noncognitive receivers is below some acceptable threshold. The interference constraint for the noncognitive users may be met by using multiple antennas to guide the cognitive signals away from the noncognitive receivers, or by using a wide bandwidth over which the cognitive signal can be spread below the noise floor, then despread at the cognitive receiver.

In general, for underlay CR settings the degradation in terms of quality of service (QoS) to the primary user is a critical aspect. In [154] interference temperature constraints (ITC) [97] were used to measure and limit this effect. In a multiple antenna system, the ITCs are distinguished in soft- and peak power-shaping constraints [156]. These constraints refer to the maximum average power and average peak power tolerated at the primary receivers, respectively. [157] considers the setting of a single secondary user sharing the same spectral band with multiple primary users. The authors provide optimal transmit beamforming strategies under ITCs for the secondary user. Furthermore, [158] characterizes the Pareto boundary of the multiple-input single-output (MISO) interference channel (IFC) through controlling the ITCs at the receivers. Convex optimization techniques for solving CR problems are studied in [159]. The coexistence of a single-input single-output (SISO) primary link and a MISO secondary link is considered in [160], where the achievable secondary rate is optimized under the primary rate constraint, assuming the primary link does not fully load its rate to achieve the Shannon capacity with equality, but there is room that can be exploited by spatial shaping (beamforming) at the secondary transmitter. Moreover, when successive decoding is viable at the secondary receiver, rate splitting at the secondary transmitter increases the achievable secondary rate compared to single-user decoding at the secondary receiver.

Another approach is underlay communication systems based on the Ultra Wide Band (UWB) transmission technology. UWB systems rely on the emission of signals characterized by a low power spectral density spread over a wide bandwidth. UWB signals can be broadly divided in the following two families

- Impulse Radio UWB (IR-UWB), where the large bandwidth required to meet the definition of UWB signal set by regulation authorities is achieved by transmitting short pulses (with typical duration in the order of 1 ns);
- OFDM UWB, where the large bandwidth is obtained by transmitting over a wide set of relatively narrowband subcarriers (e.g. 128 4 MHz sub-bands in the WiMedia standard).

Despite the good coexistence capabilities guaranteed by their spectral properties, UWB devices can still have a significant impact on narrowband systems; extensive studies showed for example the potential impact of UWB signals on GPS receivers, and led to the definition of emission masks that forced UWB devices to adopt extremely low power levels in the GPS band [161], [162]. Coexistence capabilities of UWB devices can however be significantly improved by taking advantage of spectrum shaping techniques combined with spectrum sensing, leading to UWB systems that adapt to the interference environment by sculpting the spectrum so to limit or avoid emissions in spectrum bands used by narrowband systems. Both spectrum sensing and spectrum shaping techniques depend of course on the specific characteristics of the selected UWB signal (IR vs. OFDM).

In the case of IR UWB signals the spectrum shaping can be achieved by acting on two key signal components: the code (typically, but not necessarily, a Time Hopping code adopted in combination with a Pulse Position Modulation scheme) or the pulse shape adopted at the transmitter. It can in fact be shown that the Power Spectral Density of the transmitted signal can be written as follows [163], [164]:

$$P_s(f) = \frac{1}{T_s} C(f) |P(f)|^2 P_x(f) \tag{2.12}$$

where T_s is the pulse repetition period adopted in the UWB signal, $C(f)$ is the spectrum associated to the code, $P(f)$ is the spectrum associated to the pulse and $P_x(f)$ is the spectrum associated to the transmitted data x.

Pulse generation in general is a problem widely covered in the literature with respect to implementation efficiency and accuracy, aiming at encoding information in the pulse shape itself [165], [165]. Moving to the specific problem of addressing coexistence issues by means of pulse shaping, several algorithms for selecting the best pulse shape given external constraints set by regulation and/or interference profiles were proposed in the literature. In [167] an algorithm for the generation of the pulse to be adopted in a Time-Hopping Impulse Radio UWB system was proposed, where a linear combination of pulses obtained as the derivatives of the Gaussian pulse was introduced. A heuristic approach was proposed to determine the values of the coefficients, based on the definition of a emission mask to be met by the transmitted pulse, the mask being the result of constraints imposed by the regulation (e.g., avoiding the GPS band) or resulting from the presence of other wireless services, (e.g. WiMax). The algorithm proposed in [167] generates linear combinations of the base pulses and selects the resulting pulse shape that minimizes the quadratic distance from the emission mask.

Authors in [168] face the problem of selecting the pulse by modelling the mask approximation problem as a filter design problem, assimilating the pulse response to a desired FIR filter impulse response. The problem is solved by defining an iterative algorithm based on information exchange between transmitter and receiver that leads to repeatedly execute the Parks-McLellan algorithm for the determination of the required pulse shape, until all constraints set by regulation, interference and synchronization errors are met. In the case of the code, several solutions were proposed in the literature for designing codes that increase the coexistence capabilities of an UWB signal.

Code design adds an additional opportunity to meet coexistence requirements when pulse shaping cannot efficiently be used to address such issue. In [162] authors propose to design the pulse shape so to meet the emission mask set by the FCC, delegating to the code design all additional coexistence constraints, to be met by forcing nulls in the UWB spectrum at frequencies used by other narrowband systems. The code is applied by means of coefficients weighting different Gaussian pulses, so that the coded signal is a weighted sum of such pulses spaced by a pulse repetition period. Authors in [162] show that the proposed approach can be used to generate nulls at desired frequencies while guaranteeing to meet the FCC emission masks.

A different approach was developed in [169], where a spreading code is applied to the phase of the UWB signal, leading to a higher robustness of the UWB link to the presence of narrowband interference by reducing the impact of interferers with carrier frequencies close to the carrier frequency of the UWB link.

Coexistence requirements and capabilities of OFDM-based UWB systems were investigated as well, in light of the definition of the WiMedia industrial standard [170]. MB-OFDM UWB systems provide a clear advantage over IR-UWB in terms of sensing capabilities. The FFT and IFFT blocks used for the generation and reception of the UWB OFDM signals can in fact be adapted in a straightforward manner to be used for spectrum sensing allowing the UWB devices to determine the presence of coexisting systems with a spectral resolution at least equal to the sub-carrier spacing in the UWB signal. Oppositely, sensing in IR-UWB systems can be more difficult due to the impossibility to identify which specific frequencies over the wide bandwidth of the UWB front-end filter are actually affected by interference.

In [171] the authors analyse the problem of coexistence between MB-OFDM UWB signals and WiMax signals in the 3.5 GHz band. A sensing scheme based on the use of the FFT block at the receiver is proposed, and a-priori information on the spectral characteristics of the uplink WiMax signal (based as well on a OFDM transmission scheme) is adopted in order to formulate the decision problem on the presence of such signal. Results show that high accuracy in detection of WiMax signals can be obtained with a few tens of samples, with a miss-detection probability as low as 10^{-6}.

In [172] a similar application scenario is considered, but the analysis extends to impulsive UWB systems as well, including both Time Hopping and Direct Sequence coded UWB signals. Results presented in [172] suggest that MB-OFDM UWB signals lead to lower interference levels to WiMax receivers compared to both TH-IR-UWB and DS-IR-UWB signals.

Finally, in [173], a coexistence scheme between MB-OFDM UWB devices and IEEE 802.11a networks is proposed. The scheme relies on the sensing feature inherently provided by the MB-OFDM physical layer in order to detect the presence of an IEEE 802.11a network (corresponding to the presence of interference over 5 contiguous sub-bands) and proposes the following two solutions in order to improve coexistence

- An adaptive Frequency Hopping scheme that avoids the bands where the affected sub-bands lie;
- In case all bands are affected by interference (making the adaptive FH scheme ineffective), a selective use of sub-bands, aiming at avoiding the sub-bands impacted by the narrowband interference at the price of a slightly reduced data rate.

2.6.2 Overlay Paradigm

Cognitive radio systems that have cooperation with the primary system as key feature are typically denoted as overlay cognitive radio system. In general, spectrum overlay refers to the situation where the primary system changes its transmission strategy to involve the secondary system and to set up cooperation. Cooperation between the primary and secondary system can be established for example on the transmitter side or the receiver side.

Transmit cooperation requires that the secondary system is aware of the primary signal parameters and is capable of decoding and processing primary transmissions. Consider the coexistence of primary and secondary links in the context of an overlay cognitive radio system, where the secondary users try to communicate without disturbing the incumbent primary users. In some scenarios it is reasonable to assume that the secondary transmitter has access to the message sent by the primary transmitter in a non-causal fashion. For example, whenever the primary transmitter is much closer to the secondary transmitter than to its intended receiver, the capacity of the channel to the former is much larger than that of the channel to the latter. This allows the secondary transmitter to obtain the message in a fraction of the total transmission time. This channel model is known as the cognitive radio channel or the interference channel (IFC) with degraded message sets [174]-[178]. The additional knowledge allows for a form of asymmetric cooperation between the two transmitters. For example, one possible strategy is to have the secondary transmitter employ part of its resources to help the communication between the primary users, so that their communication is not disturbed or is even improved (e.g. in terms of rates). The remaining resources are used for private communication to the secondary receiver. Moreover, with accurate channel state information, the secondary transmitter can use its knowledge of the interference experienced by the primary receiver (or the secondary receiver) to pre-cancel it, for example using dirty paper coding (DPC) [179]. This strategy was shown to achieve capacity in the weak interference regime in [175] and [176]. In contrast, the capacity of part of the strong interference regime was obtained in [177] using superposition coding and interference decoding. In many scenarios the associated capacity gains over non-cooperative transmission could serve as a motivation for having the primary transmitter share its codebook and message with the secondary transmitter [178].

More often, in a typical setup, the primary and secondary systems agree on a cooperative strategy, and the primary system transfers the required information to the secondary system during an initial transmission phase. In [180], [181], it is suggested that a cognitive radio can learn the primary message by overhearing primary automatic repeat request (ARQ) transmissions and utilize knowledge of the message to perform spectrum overlay during retransmissions of the primary system. As an alternative [182] and [183] consider explicit cooperation of the primary and secondary systems. In any case, learning the primary message requires the secondary transmitter to be passive for certain duration in time, and it leads therefore inevitably to a rate loss for the secondary system which may lower the attractiveness of overlay strategies. A cooperative transmission (for example using distributed multiple-antenna/space-time and channel coding techniques) is then carried out in a second phase. Depending on the chosen communication strategy the primary receiver may or may not be changed. The primary system potentially gains diversity, throughput, or coverage through this cooperation and can save energy. The secondary system on the other hand can utilize the cooperative transmission for its own purpose and embed own data in the cooperative transmission. A secondary transmitter can for example compensate for and control the interference due to embedded secondary data by spending additional power for the message of the primary system, by using (multiple-antenna) interference cancelation techniques, or by combining both strategies. In this way, secondary transmit opportunities are created. Since the effectiveness of transmitter cooperation is limited by the first initial transmission phase, transmit cooperation is mostly relevant if the primary and secondary transmitters are close and can transfer the primary's message effectively using high transmission rates and low transmit powers.

Receive cooperation can be an alternative strategy if the primary and secondary receivers are close to each other such that they can establish efficient communication among them. In receive cooperation, the secondary system after decoding its own message can forward side information to the primary system. This side information can contain additional information on the secondary's message which then allows the primary system to decode and cancel out the interference from the secondary, or it can forward a compressed version of its residual signal after decoding, which can be used by the primary receiver to enhance the signal-to-noise-and-interference ratio for the desired signal component. Receiver cooperation can essentially provide the same benefits as transmit cooperation; however, it requires a modification of the primary's receiver while the primary transmitter can (but needs not to) be ignorant to the cooperation.

2.6.3 Interweave Paradigm

An interweave cognitive radio is an intelligent wireless communication system that periodically monitors the radio spectrum, intelligently detects occupancy in the different parts of the spectrum, and then opportunistically communicates over spectrum holes with minimal interference to the active user. Cognitive user transmits simultaneously with a non-cognitive user only in the event of a false spectral hole detection. Cognitive user's transmit power is limited by the range of its spectral hole sensing.

In the case of interweave cognitive radio systems, secondary users utilize vacant primary users spectrum for their own communication purposes. This accentuates the necessity of reliable detection of the available spectrum currently not utilized by any primary user. Inaccurate detection can result in excessive interference to the primary user systems and can severely affect their performance. A possible method for vacant spectrum (i.e. primary user absence) detection is spectrum sensing that utilizes techniques which strongly rely on signal processing. There are several spectrum sensing techniques, which differ according to the amount of needed a priori information for proper operation, implementation complexity, accuracy etc.

There are numerous factors affecting the spectrum sensing reliability. The most essential ones are real-time operation and robustness to channel variations depending on the device performance and the channel state. The sensing period and the computational complexity have a strong influence on the real-time sensing capabilities, e.g. long sensing periods or methods with higher computational complexity increase the detection performance, but decrease the real-time operation. The robustness to channel variations is mainly influenced by the impact of the noise and the fading, which may affect the reliability and the performance of the spectrum sensing techniques. Many solutions propose to mitigate the negative noise and fading effects by introducing complex signal processing techniques as well as cooperation between multiple sensing devices.

As already elaborated, real-time operation is a vital reliability factor of any spectrum sensing technique which is tightly correlated with its detection performance. For example, in the case of AWGN channel, the detection performance of the conventional energy based detector [184], which uses only the power of the received samples, increases when the number of sensed samples increases

$$P_D = Q_{N/2}(\sqrt{N_\gamma}, \sqrt{\lambda_E/2}) \tag{2.13}$$

$$P_F = \frac{\Gamma(N/2, \lambda_E/2)}{\Gamma(N/2)} \tag{2.14}$$

where P_D, P_F, N, γ and λ_E represent the probability of detection, probability of false alarm, number of sensed samples, channel SNR and SNR threshold, respectively, while $Q_{N/2}(\cdot,\cdot), \Gamma(\cdot)$ and $\Gamma(\cdot,\cdot)$ denote the generalized Marcum Q-function, Gamma and incomplete Gamma functions, respectively. Equation 2.14 shows that higher number of sensed samples can be obtained either when increasing the sensing time or the sampling frequency of the device

$$N = T_s f_s \tag{2.15}$$

where T_s and f_s, denote the sampling frequency and the sensing time, respectively. Hence, the spectrum sensing techniques cannot use very long sensing periods in order to stay in the boundaries of real-time operation. The same conclusions, about the real-time operation, can be made for all types of energy based detectors (e.g. eigenvalue detector, Higher Order Statistics - HOS detector etc.).

In the case of feature detection techniques, the real-time operation reliability factor is also related to the sensing time and the computational complexity. Longer observation times usually result in higher reliability since the feature based sensing techniques exploit the correlation properties of the primary user signal type. However, [141] proves that the length of the sensing time of a cyclostationarity based detector, needed for reliable primary detection, is significantly small and satisfies the real-time requirements. On the other hand, the computational complexity can have a significant impact on the real-time performance of feature based spectrum sensing techniques. Due to the complex mathematical operations, these spectrum sensing techniques require devices with high processing power. Compared to the energy based, feature based techniques prove to struggle more in terms of the real-time reliability factor.

As previously mentioned, another essential reliability factor of the spectrum sensing techniques is the robustness to channel variations in terms of noise and fading. It is proven that in noisy environments the conventional energy detection underperforms due to the noise uncertainty [155]. In this case, if the noise level is not precisely known, the detection becomes impossible for low signal levels. More sophisticated energy based detection techniques (e.g. eigenvalue detector, HOS detector etc.), feature based detectors, as well as cooperative spectrum sensing techniques overcome the noise uncertainty problem and provide reliable performance in cases of highly noised channels.

There are many incumbent primary communication systems (e.g. DTV, radar, DME etc.) which implement sparse frequency planning with large interference margins. This leads to an underutilization of frequency spectrum in a given geographic area and a secondary user operating on a vacant frequency spectrum chunk at relatively low power level would not need a great separation from co-channel and adjacent channel primary users to avoid causing interference. This opportunistic operation of secondary users in the interleaved spectrum holes is conditioned on their ability to avoid harmful interference to licensed primary users of these bands. Therefore, the secondary users must be aware of the geographical and frequency characteristics of the primary system within the area of current location. However, the secondary users must also incorporate certain regulatory rules which govern the particular frequency band and geographical location.

For example, the FCC rules [185][186][187] define a fixed permitted maximum transmit power for different types of TV white space devices. The maximum Equivalent Isotropicaly Radiated Power (EIRP) for a fixed TV white space device with an antenna height below 30 m is 39 dBm. For a mobile device, the EIRP limit is 20 dBm. There is an additional protection distance in which white space devices are not allowed to operate at all on the same channel around each TV transmitter coverage area. Outside this area, the permitted transmit power immediately goes up to the maximum allowed value. The FCC rules also forbid white space device usage in the first adjacent channel to an occupied DTV channel, but in this case the protection distance is smaller. For a white space device with antenna height between 10 m and 30 m, the added co-channel protection zone is 14.4 km and the adjacent channel protection zone is 0.74 km. Beyond the first adjacent channel there are no limitations from the viewpoint of one particular transmitter.

On the other hand, the ECC rules [188] allowed secondary users to transmit at different power levels based on their distance to the coverage area. The protection principle is implemented as a boundary condition of the maximum transmission power. The method developed by SE43 calculates the permitted maximum transmit power for a white space device at a given location. The calculation lays on the given permitted degradation of location probability for TV reception. Furthermore, the ECC has left specification of white space device spectrum masks to manufactures, while FCC has prescribed stringent masks.

2.7 Potential Applications of Cognitive Radio

Cognitive radio concepts can be applied to a variety of wireless communications scenarios, a few of which are described below [92]:

- *Next generation wireless networks*: Cognitive radio is expected to be a key technology for next generation heterogeneous wireless networks. Cognitive radio will provide intelligence to both the user-side and provider-side equipments to manage the air interface and network efficiently. At the user-side, a mobile device with multiple air interfaces (e.g. WiFi, WiMAX, cellular) can observe the status of the wireless access networks (e.g. transmission quality, throughput, delay, and congestion) and make a decision on selecting the access network to connect with. At the provider-side, radio resource from multiple networks can be optimized for the given set of mobile users and their QoS requirements. Based on the mobility and traffic pattern of the users, efficient load balancing mechanisms can be implemented at the service provider's infrastructure to distribute the traffic load among multiple available networks to reduce network congestion.

- *Coexistence of different wireless technologies*: New wireless technologies are being developed to reuse the radio spectrum allocated to other wireless services (e.g. TV service). Cognitive radio is a solution to provide coexistence between these different technologies and wireless services. For example, IEEE 802.22-based WRAN users can opportunistically use the TV band when there is no TV user nearby or when a TV station is not broadcasting [189]. Spectrum sensing and spectrum management will be crucial components for IEEE 802.22 standard-based WRAN technology to avoid interference to TV users and to maximize throughput for the WRAN users.

- *eHealth services*: Various types of wireless technologies are adopted in health care services to improve efficiency of the patient care and health care management. However, using wireless communication devices in health care application is constrained by EMI (electromagnetic interference) and EMC (electromagnetic compatibility) requirements. Since the medical equipments and biosignal sensors are sensitive to EMI, the transmit power of the wireless devices has to be carefully controlled. Also, different biomedical devices (e.g. surgical equipment, diagnostic and monitoring devices) use RF transmission. The spectrum usage of these devices has to be carefully chosen to avoid interference with each other. In this case, cognitive radio concepts can be applied. For example, many wireless medical sensors are designed to operate in the ISM (industrial, scientific, and medical) band, which can use cognitive radio concepts to choose suitable transmission bands to avoid interference.

- *Intelligent transportation system*: Intelligent transportation systems (ITS) will increasingly use different wireless access technologies to enhance the efficiency and safety of transportation by vehicles. Two different types of communications scenarios arise in an ITS system vehicle-to-roadside (V2R) communication and vehicle-to-vehicle (V2V) communication. In vehicle-to-roadside communications, information is exchanged between the roadside unit (RSU) and the onboard unit (OBU) in a vehicle. In vehicle-to-vehicle communications, a special form of ad hoc network, namely, a vehicular ad hoc network (VANET), is formed among vehicles to exchange safety-related information. High mobility of the vehicles and rapid variations in network topologies pose significant challenges to efficient V2R and V2V communications. Cognitive radio concepts can be used in both OBUs and RSUs so that they can adapt their transmissions to cope with the rapid variations in the ambient radio frequency environment [190]. With multi-radio capabilities at the OBUs, they should be able to adaptively choose the radio to communicate with the RSUs.

- *Emergency networks*: Public safety and emergency networks can take advantage of the cognitive radio concepts to provide reliable and flexible wireless communication. For example, in a disaster scenario, the standard communication infrastructure may not be available, and therefore, an adaptive wireless communication system (i.e. an emergency network) may need to be established to support disaster recovery. Such a network may use the cognitive radio concept to enable wireless transmission and reception over a broad range of the radio spectrum.

- *Military networks*: With cognitive radio, the wireless communication parameters can be dynamically adapted based on the time and location as well as the mission of the the soldiers. For example, if some frequencies are jammed or noisy, the cognitive radio transceiver can search for and access alternative frequency bands for communication. Also, location-aware cognitive radio can control the transmitted waveform in a particular region to avoid interference to the high priority military communication systems [191].

2.8 Research Challenges in Cognitive Radio

Research in cognitive radio poses a number of challenges. Below are some of the major challenges [92].

2.8.1 Issues in Spectrum Sensing

Spectrum sensing gives rise to several physical and media access control (MAC) layer research issues. While the physical layer issues are mostly related to signal processing, the MAC layer issues are related to optimization of spectrum sensing.

- *Sensing interference limit*: One objective of spectrum sensing, especially for interference-based sensing, is to obtain the status of the spectrum (i.e. idle/occupied), so that the spectrum can be accessed by an unlicensed user under the interference constraint. The challenge lies in the interference measurement at the licensed receiver caused by transmissions from unlicensed users. First, an unlicensed user may not know exactly the location of the licensed receiver which is required to compute interference caused due to its transmission. Second, if a licensed receiver is a passive device, the transmitter may not be aware of the receiver.

- *Spectrum sensing in multiuser networks*: Multiple users, both licensed and unlicensed, may share the radio spectrum in a network. Also, multiple networks can coexist for which transmissions in one network may interfere with transmissions in other networks. In such a case, coordinated and cooperative spectrum sensing would be preferred since it can detect the spectrum access status by the licensed users in different locations in the network. The spectrum sensing information can be used to obtain a spectrum map which can be utilized by the unlicensed users to make spectrum access decisions.

- *Optimizing the period of spectrum sensing*: In spectrum sensing, the longer the observation period, the more accurate will be the spectrum sensing result. However, during sensing, a single-radio wireless transceiver cannot transmit in the same frequency band. Consequently, a longer observation period will result in lower system throughput (Figure 2.3). This performance tradeoff can be optimized to achieve an optimal spectrum sensing solution. If the accuracy of spectrum sensing is low, collision and interference to the transmissions by licensed users could occur to degrade the performances of both licensed and unlicensed users. Classical optimization techniques (e.g. convex optimization) can be applied to obtain the optimal solution.

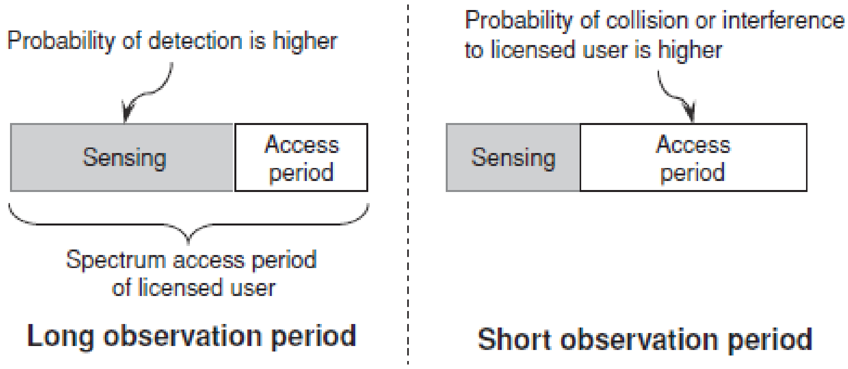

Figure 2.3: Tradeoff between spectrum sensing time and user throughput. [92].

- *Spectrum sensing in multichannel networks*: Multichannel transmission (e.g. OFDM-based transmission) would be typical in a cognitive radio network. However, the number of available channels would be larger than the number of available interfaces at the radio transceiver. Therefore, only a fraction of the available channels can be sensed simultaneously. Selection of the channels (among all available channels) to be sensed will affect the performance of the system. For spectrum sensing, a channel which is mostly occupied by the licensed user(s) should be less preferred to a channel which is occasionally occupied. In a multichannel environment, selection of the channels should be optimized for spectrum sensing to achieve the optimal system performance under hardware constraints at the cognitive radio transceiver.

2.8.2 Spectrum Management Issues

The main objective of spectrum management is to observe and control access to the spectrum holes by the unlicensed users. The research issues in spectrum management are related to spectrum analysis and spectrum access decisions.

- *Issues in spectrum analysis*: Based on the spectrum sensing result, spectrum analysis is performed to estimate spectrum quality. One of the issues here is how to quantify the quality of the spectrum opportunity which can be accessed by an unlicensed user. This quality can be characterized by the signal-to-noise ratio (SNR), the average duration and correlation of the availability of spectrum holes. The information about this spectrum quality available to a cognitive radio user can be imprecise and noisy. Learning algorithms from artificial intelligence is one of the candidate techniques that can be used by the cognitive radio users for spectrum analysis.

- *Issues in the spectrum access decision*: Some of the research issues related to the spectrum access decision of an unlicensed user are described below:
  - *Decision model*: A decision model is required for spectrum access. The complexity of this decision model depends on the parameters considered during spectrum analysis (e.g. the average duration of spectrum holes and the SNR of the target frequency band) as well as the utility of the cognitive user obtained through accessing the spectrum holes. The decision model becomes more complex when an unlicensed user has multiple objectives. For example, an unlicensed user may intend to maximize its throughput while minimizing the interference caused to the licensed user. Stochastic optimization methods (e.g. the Markov decision process) will be an attractive tool to model and solve the spectrum access decision problem in a cognitive radio environment.
  - *Competition/cooperation in a multiuser environment*: When multiple users (both licensed and unlicensed users) are in the system, their preference will affect the spectrum access decision. These users can be cooperative or non-cooperative in accessing the spectrum.

    In a non-cooperative environment, each user has its own objective, while in a cooperative environment, all users can cooperate to achieve a single objective (Figure 2.4). For example, multiple unlicensed users may compete with each other to access the radio spectrum (e.g. O1, O2, O3, and O4 in Figure 2.4) so that their individual throughput is maximized. During this competition between unlicensed users, all of them have to ensure that the interference caused to the licensed user(s) is maintained below the corresponding interference temperature limit. Non-cooperative game theory is the most suitable tool to obtain the equilibrium solution for the spectrum access problem in such a scenario. This equilibrium solution would guarantee that none of the users will unilaterally deviate to achieve higher payoff (which could degrade the payoff of other users).

    In a cooperative environment, the cognitive radios cooperate with each other to make the spectrum access decision to maximize a common objective function under given constraints. In such a scenario, a central controller may coordinate the spectrum management. Alternatively, the cognitive radios can communicate among themselves in a distributed manner and a mechanism for information exchange, negotiation, and synchronization would therefore be required.
  - *Distributed implementation of spectrum access control*: In a distributed multiuser environment, for non-cooperative spectrum access, each user can reach an optimal decision independently by observing the historical behavior/action of other users in the system. Therefore, a distributed algorithm is required for an unlicensed user to make the decision on spectrum access autonomously. The stability and convergence property of the distributed algorithm needs to be evaluated to ensure that it achieves the desired solution for an unlicensed user.

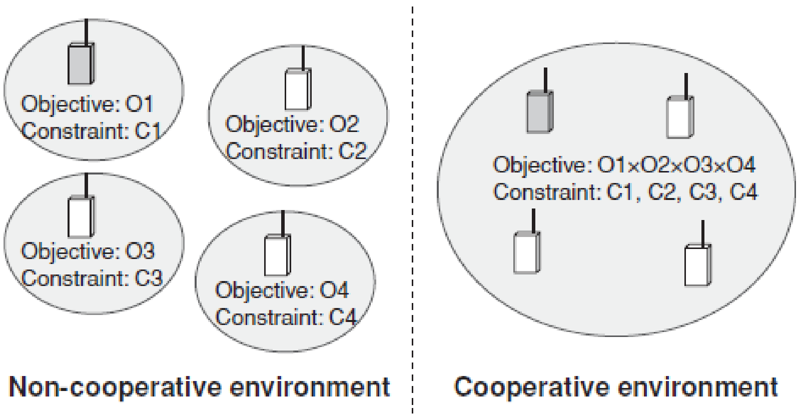

Figure 2.4: Cooperative and non-cooperative spectrum access. [92].

2.8.3 Spectrum Mobility Issues

The spectrum mobility functions in a cognitive radio network allow an unlicensed user to change its operating spectrum dynamically based on the spectrum condition. The research issues in spectrum mobility relate to switching between available frequency bands to provide smooth spectrum access without interruption to both application and service due to the change in the radio environment.

- *Search for the best frequency bands*: A cognitive radio must keep track of available frequency bands so that if necessary (e.g. a licensed user is detected), it can switch immediately to other frequency bands. During transmission by an unlicensed user, the condition of the frequency band has to be observed. In a similar way to spectrum sensing, this would of course incur some overhead. The observation can be performed in a proactive manner or in an on-demand basis [192]. In the proactive approach, the condition of the available channels is periodically observed and the knowledge about these channels is continuously updated. When a spectrum handoff is required, this knowledge can be used by an unlicensed user to switch to a new frequency band. In contrast, with an on-demand approach, channel observation can be performed only when an unlicensed user needs to switch the channel. While the proactive approach incurs a larger overhead due to periodic observation, the latency of spectrum handoff would be smaller in this case.

- *Protocol stack adaptation*: Since the latency due to spectrum handoff could be high, the modification and adaptation of other components in the protocol stack are required. For example, when an unlicensed user switches channel, the transmission control protocol (TCP) timer at the transport layer can be frozen to avoid any mis-interpretation of the delay incurred for the acknowledgement message. A cross-layer optimized framework for protocol adaptation has to be developed to cope with spectrum mobility.

- *Self-coexistence and synchronization*: When an unlicensed (or secondary) user performs spectrum handoff, two issues have to be taken into account. First, the target channel must not currently be used by any other secondary user (i.e. the self-coexistence requirement), and the receiver of the corresponding secondary link must be notified of the spectrum handoff (i.e. the synchronization requirement). For the self-coexistence issue, a spectrum broker can be used to manage spectrum allocation.

However, this issue becomes challenging when such a broker is not available in the system. For synchronization, the MAC protocol must be designed with provision for spectrum handoff information exchange.

2.8.4 Network Layer and Transport Layer Issues

The major issue in the network layer is the design of the routing protocol for multihop cognitive radio networks. The routing algorithm needs to be integrated with spectrum management in order to improve the overall system performance. It was observed that the performance of the cross-layer approach is much better than the performance of the decoupled approach for which routing algorithm and spectrum management perform separately [193][194]. In the cross-layer approach, the routing algorithm (e.g. dynamic source routing (DSR)) considers the spectrum allocation in each hop. In the decoupled approach [195], the shortest-path and spectrum sharing algorithms are performed independently. Although integration of routing algorithms and spectrum management can achieve better performance, many issues related to routing in the network layer remain to be investigated.

- *Message broadcasting mechanism*: Given the routing metric, a routing algorithm requires information exchange among the network nodes to choose the best route. However, since in a cognitive radio network a common channel for this information exchange may not be available, an efficient message broadcasting mechanism based on dynamic spectrum access would be required.

- *Routing metrics and route selection*: Due to the activity of licensed users, connectivity between the nodes of unlicensed users can be dynamically changed. Also, the routing metric has to be jointly defined based on network parameters (e.g. hop-counts and link quality) and spectrum management parameters (e.g. interference to licensed users and the average number of available channels). For example, in Figure 2.5, unlicensed user 1 may require to use the route through users 2 and 4 to the destination user 5 for which the number of hops is more than that of the route through user 3 (i.e. three hops versus two hops).This is because using the shorter route may cause interference to the licensed user. However, during periods when the licensed transmitter is inactive, the route through unlicensed user 3 can be selected.

In the transport layer, modifications have to be made to TCP and user datagram protocol (UDP) working in a cognitive radio environment to avoid performance degradation [196]. Congestion control in TCP depends on the packet loss rate and the round-trip-time (RTT). With a wireless link, a TCP sender could mis-interpret packet loss due to wireless error as a sign of congestion. As a result, congestion avoidance and slow start mechanisms would be invoked. Some variants of TCP were proposed to cope with this problem in a wireless environment. For example, an indirect-TCP (I-TCP) splits a connection of wireless link from the wired link, so that each TCP connection can be optimized for wireless and wired networks, respectively.

In cognitive radio networks, many factors such as the transmit power, the bandwidth of the spectrum hole, and the interference level can affect the packet loss rate. Similarly, RTT can be affected by the delay due to spectrum sensing and spectrum handoff, for which when the current channel becomes unusable for an unlicensed user, the unlicensed user has to search for a new channel. Therefore, the transport layer protocol has to consider these effects to optimize end-to-end rate control.

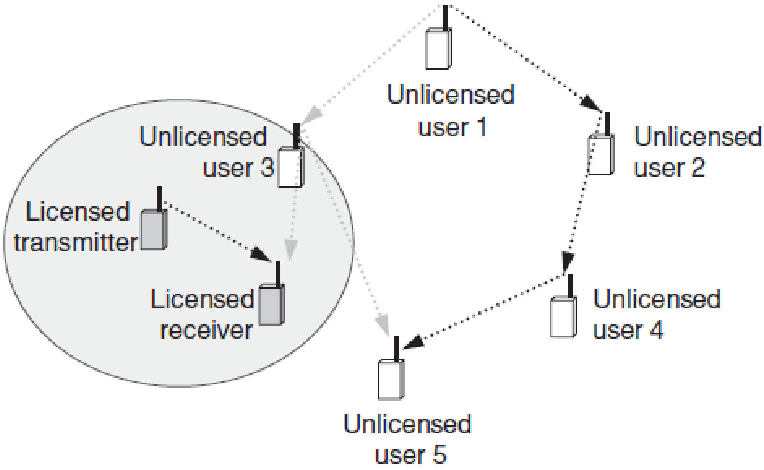

Figure 2.5: Routing in the presence of licensed users. [92].

2.8.5 Cross-layer Design for Cognitive Radio Networks

Communication systems are usually designed based on a layered architecture. The layered architecture promotes the modularity, standardization, and expandability of the system. Since the communication functionalities are separated into different layers, with those that are closely related grouped in one layer, each of the layers can be designed independently. In addition, the components in each layer can be updated, changed, and expanded independently without any side effect on other components. The layered structure provides explicit abstraction of the functions in each layer and supports well defined interfaces between the layers. Therefore, components developed or implemented by different manufacturers can interoperate with each other.

However, since the different components are ordered in the layered structure, each component has to operate sequentially (e.g. a lower layer has to wait until a higher layer has finished processing). This sequential operation results in computational overhead and latency. With the layers being isolated, components in one layer may not be able to access information in other layers. As a result, the interaction among the components in the different layers is limited. The performance of the entire system may therefore not be optimized due to the lack of global information exchange. Also, some components can have redundant functions (e.g. error control and recovery in both MAC and physical layers). Wireless systems with layered protocol structures may lack adaptability with channel variations. Since the interaction between the layers has to be performed only through a standard interface, the communication system may not be able to respond immediately when the radio environment changes. As a result, the overall system performance could be degraded.

Some of the limitations of layered protocol structure in a communication system can be mitigated through cross-layer design and optimization methods [197] [198]. One objective of cross-layer design is to increase the information flow between components in the different layers. Cross-layer optimization aims to improve the overall performance of a communication system through optimization of decision variables and parameters in different layers simultaneously.

An example of cross-layer optimization in cognitive radio networks was presented in

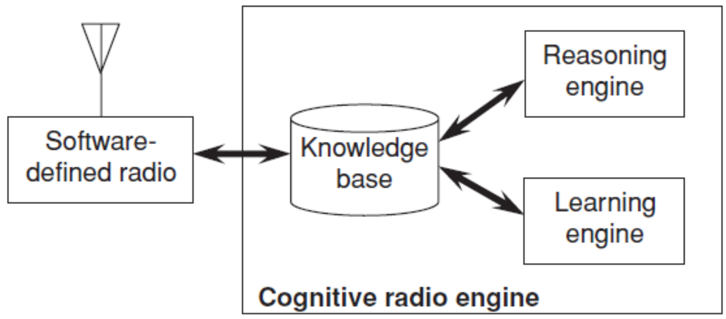

Figure 2.6: Cognitive radio architecture with machine learning [92].

[199]. In a cognitive radio environment, the information gathered (e.g. signal quality) by a cognitive radio could often be imprecise. Therefore, the radio interface and protocols in a cognitive radio have to be designed to process noisy and inaccurate information. In [163], fuzzy logic was used as a solution to process imprecise information in a cognitive radio environment using the concept of cross-layer design.
Using a fuzzy logic controller can reduce the complexity of the system. Specifically, using predefined rules for fuzzification and defuzzification processes in a fuzzy logic-based system often reduces the computational complexity significantly when compared to the complexity of solving an optimization problem in an exact manner.

In a fuzzy logic system, the protocol parameters in the different layers can be modeled as fuzzy variables which can be accessed and modified by the fuzzy controller. The values of these fuzzy variables are classified into fuzzy sets with certain probability. The values of input fuzzy variables can be determined by the fuzzification process applied to the measured values. Then, the fuzzy controller applies the inference rules to the input variables and the defuzzification process is used to obtain the values of output variables which are used to control the protocol parameters.

2.8.6 Artificial Intelligence Approach for Designing Cognitive Radio

Artificial intelligence (AI) techniques for learning and decision making can be applied to design efficient cognitive radio systems [200][201][202]. One example was illustrated in [200], where the concept of machine learning was applied to cognitive radio for capacity maximization and dynamic spectrum access.

The proposed system architecture is shown in Figure 2.6. Here, the knowledge base maintains the states of the system and the available actions [203]. The reasoning engine uses the knowledge base to select the best action. The learning engine performs knowledge manipulation based on the observed information (e.g. information on channel availability, channel error rate). In the knowledge base, two data structures, namely, predicate and action, are defined. The predicate (or inference rule) is used to represent the state of the environment. Based on this state, an action can be performed to change the state so that the system objectives can be achieved. For example, a predicate can be defined as “modulation==QPSK AND SNR==5dB”, while the action can be defined as “decrease modulation mode” with precondition “SNR 8 dB” and postcondition “modulation==BPSK". Given the input(which is obtained from measurement), the reasoning engine matches the current state (e.g. modulation and SNR in this case) with the predicates and determines the predicate results (i.e. true or false). Then, from the set of predicate results, an appropriate action is taken. In the above example, if the current SNR is equal to 5 dB and current modulation is QPSK, the precondition will be true and the predicate will be active. As a result, the cognitive engine will decide to reduce the modulation mode. In this case, the modulation will be changed to BPSK, as stated in the corresponding postcondition.

A learning algorithm is used to update both the state of the system and the available actions according to the radio environment. This update can be done using an objective function (e.g. minimize the bit error rate) with a goal to determine the best action given the input (e.g. channel quality) and the available knowledge. Different learning algorithms can be used in a cognitive radio network (e.g. based on a hidden Markov model [204], neural network [205], reinforcement learning [206], or genetic algorithm [207]).

2.8.7 Location-aware Cognitive Radio

Location information can be used to improve the performance of wireless systems. For example, in mobile cellular networks, the location information of the mobile users can be used to optimally reserve the channels for handoff, e.g. using the concept of shadow cluster [208][209]. Other examples are location-assisted dynamic spectrum management, transceiver algorithm development and optimization (e.g. location-aided adaptive beamforming), and environment characterization (e.g. location-assisted propagation environment identification) [210][211]. The location awareness was also used in the context of a cognitive radio system [212][213]. Two dynamic spectrum access schemes, which were proposed by the FCC to utilize location information for spectrum allocation, are geolocation-database and local beacon [214]. These schemes were proposed for an unlicensed system to access TV bands without interfering with a TV service (i.e. the licensed service).

In a geolocation-database scheme, the licensed services (i.e. TV broadcasters) use location estimation devices (e.g. global positioning system or GPS) to obtain their location information. Then, this information is sent by the licensed service to the FCC central database. This FCC database broadcasts the collected TV band and the location information from the corresponding licensed services to the unlicensed users. Similarly, the unlicensed users also use location estimation devices to obtain their location information. Based on the information from the FCC database and their own location information, the unlicensed users identify available TV bands that they can use without interfering with the licensed services. This step can be performed locally by the unlicensed users. After the unlicensed users determine the TV bands to be used, they submit the request with their location information to the cognitive base station. This cognitive base station allocates the spectrum to the unlicensed users and also reports to the FCC database about the occupancy of the TV bands.

In a similar way to the geolocation-database scheme, a local beacon scheme utilizes the location information to identify the TV bands to be used by the unlicensed users. However, in this scheme, the database is located in a local cell to manage the spectrum allocation. The licensed services report periodically to update their location and TV band information in the local database. The cognitive radio base station broadcasts the geolocation-database to the unlicensed user. The unlicensed user receives this information and uses it to identify available TV bands. Again, its location information is used. The spectrum access plan (e.g. which TV band to access and for how long) is sent to the cognitive radio base station to maintain information on the current spectrum allocation.

Although the proposed dynamic spectrum access can improve the performance of spectrum allocation, there are some issues that need to be addressed. For example, the accuracy of the location information will have an effect on the interference caused to the licensed service, especially when the unlicensed user is located in a place where the geolocation signal cannot be accurately estimated (e.g. indoor). Adaptive position systems based on cognitive radios as proposed in [210] can be applied to mitigate the problem.

Chapter 3

Design of Non-Uniform Antenna Arrays Using Genetic Algorithm

3.1 Introduction

The performance of a single-element antenna is somewhat limited. To obtain high directivity, narrow beamwidth, low side-lobes, point-to-point and preferred-coverage pattern characteristics, etc., antenna arrays are used [7]. An antenna array is an assembly of individual radiating antennas in an electrical and geometrical configuration. Nowadays, antenna arrays appear in wireless terminals and smart antennas, so robust and efficient array design is increasingly becoming necessary.

The design of an array involves mainly the selection of elements and array geometry first, and then the determination of the element excitations required for achieving a particular performance. In antenna arrays, it is frequently desirable to achieve both a narrow beamwidth and a low side-lobe level. In linear antenna arrays, a uniform array (having uniform inter-element spacing and uniform amplitude excitation) yields the smallest beamwidth and hence the highest directivity. It is followed, in order, by the Dolph-Chebyshev and Binomial arrays. In contrast, Binomial arrays usually possess the smallest side-lobes followed, in order, by the Dolph-Chebyshev and uniform arrays.

Binomial and Dolph-Chebyshev arrays are typical examples of non-uniform arrays. Non-uniform linear antenna arrays have uniform inter-element spacing and non-uniform amplitude distributions.

It will be shown that using genetic algorithm it is possible to design a non-uniform linear array that approximates the beamwidth of a uniform array and having smaller side-lobe level than the Dolph-Chebyshev array. The result is that the designed antenna array exhibits the largest directivity as compared to the uniform, Binomial and Dolph-Chebyshev arrays. In the design, the genetic algorithm is employed to generate the excitation amplitudes of the antenna array. Although over the past decades, the theory of antenna array design has been studied in depth and is certainly well documented [7], it is only recently that the applications of genetic algorithms to engineering electromagnetics [215]-[217] and antenna array design and synthesis [218]-[221] have attracted much attention.

This chapter is organized as follows. The problem formulation is presented in Section 3.2. Section 3.3 describes how the genetic algorithm is applied to the problem at hand.

In Section 3.4, some representative numerical results are presented. Finally concluding remarks are made in Section 3.5.

3.2 Problem Formulation

Consider a uniformly spaced linear array of N elements places along the z-axis. Suppose the distance between any two adjacent elements is d and the array is operated at wavelength λ. The array factor is (1.6)

$$AF(\theta) = \sum_{n=1}^{N} a_n e^{j(2\pi nd\cos\theta)/\lambda} \tag{3.1}$$

The feeding coefficient a_n can be written as

$$a_n = |a_n|e^{j\alpha_n} \tag{3.2}$$

where α_n is the phase of the excitation current.

In uniform arrays, the elements have equal amplitude and a constant phase difference between adjacent ones whereas binomial and Dolph-Chebyshev arrays, which are typical examples of non-uniform arrays, have amplitude excitations derived from the binomial series and Chebyshevs polynomials, respectively [7].

As stated above, in antenna system design it is frequently desirable to achieve both a narrow beamwidth and a low side-lobe level [222]. A uniform array yields the smallest beamwidth and the highest directivity. It is followed, in order, by the Dolph-Chebyshev and binomial arrays. In contrast, binomial arrays usually possess the smallest side-lobes followed, in order, by the Dolph-Chebyshev and uniform arrays [7].

Our objective is to design, using GA, a non-uniform linear array that approximates the beamwidth of uniform arrays and produces smaller side-lobe level than that of Dolph-Chebyshev array. The array so designed will posses, as will be shown, the highest directivity than uniform, binomial, and Dolph-Chebyshev arrays.

From Equation (3.1), the array factor for a non-uniform broadside ($\alpha_n = 0$) array is

$$AF(\theta) = \sum_{n=1}^{N} a_n e^{j(2\pi nd\cos\theta)/\lambda} \tag{3.3}$$

where a_n is real.

To design the array, first the number of array elements N and the inter-element spacing d are specified. The genetic algorithm generates N excitation coefficients $(a_1, a_2 \ldots, a_n)$ and forms the non-uniform array factor $AF(\theta)$ (3.3). By successive generation of a_n's through the GA, the desired array factor is made to approximate a hypothetical array factor $AF_h(\theta)$ in some acceptable sense. The array factor $AF_h(\theta)$ is one which, in the region of the main lobe, is the same as a uniform broadside array with the same N and

d, but is zero elsewhere-i.e., with no side-lobes.

$$AF_h(\theta) = \begin{cases} \dfrac{1}{N} \dfrac{\sin\left(\dfrac{\pi N d}{\lambda}\cos\theta\right)}{\sin\left(\dfrac{\pi d}{\lambda}\cos\theta\right)}, & \text{for } \cos^{-1}\left(\frac{\lambda}{Nd}\right) \leq \theta \leq \pi - \cos^{-1}\left(\frac{\lambda}{Nd}\right); \\ 0, & \text{otherwise.} \end{cases} \tag{3.4}$$

Since the required non-uniform array $AF(\theta)$ is to approximate $AF_h(\theta)$, the mean-squared error of the difference between $AF(\theta)$ and $AF_h(\theta)$ is passed to the genetic algorithm as an objective or fitness function, $f(\theta; a_1, \ldots, a_N)$, to be minimized, where

$$f(\theta; a_1, \ldots, a_N) = \|AF(\theta) - AF_h(\theta)\|^2, \text{or}$$

$$\boxed{f = \begin{cases} \left\| \displaystyle\sum_{n=1}^{N} a_n e^{j(2\pi n d\cos\theta)/\lambda} - \frac{1}{N}\frac{\sin\left(\frac{\pi N d}{\lambda}\cos\theta\right)}{\sin\left(\frac{\pi d}{\lambda}\cos\theta\right)} \right\|^2, & \text{for } \cos^{-1}\left(\frac{\lambda}{Nd}\right) \leq \theta \leq \pi - \cos^{-1}\left(\frac{\lambda}{Nd}\right); \\ \left\| \displaystyle\sum_{n=1}^{N} a_n e^{j(2\pi n d\cos\theta)/\lambda} \right\|^2, & \text{otherwise.} \end{cases}} \tag{3.5}$$

3.3 Applying the Genetic Algorithm

The genetic algorithm is a method for solving optimization problems that is based on the evolutionists' natural selection concept. The GA repeatedly modifies a population of individual solutions. At each step, the GA selects individuals at random from the current population to be parents and uses them produce the children for the next generation. Over successive generations, the population 'evolves' toward an optimal solution. At each step of the iteration, the GA uses the selection, crossover and mutation rules to create the next generation from the current population.

The GA can be applied to solve a variety of optimization problems that are not well suited for standard optimization algorithms, including problems in which the objective function is discontinuous, non-differentiable, stochastic, or highly nonlinear.

The algorithm begins by creating a random initial population- in our case, a set of random excitation amplitudes in a given range, say, twenty sets of N a_n's. The algorithm then creates a sequence of new populations, or generations. At each step, the algorithm uses the individuals in the current generation to create the next generation. To create the new generation, the algorithm performs the following steps: scores each member of the current population by computing its fitness value. The fitness value of an individual is the value of the fitness function for that individual. The fitness or objective function is the function to be optimized. In the non-uniform array context, the fitness function is the mean-squared error of the difference between the array factors generated by individual members of a generation and the hypothetical side-lobe free uniform array (3.5). The algorithm then selects parents with the lowest fitness values. Children are produced from parents either by making random changes to a single parent- mutation, or by combining the vector entries of a pair of parents- crossover. The current population is replaces with the children to form the next generation. Finally the algorithm stops when one of the stopping criteria is met. Usually the stopping criteria is when the number of generations reaches a pre-set maximum number of generations or when the value of the fitness function for the best point in the current population is less than or equal to a pre-set fitness value.

3.4 Results

As it is well known in optimization problems, the number of local minima gets on exploding as the number of optimization variables increase. This is to be expected in antenna array design, since the number of nulls increase as N increases. Compared to standard optimization algorithms, the genetic algorithm is strong at escaping the local minima [223].

The non-uniform array designed using the genetic algorithm exhibits the highest directivity, will have a narrow beamwidth comparable to uniform array and displays lower side-lobe levels than Dolph-Chebyshev or uniform arrays. In Dolph-Chebyshev arrays, the side-lobe levels are assumed to be 20 dB below the maximum of the major lobe. Some representative results will be considered. In the sample results below, Matlab's GA toolbox with default parameters is used.

Result 1 For a linear array with $N = 10$ and $d = 0.25\lambda$, a broadside uniform, binomial, and Dolph-Chebyshev arrays are produced. With the same N and d, a non-uniform array is designed using the genetic algorithm. The result is displayed in Figure 3.1. The excitation coefficients of the non-uniform array as produced by the genetic algorithm are shown in Table 3.1. The directivities in descending order are shown in Table 3.2.

Table 3.1: Excitation coefficients for $N = 10, d = 0.25\lambda$

$a_1 = 1.5051$	$a_2 = 0.8778$
$a_3 = -0.4210$	$a_4 = 3.5444$
$a_5 = -0.3286$	$a_6 = 0.9350$
$a_7 = 2.3436$	$a_8 = 0.5822$
$a_9 = 0.2470$	$a_{10} = 1.7174$

Table 3.2: Directivities for $N = 10, d = 0.25\lambda$

Array	**Directivity**
Using GA	5.4382
Uniform	5.1658
Dolph-Chebyshev	4.9253
Binomial	2.6967

As claimed earlier, the array designed using the genetic algorithm exhibits the largest directivity while keeping its beamwidth as narrow as the uniform array.

Result 2 As in Result 1 above, but with $N = 20$ and $d = 0.25\lambda$, the result is displayed in Figure 3.2. The excitation coefficients and directivities are shown, respectively, in Tables 3.3 and 3.4.

Table 3.3: Excitation coefficients for $N = 20, d = 0.25\lambda$

$a_1 = 1.4647$	$a_2 = -0.0557$	$a_3 = 0.7709$	$a_4 = 1.6612$
$a_5 = 0.2775$	$a_6 = 1.1205$	$a_7 = 0.9641$	$a_8 = 1.6770$
$a_9 = 0.6786$	$a_{10} = 0.2991$	$a_{11} = 3.1648$	$a_{12} = -0.5235$
$a_{13} = 1.3070$	$a_{14} = 1.6972$	$a_{15} = 1.0998$	$a_{16} = -0.1354$
$a_{17} = 1.7464$	$a_{18} = 1.0624$	$a_{19} = -0.4338$	$a_{20} = 1.4978$

Table 3.4: Directivities for $N = 20, d = 0.25\lambda$

Array	**Directivity**
Using GA	10.1630
Uniform	10.1593
Dolph-Chebyshev	10.0092
Binomial	3.8884

Result 3 When the inter-element spacing d becomes larger, the number of side-lobes proportionally increases. This means the fluctuations between nulls and side-lobe peaks increases and the efficiency of the genetic algorithm decreases. This effect can be illustrated by taking $N = 10$ and $d = 0.5\lambda$. The result is displayed in Figure 3.3 and the excitation coefficients are shown in Table 3.5 while the directivities are shown in Table 3.6.

Table 3.5: Excitation coefficients for $N = 10, d = 0.5\lambda$

$a_1 = 0.4950$	$a_2 = 0.6905$
$a_3 = 0.7415$	$a_4 = 0.8094$
$a_5 = 0.8379$	$a_6 = 0.8401$
$a_7 = 0.8126$	$a_8 = 0.7458$
$a_9 = 0.6782$	$a_{10} = 0.5018$

Result 4 : If the inter-element spacing d becomes smaller, the number of side-lobes proportionally decreases. The array factor becomes smoother. This increases the efficiency of the genetic algorithm. The effect can be illustrated by taking $N = 10$ and $d = 0.15\lambda$. The result is displayed in Figure 3.4. The excitation coefficients and directivities are shown, respectively, in Tables 3.7 and 3.8.

3.5 Conclusion and Recommendations

As demonstrated above, genetic algorithm can be used to design an efficient non-uniform array. The designed array exhibits the largest directivity and a beamwidth approximating that of uniform arrays. Besides, the side-lobe level is smaller than that of either uniform or Dolph-Chebyshev arrays.

For inter-element spacing greater than 0.5λ, the efficiency of the designed array relatively decreases as opposed to smaller spacing. This is not a problem in practical terms since real arrays will have inter-element spacing less than or equal to 0.5λ to

Table 3.6: Directivities for $N = 10, d = 0.5\lambda$

Array	**Directivity**
Uniform	9.9980
Using GA	9.7197
Dolph-Chebyshev	9.6203
Binomial	5.3914

avoid large number of side-lobes and perhaps grating lobes.

For future work, the excitation amplitude and excitation phases can be simultaneously used to design the non-uniform array using GA. Since the optimization parameters are doubled, a better performance can be expected than the results presented here.

Table 3.7: Excitation coefficients for $N = 10, d = 0.15\lambda$

$a_1 = -2.8430$	$a_2 = -1.0364$
$a_3 = -0.5084$	$a_4 = -0.0046$
$a_5 = -3.3524$	$a_6 = -1.5005$
$a_7 = -3.2832$	$a_8 = 1.2169$
$a_9 = -0.0279$	$a_{10} = -4.1288$

Table 3.8: Directivities for $N = 10, d = 0.15\lambda$

Array	**Directivity**
Using GA	3.6364
Uniform	3.2045
Dolph-Chebyshev	3.2045
Binomial	1.6826

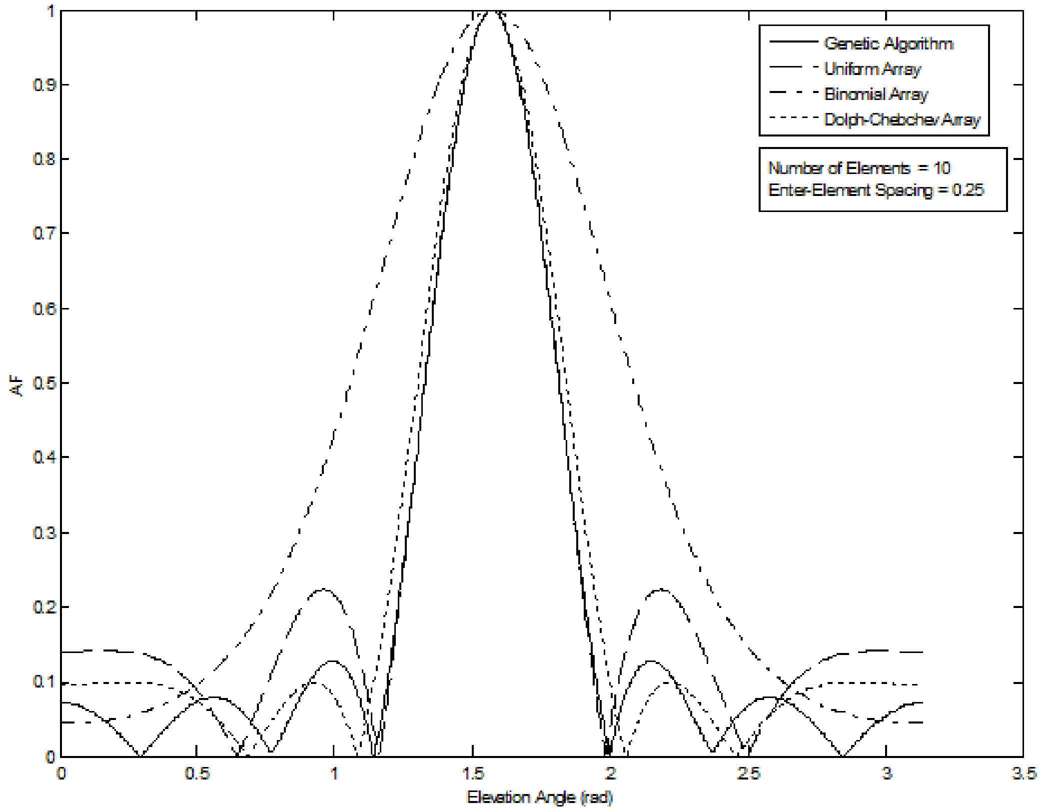

Figure 3.1: Magnitude of normalized array factor, $|AF|$, versus θ for $N = 10, d = 0.25\lambda$.

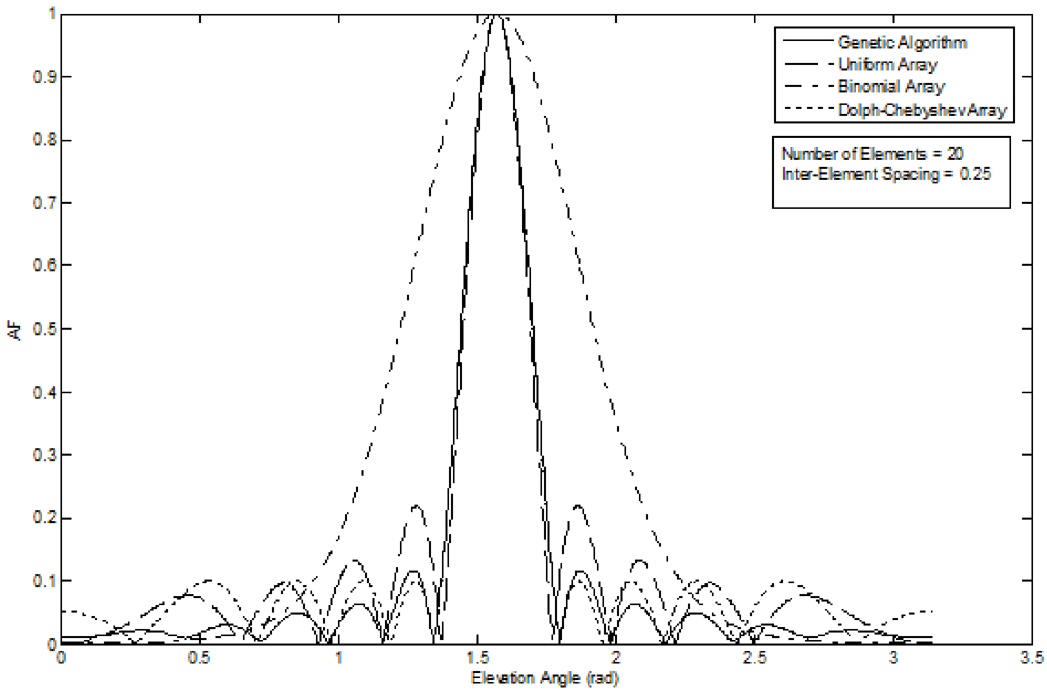

Figure 3.2: Magnitude of normalized array factor, $|AF|$, versus θ for $N = 20, d = 0.25\lambda$.

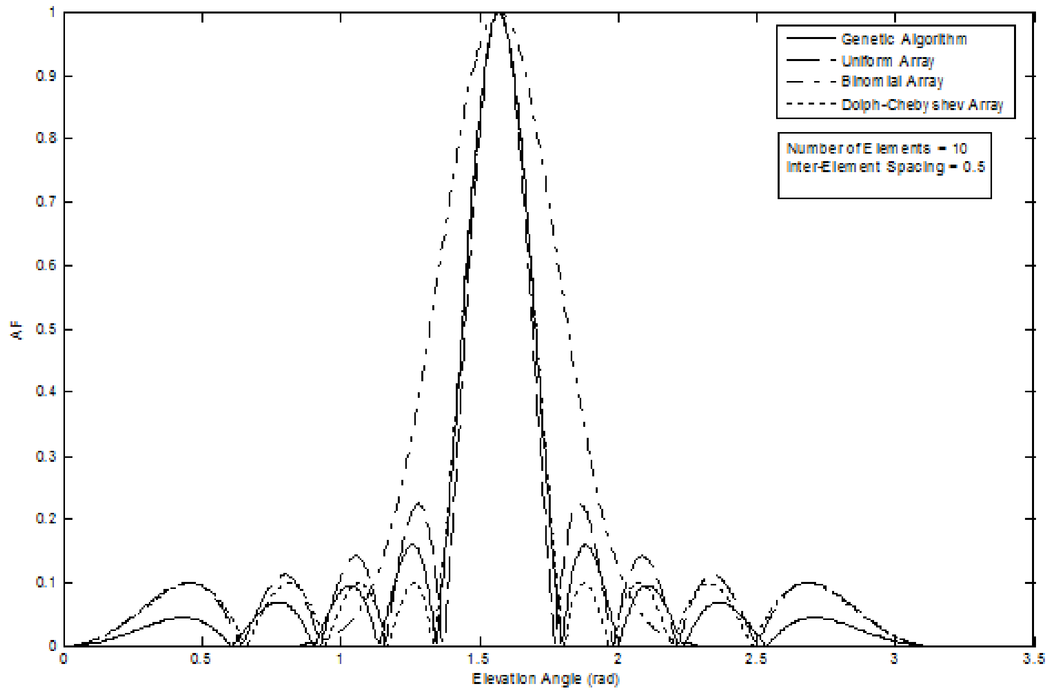

Figure 3.3: Magnitude of normalized array factor, $|AF|$, versus θ for $N = 10, d = 0.5\lambda$.

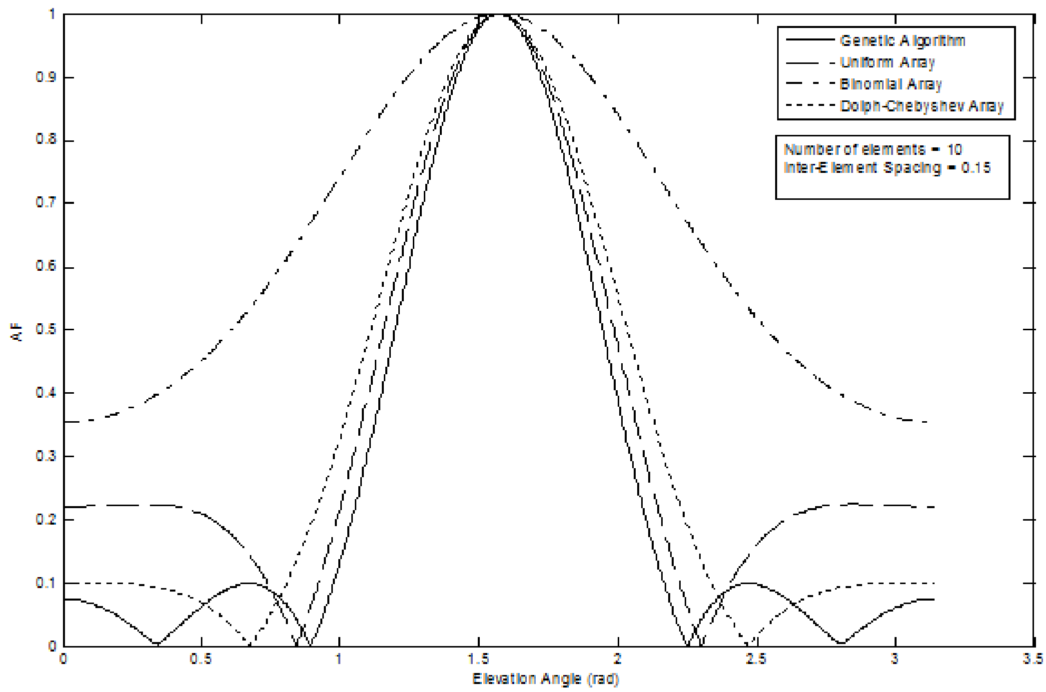

Figure 3.4: Magnitude of normalized array factor, $|AF|$, versus θ for $N = 10, d = 0.15\lambda$.

Chapter 4

Smart Antennas in Cognitive Radio System

4.1 Introduction

It was pointed out in Section 2.4 that conventional cognitive radios exploit the licensed spectrum by opportunistically seeking the under-utilized radio resource in time, frequency and space domains. However, there are other dimensions that need to be explored further for spectrum opportunity. The *angle dimension* is a typical example [100]. The literatures surveyed point to the fact that little work has been done in this dimension. This chapter, which constitutes core work of the dissertation, further explores the angle dimension.

It is to be noted that angle dimension is different than geographical space dimension. In angle dimension, a primary and a secondary user can be in the same geographical area and share the same channel. However, geographical space dimension refers to physical separation of radios in distance such as those in different mobile cells (see Figure 2.2).

To exploit the angle opportunity, the cognitive transmitter (CT) can be equipped with a smart antenna so that it directs its main lobe in the direction of the cognitive receiver (CR) while minimizing or nulling its interference in the direction of the primary receiver (PR).

The chapter investigates performance of CR systems in utilizing the angle diversity in Rayleigh fading channel. As proposed, the CT equipped with smart antenna should keep the interference to the primary receiver below a given threshold while at the same time ensuring high enough SINR at the cognitive receiver. For a given cognitive transmitter location, the region where cognitive receivers can be deployed is determined under the fading channel and compared with a non-fading (large-scale fading) channel.

The authors in [226] proposed opportunistic spectrum access scheme based on angle diversity and smart antenna technology. In their proposed non-intrusive cognitive scheme they showed that, depending on the relative location of the CR and PR, interference from primary transmitter (PT) to CR can be made very small in a large area coined by them as the 'decodable zone'. Consequently, the CT and PT can transmit to their respective receivers with high enough SINR when the CRs are deployed in the decodable zone. The present work is partially an extension of the model developed by [226] to Rayleigh fading channel.

This chapter is organized as follows. The system model is presented in Section 4.2. Section 4.3 sets the problem statement and describes the algorithm for a successful deployment of the CR in the allowable region. Section 4.4 provides some representative numerical results. Finally in Section 4.5 concluding remarks and further research areas are hinted.

4.2 System Model

Assume there are two wireless communication links coexisting in the same geographical region. The primary users (PT and PR) are the licensed users while the secondary or cognitive users (CT and CR) are allowed to opportunistically access the primary user's spectrum under the conditions to be outlined below. The system setup is shown in Figure 4.1.

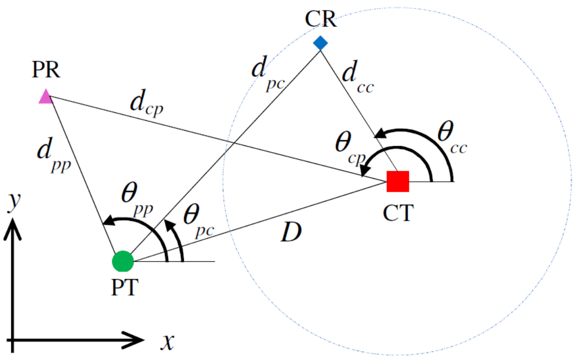

Figure 4.1: Cognitive radio system with primary users.

For a PT located at (x_0, y_0), the separation distance between PT and CT is

$$D = \sqrt{(x_0 - x_1)^2 + (y_0 - y_1)^2} \tag{4.1}$$

The PR is randomly distributed within the circle of radius D while the CR is deployed in a small region centered on the CT at (x_1, y_1). Subscripts $()_p$ and $()_c$ indicate, respectively, primary and cognitive users. d_{ij} and θ_{ij} for $i, j = p, c$ represent, respectively, the distance and azimuth angle from the i's transmitter to the j's receiver. For example, d_{pc} represent the distance between PT and CR while d_{cp} represents the separation distance between CT and PR.

To exploit the angle opportunity, the CT should be equipped with beamforming smart antenna so that it minimizes its interference to the PR while maximizing its radiation in the direction of the CR. Assume that the CT is using a 2-D uniform circular array with M array elements and consider, for simplicity, the azimuth angle. The array beamforming gain in the direction of the azimuth angle θ becomes

$$G(\theta) = \mathbf{w}^H \mathbf{a}(\theta) = \sum_{m=1}^{M} w_m e^{-j2\pi(R/\lambda)\cos(\theta-\theta_m)} \tag{4.2}$$

where $\mathbf{w} = [w_1, w_2, \ldots, w_M]^H \in \mathcal{C}^{M\times 1}$ is the transmit beamforming vector, $a(\theta) = [a_1(\theta), a_2(\theta), \ldots, a_M(\theta)]^T$ is the array steering vector. The superscript H is the hermitian transpose while T is the transpose operator. R is the array radius, λ is the carrier wavelength and $\theta_m = \frac{2\pi}{M}m, m = 1, \ldots, M$ is the angular location of the array elements with respect to the horizontal axis.

The instantaneous signal-to-interference-plus noise ratio, SINR, at the PR and CR, respectively, are

$$SINR_p = \frac{P_{pp}|G(\theta_{pp})|^2}{N_0 + P_{cp}|G(\theta_{cp})|^2} \tag{4.3}$$

$$SINR_c = \frac{P_{cc}|G(\theta_{cc})|^2}{N_0 + P_{pc}|G(\theta_{pc})|^2} \tag{4.4}$$

where P_{ij} for $i, j = p, c$ is the instantaneous received power at receiver j that was transmitted by the ith source. G_p and G_c are, respectively, the primary and cognitive transmit beamforming gains.

4.2.1 Rayleigh Fading Channel

In a Rayleigh fading channel, the received power is exponentially distributed. Let Ω_{ij} be the average received power (including path loss and shadowing) at receiver j that was transmitted by the ith source. Then

$$\Omega_{ij} = \mathbb{E}\left\{P_i d_{ij}^{-\alpha} + X\right\} = P_i d_{ij}^{-\alpha} \tag{4.5}$$

where $\mathbb{E}\{\cdot\}$ is the expectation operator, P_i is the power transmitted by source $i(= p, c)$, α is the path loss factor and X is the large-scale shadowing power with zero mean.

The probability density function (pdf) of the instantaneous power P_{ij} is

$$f_{P_{ij}}(P_{ij}) = \begin{cases} \frac{1}{\Omega_{ij}} e^{-P_{ij}/\Omega_{ij}}, & P_{ij} \geq 0; \\ 0, & \text{otherwise.} \end{cases} \tag{4.6}$$

Thus, the SINRs (4.3) and (4.4) in are random variables of the form

$$Z = \frac{aX}{b + cY} \tag{4.7}$$

where X and Y are exponentially distributed independent random variables and $a, b, c > 0$ are real numbers.

4.2.2 Distribution of SINR

As shown above, the SINR is expressed as a ratio of two random variables. The distribution of the ratio of two random variables has been extensively investigated by many authors especially when X and Y are independent and identically distributed (i.i.d.) random variables [227][228].

To determine the pdf of (4.7), define an auxiliary random variable

$$W = b + cY \tag{4.8}$$

The joint distribution of Z and W becomes

$$\begin{aligned} f_{ZW}(z, w) &= f_{XY}(x, y)|J(x, y)|^{-1} \\ &= f_{XY}\left(\frac{wz}{a}, \frac{w - b}{c}\right)\left|\frac{w}{ac}\right| \end{aligned}$$

where $J(x,y)$ is the Jacobian of the transformation

$$J(x,y) = \begin{vmatrix} \frac{\partial Z}{\partial x} & \frac{\partial Z}{\partial y} \\ \frac{\partial W}{\partial x} & \frac{\partial W}{\partial y} \end{vmatrix} \tag{4.9}$$

It will be assumed $f_X(x)$ and $f_Y(y)$ to be i.i.d. exponential random variables with mean Ω_x and Ω_y. Hence, integrating over W, the marginal pdf of Z becomes

$$\begin{aligned} f_Z(z) &= \int_{-\infty}^{\infty} f_{ZW}(z,w)\, dw \\ &= \int_{-\infty}^{\infty} f_{XY}\left(\frac{wz}{a}, \frac{w-b}{c}\right) \left|\frac{w}{ac}\right| dw \\ &= \int_{b}^{\infty} \frac{w}{ac} f_X\left(\frac{wz}{a}\right) f_Y\left(\frac{w-b}{c}\right) dw \\ &= \int_{b}^{\infty} \frac{w}{ac} \left[\frac{1}{\Omega_x} e^{-wz/a\Omega_x}\right] \left[\frac{1}{\Omega_y} e^{-(w-b)/c\Omega_y}\right] dw \end{aligned}$$

carrying the integration,

$$\boxed{f_Z(z) = \begin{cases} \dfrac{bc\Omega_y z + a\Omega_x(b + c\Omega_y)}{(a\Omega_x + c\Omega_y z)^2} e^{-bz/a\Omega_x}, & z \geq 0; \\ 0, & \text{otherwise.} \end{cases}} \tag{4.10}$$

The mean of Z becomes

$$\mathbb{E}\{Z\} = \frac{a\Omega_x e^{b/c\Omega_y}}{c\Omega_y} \Gamma\left(0, \frac{b}{c\Omega_y}\right) \tag{4.11}$$

where

$$\Gamma(a,z) = \int_z^{\infty} t^{a-1} e^{-t}\, dt \tag{4.12}$$

is the incomplete gamma function.

The probability of $Z \geq T$ becomes

$$\begin{aligned} P_T &\equiv P\{Z \geq T\} \\ &= \int_z^{\infty} \frac{bc\Omega_y z + a\Omega_x(b + c\Omega_y)}{(a\Omega_x + c\Omega_y z)^2} e^{-bz/a\Omega_x}\, dz \\ &= \frac{a\Omega_x e^{-(b/a\Omega_x)T}}{a\Omega_x + c\Omega_y T} \end{aligned} \tag{4.13}$$

4.3 Problem Statement

Consider a scenario where the primary users (PT, PR) and the cognitive receiver CR use omnidirectional antennas while the cognitive transmitter CT is equipped with a beam-forming smart antenna. For communication of cognitive radio systems to be established, the CT has to guarantee that its average interference to the PR is below a threshold I_0 while at the same time keeping high enough $SINR_c$ at the CR.

The cognitive radio has to be aware of the approximate location of the PR. Assume that the distance to the PR, d_{cp}, is known exactly while its angle information θ_{cp} is uncertain by $\Delta\phi$. Let g_c be the worst interference gain in the direction of PR, then

$$g_c = \max_{\theta_{cp}-\Delta\phi \leq \theta \leq \theta_{cp}+\Delta\phi} G_c(\theta) \tag{4.14}$$

The optimal CT beamforming can be stated as:

$$\boxed{\begin{array}{l} \max\limits_{\mathbf{w}_c} SINR_c \\ \text{subject to} \\ \Omega_{cp}|g_c|^2 \leq I_0 \\ |G_c(\theta_{cc})| = 1 \\ |G_c(\theta_{cj}| \leq 1/2, \theta_{cj} \notin [\theta_{cc}-\Delta\theta, \theta_{cc}+\Delta\theta] \\ P_c \leq P_{\max} \end{array}} \tag{4.15}$$

where $\Omega_{cp} = P_c d_{cp}^{-\alpha}$. The first constraint guarantees that the worst interference to the PR has to be kept below I_0. $|G_c(\theta_{cj})| \leq 1/2$ is a constraint on the sidelobe leakage of the CT antenna beam with half-power beamwidth $2\Delta\theta$. $P_{\max}$ is the maximum transmission power of the CT

$$P_{\max} = \bar{\gamma}_c N_0 d_{cc}^{\alpha} \tag{4.16}$$

where $\bar{\gamma}_c$ is the average SNR requirement of the CR.

From the optimization problem (4.15), $\mathbf{w}_c$ is determined. Note that when $\theta_{cc} \in [\theta_{cp}-\Delta\phi, \theta_{cp}+\Delta\phi]$, the gain becomes $g_c = 1$.

After determining the optimal $\mathbf{w}_c$ for the CT, the CT's transmission power becomes

$$P_c = \min\left\{I_0|g_c|^{-2}d_{cp}^{\alpha}, \bar{\gamma}_c N_0 d_{cc}^{\alpha}\right\} \tag{4.17}$$

The first term in (4.17) comes from the interference constraint $P_c d_{cp}^{-\alpha}|g_c|^2 \leq I_0$ while the second term is from $P_{\max}$ in (4.16).

For successful communication of the cognitive system, the $SINR_c$ at the CR has to be greater than a minimum value T with a high probability p.

P_T in (4.13) for the CR with $Z = SINR_c$ and referring to (4.4) and (4.7), with

$$\begin{aligned} a &= |G_c(\theta_{cc})| = 1, \\ b &= N_0, \\ c &= |G_p(\theta_{pc})| = 1, \\ \Omega_x &= P_c d_{cc}^{-\alpha}, \quad \text{and} \\ \Omega_y &= P_p d_{pc}^{-\alpha} \end{aligned}$$

and so that

$$P_T \equiv Pr\{SINR_c \geq T\} = \frac{P_c d_{cc}^{-\alpha} e^{-N_0 T/P_c d_{cc}^{-\alpha}}}{P_c d_{cc}^{-\alpha} + P_p d_{pc}^{-\alpha} T} \tag{4.18}$$

To meet the power constraint (4.17),

$$P_{T_1} \equiv P_T|_{P_c=I_0|g_c|^{-2}d_{cp}^{\alpha}} = \frac{k\left(\frac{d_{cp}}{d_{cc}}\right)^2 |g_c|^{-2} e^{-T/k(\frac{d_{cp}}{d_{cc}})^{\alpha}|g_c|^{-2}}}{k\left(\frac{d_{cp}}{d_{cc}}\right)^2 |g_c|^{-2} + \overline{\gamma}_p\left(\frac{d_{pp}}{d_{pc}}\right)^2 T} \tag{4.19}$$

$$P_{T_2} \equiv P_T|_{P_c=\overline{\gamma}_c N_0 d_{cc}^{\alpha}} = \frac{\overline{\gamma}_c e^{-T/\overline{\gamma}_c}}{\overline{\gamma}_c + \overline{\gamma}_p\left(\frac{d_{pp}}{d_{pc}}\right)^2 T} \tag{4.20}$$

where $P_p = \overline{\gamma}_p d_{pp}^{\alpha} N_0$ and $k = I_0/N_0$. Therefore,

$$\begin{aligned} P_T &= \min\{P_{T_1}, P_{T_2}\} \\ &= \min\left\{\frac{k\left(\frac{d_{cp}}{d_{cc}}\right)^2 |g_c|^{-2} e^{-T/k(\frac{d_{cp}}{d_{cc}})^{\alpha}|g_c|^{-2}}}{k\left(\frac{d_{cp}}{d_{cc}}\right)^2 |g_c|^{-2} + \overline{\gamma}_p\left(\frac{d_{pp}}{d_{pc}}\right)^2 T}, \frac{\overline{\gamma}_c e^{-T/\overline{\gamma}_c}}{\overline{\gamma}_c + \overline{\gamma}_p\left(\frac{d_{pp}}{d_{pc}}\right)^2 T}\right\} \end{aligned} \tag{4.21}$$

The CT, subject to (4.15) and (4.21), can establish communication with the CR at high probability p when

$$\boxed{P_T \equiv Pr\{SINR_c \geq T\} \geq p} \tag{4.22}$$

For a fixed CT location, the area in space where (4.22) is satisfied defines the *region* where the CRs can be deployed to have permissible communication.

If only large-scale path loss (non-fading channel) is considered, communication is established when $SINR_c \geq T$ with

$$SINR_c = \min\left\{\frac{k\left(\frac{d_{cp}}{d_{cc}}\right)^{\alpha} |g_c|^{-2}}{1+\gamma_p\left(\frac{d_{pp}}{d_{pc}}\right)^{\alpha}}, \frac{\gamma_c}{1+\gamma_p\left(\frac{d_{pp}}{d_{pc}}\right)^{\alpha}}\right\} \tag{4.23}$$

Define the *angle spectral efficiency* as

$$\begin{aligned} \eta_a &= \frac{\text{allowable area}}{\text{total area}} \\ &= \frac{\int_{P_T \geq p: d_{cc}\in[d_{\min}, d_{\max}], \theta\in[0,2\pi]} dA}{\pi(d_{\max}^2 - d_{\min}^2)} \end{aligned} \tag{4.24}$$

Thus η_a represents the improvement on angle spectral usage.

4.4 Numerical Results

In the examples below, the following assumptions are made:

- Physical location of the PR is fixed. It implies that $d_{pp}, d_{cp}, \theta_{cp}$ are fixed.
- CR is randomly deployed with d_{cc} and θ_{cc} uniformly distributes, i.e.,

$$d_{cc} \sim U(d_{\min}, d_{\max}), \tag{4.25}$$
$$\theta_{cc} \sim U(0, 2\pi) \tag{4.26}$$

- In the simulations, 2000 random positions of CR are generated.
- $d_{\max} = D, d_{\min} = 10$ m,
- $\Delta\phi = 10^{\circ}$, the pass loss factor to be $\alpha = 2$, and $I_0 = 0.1N_0$.
- CT is equipped with a smart antenna which uses a circular array of 8 elements with array radius $R = \lambda$.

The allowable region where the CR can be deployed is simulated using the Monte-Carlo simulation (see Appendix A) for different combinations of $\bar{\gamma}_c, \bar{\gamma}_p, T$ and p. The following sample results are obtained:

1. For $\bar{\gamma}_c = 20$ dB, $\bar{\gamma}_p = 10$ dB, $T = 6$ dB, and $p = 0.70$, the allowable region, both for non-fading and Rayleigh fading channels, is shown in Figure 4.2. The angle spectrum efficiencies, respectively, for the non-fading and Rayleigh channels are 80.89% and 71.80%.

2. The second simulation is carried as in the above example, except for $\bar{\gamma}_c = 15$ dB. The result is shown in Figure 4.3. The angle spectrum efficiencies are respectively 64.27% and 10.38% for the non-fading and Rayleigh fading channels.

3. Simulation Figure 4.4 shows the effect of varying p in a Rayleigh channel. In both simulations $\bar{\gamma}_c = 20$ dB, $\bar{\gamma}_p = 10$ dB, and $T = 6$ dB is taken, while p is set to 0.85 and 0.90. The resulting angle spectrum efficiencies become $\eta_a|_{p=0.85} = 34.22\%$, and $\eta_a|_{p=0.90} = 2.0\%$.

4. Variation of the spectral efficiency η_a as a function of the average SINR at the CR, $\bar{\gamma}_c$, for non-fading and Rayleigh fading is shown in Figure 4.5. The Rayleigh channel is parameterized against different values of p. From the figure, one can infer that the angle spectral efficiency jumps from zero to approximately 70% in almost 5 dB $\bar{\gamma}_c$ interval and then saturates.

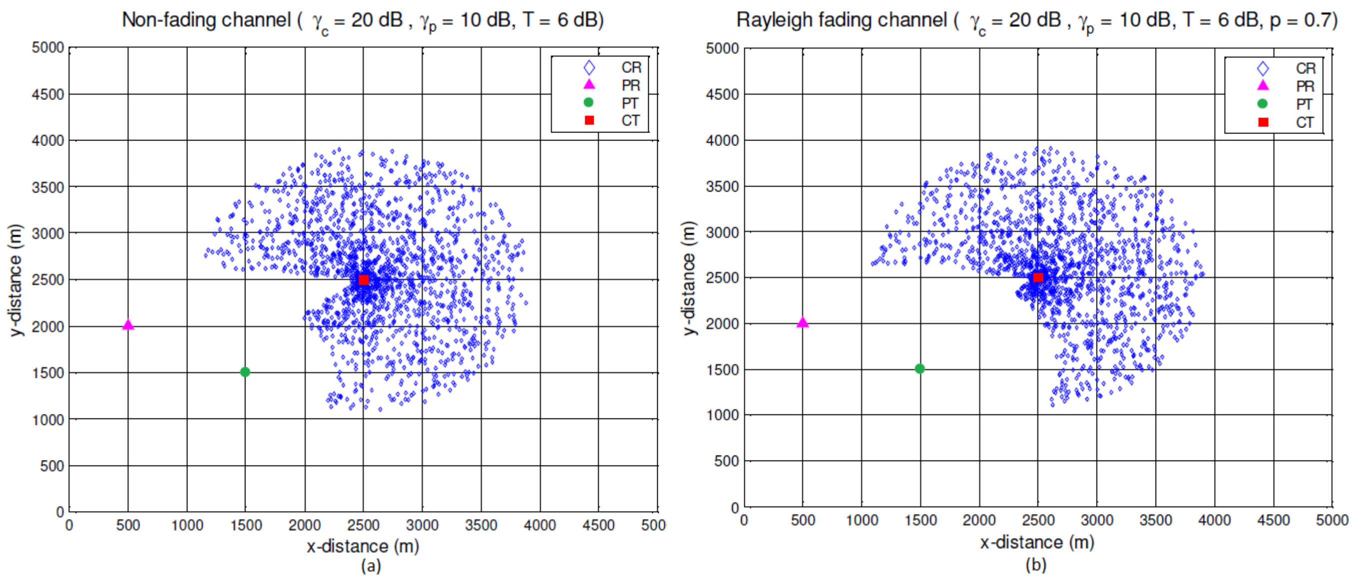

Figure 4.2: (a) Non-fading $\eta_a = 80.89\%$ (b) Rayleigh fading $\eta_a = 71.80\%$

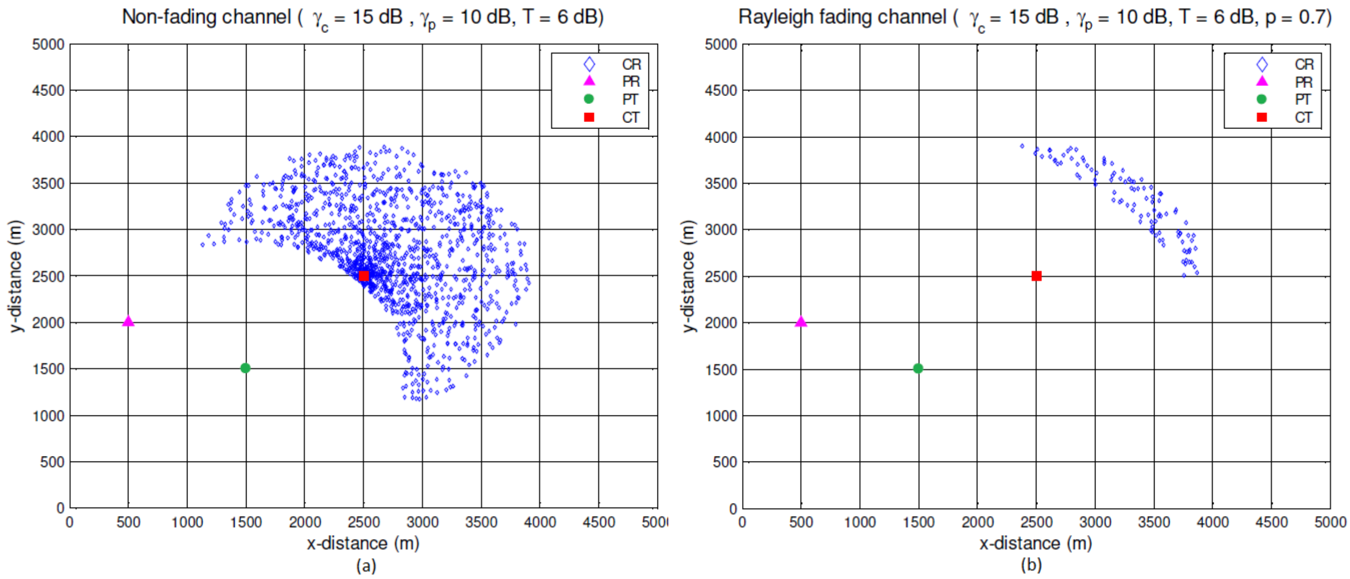

Figure 4.3: (a) Non-fading $\eta_a = 64.27\%$ (b) Rayleigh fading $\eta_a = 10.38\%$

4.5 Conclusions and Recommendations

In this chapter it has been shown that the angle spectrum in cognitive radio system can be greatly exploited using smart antenna and thus leading to multiplexing of multiple users in the same channel at the same time in the same geographical area. The resulting efficiency in spectrum utilization greatly relieves the already congested radio spectrum.

The region where the CRs are to be deployed for a given PT, PR and CT locations is determined for Rayleigh fading channel and compared with the non-fading channel.

The angle spectral efficiency for Rayleigh channel is lower as compared to a non-fading channel with the same power levels and radio terminal locations. It has also been shown that increasing the CT power beyond a certain level has negligible effect on the spectral efficiency.

Future work might extend the present model to scenarios where multiple primary and cognitive users are present. Other types of fading channels can also be considered such as fast fading and frequency selective Rayleigh channels. Real world 3D scenarios can also be considered for future work.

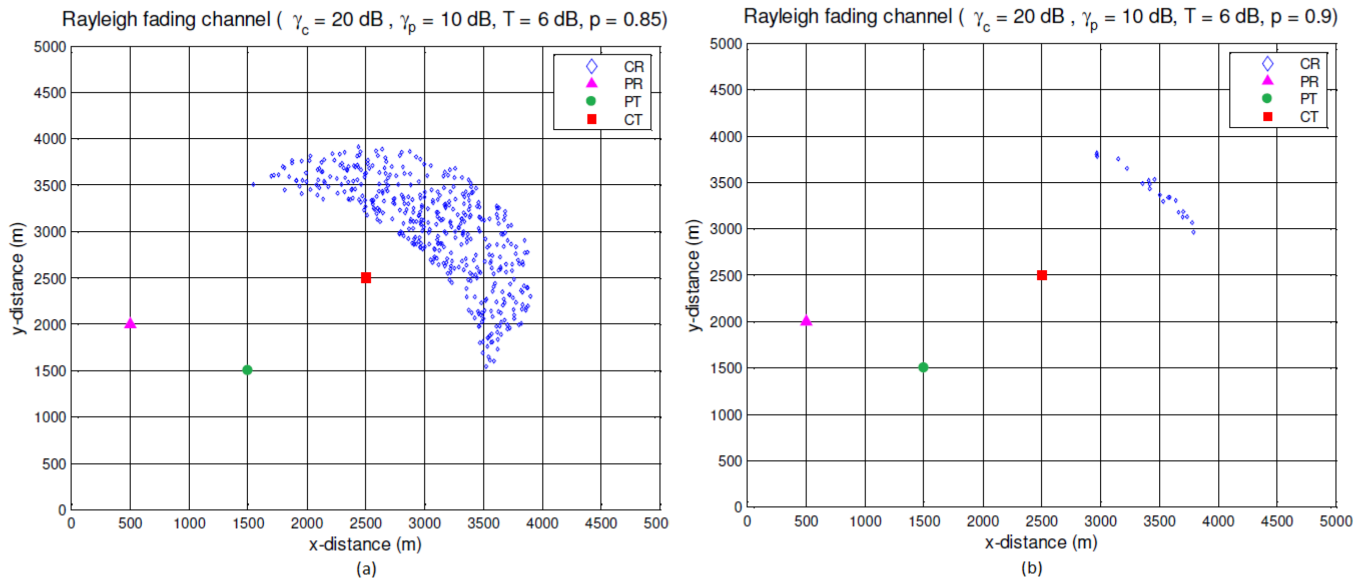

Figure 4.4: (a) Rayleigh fading $\eta_a = 34.22\%$ (b) Rayleigh fading $\eta_a = 2.0\%$

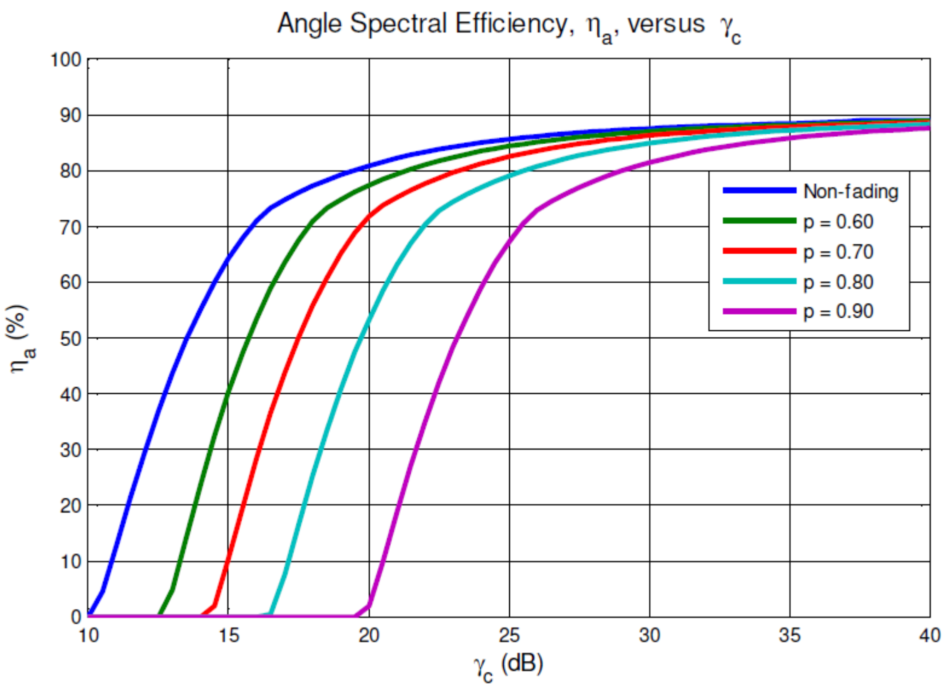

Figure 4.5: Angle spectral efficiency, η_a, as a function of $\overline{\gamma}_c$.

Chapter 5

Distributions of SIR in a Rayleigh Fading Channel

5.1 Introduction

In Chapter 4, a situation was encountered calling for the determination of the probability distribution of SINR in Rayleigh fading. In fading channels when the interfere signal is a random variable, the resulting signal-to-interference-plus-noise ratio (SINR) or signal-to-interference ratio (SIR) is also random and its distribution has to be known for a correct description of the receiver. The distribution of SINR was derived when only one interfere is present. This chapter extends the result when more than one Rayleigh distributed interfere signals are present.

SINR or SIR involve the sum and ratio of random variables. When the interfere signals are more than one, it becomes very difficult, if not impossible, to obtain a tractable closed form expression of the pdf of SINR or SIR. The SIR is studied in noise limited systems, i.e. where the interfere signals dominate over noise. If the noise is to be accounted for, which is typically AWGN, the SINR may be studied. In our case, adding AWGN has no effect on the overall distribution except for a change in its moments. So to keep the mathematical complexity at bay, only the SIR is considered.

The chapter is arranged as follows. Section 5.2 gives a quick revision of the basic mathematical tools needed to deal with the algebra of random variables. In Section 5.3, a closed form expression for the sum of N exponential random variables is derived. Finally in Section 5.4 the distribution of SIR in Rayleigh fading channel is determined.

5.2 Mathematical Preliminaries

In this section a few basic concepts on functions of random variables, which are often referred in the subsequent sections, will be considered.

Sum: Consider a random variable Z defined as the sum of two random variables X_1 and X_2,

$$Z = X_1 + X_2 \tag{5.1}$$

The range R_z of Z corresponding to the event $(Z \leq z) = (X_1 + X_2 \leq z)$ is the set of points (x_1, x_2) which lie on and to the left of the line $z = x_1 + x_2$ (Figure 5.1). Thus,

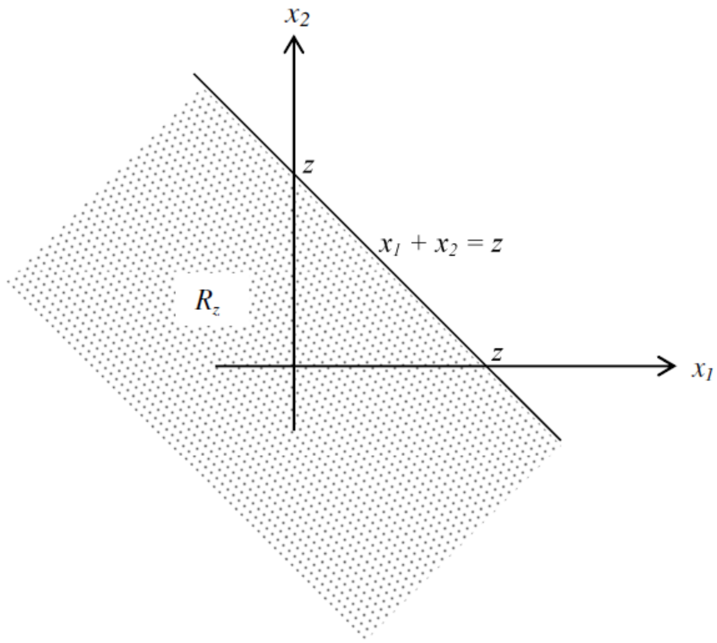

Figure 5.1: Sum of two random variables.

$$F_z(z) = Pr(X_1 + X_2 \leq z) = \int_{-\infty}^{\infty} \left[\int_{-\infty}^{z-x_1} f_{X_1X_2}(x_1, x_2) dx_2 \right] dx_1$$

Then, the pdf of Z becomes

$$f_z(z) = \frac{d}{dz} F_z(z) = \int_{-\infty}^{\infty} f_{X_1X_2}(x_1, z - x_1) dx_1 \tag{5.2}$$

If X_1 and X_2 are independent, (5.2) reduces to

$$\boxed{f_z(z) = \frac{d}{dz} F_z(z) = \int_{-\infty}^{\infty} f_{X_1}(x_1) f_{X_2}(z - x_1) dx_1} \tag{5.3}$$

which is the convolution integral.

Quotient: Now let's consider the quotient Z of two random variables, i.e.,

$$Z = X_1/X_2 \tag{5.4}$$

Set $W = X_2$. The joint pdf of Z and W is given by

$$f_{ZW}(z, w) = f_{X_1X_2}(x_1, x_2) |J(z, w)| \tag{5.5}$$

where $J(z, w)$ is the Jacobian of the transformation

$$J(z, w) = \begin{vmatrix} \frac{\partial x_1}{\partial z} & \frac{\partial x_1}{\partial w} \\ \frac{\partial x_2}{\partial z} & \frac{\partial x_2}{\partial w} \end{vmatrix}$$

The pdf of Z is the marginal pdf

$$f_Z(z) = \int_{-\infty}^{\infty} f_{ZW}(z, w) dw \tag{5.6}$$

Thus using (5.5) and (5.6), the pdf of (5.4) for independent X_1 and X_2 becomes

$$\boxed{f_Z(z) = \int_{-\infty}^{\infty} |w| f_{X_1}(zw) f_{X_2}(w) dw} \tag{5.7}$$

Square: Consider the square of a random variable X for $x > 0$

$$Z = X^2 \tag{5.8}$$

then

$$F_Z(z) = Pr(Z \leq z) = Pr(X^2 \leq z) = Pr(X \leq \sqrt{z})$$

therefore, the pdf of Z becomes

$$\boxed{f_Z(z) = \frac{d}{dz} F_X(\sqrt{z}) = \begin{cases} \frac{1}{2\sqrt{z}} f_X(\sqrt{z}), & \text{for } z > 0; \\ 0, & \text{otherwise.} \end{cases}} \tag{5.9}$$

5.3 Sum of N Exponential Random Variables

In a Rayleigh fading channel, the signal power is distributed exponentially with pdf

$$f_X(x) = \begin{cases} \lambda e^{-\lambda x}, & x \geq 0; \\ 0, & \text{otherwise.} \end{cases} \tag{5.10}$$

where λ is the rate parameter and related to the average signal power Ω by

$$\Omega = \mathbb{E}(X) = \frac{1}{\lambda} \tag{5.11}$$

where $\mathbb{E}(\cdot)$ is the expectation operator.

To find the expression for the sum of N independent exponential random variables, first the expressions for $N = 2$ and $N = 3$ are obtained. Then the results are extended to the general case and proved using mathematical induction.

Theorem 1. *The pdf of $Z = X_1 + X_2$, where X_1 and X_2 are independent exponential random variables is*

$$f_Z(z) = \begin{cases} \frac{\lambda_1 \lambda_2}{\lambda_2 - \lambda_1} e^{-\lambda_1 z} + \frac{\lambda_1 \lambda_2}{\lambda_1 - \lambda_2} e^{-\lambda_2 z}, & z \geq 0; \\ 0, & \textit{otherwise.} \end{cases} \tag{5.12}$$

Proof. Using (5.3),

$$\begin{aligned} f_Z(z) &= \int_0^z f_{X_1}(x_1) f_{X_2}(z - x_1)\, dx_1 \\ &= \lambda_1 \lambda_2 e^{-\lambda_2 z} \int_0^z e^{x_1(\lambda_2 - \lambda_1)}\, dx_1 \\ &= \frac{\lambda_1 \lambda_2}{\lambda_2 - \lambda_1} \left[e^{-\lambda_1 z} - e^{-\lambda_2 z} \right] \\ &= \frac{\lambda_1 \lambda_2}{\lambda_2 - \lambda_1} e^{-\lambda_1 z} + \frac{\lambda_1 \lambda_2}{\lambda_1 - \lambda_2} e^{-\lambda_2 z} \qquad \blacktriangleleft \end{aligned}$$

Corollary 1. *The pdf of $Z = X_1 + X_2 + X_3$, where X_1, X_2 and X_3 are independent exponential random variables is*

$$f_Z(z) = \begin{cases} \dfrac{\lambda_1\lambda_2\lambda_3}{(\lambda_2-\lambda_1)(\lambda_3-\lambda_1)}e^{-\lambda_1 z} + \dfrac{\lambda_1\lambda_2\lambda_3}{(\lambda_1-\lambda_2)(\lambda_3-\lambda_2)}e^{-\lambda_2 z} + \dfrac{\lambda_1\lambda_2\lambda_3}{(\lambda_1-\lambda_3)(\lambda_2-\lambda_3)}e^{-\lambda_3 z}, & z \geq 0; \\ 0, & \textit{otherwise.} \end{cases} \tag{5.13}$$

Proof. Set $Y = X_1 + X_2$, $Z = Y + X_3$. The pdf of Y is (5.12). Then

$$\begin{aligned} f_Z(z) &= \int_0^z f_{X_3}(x_3) f_Y(z-x_3)\, dx_3 \\ &= \int_0^z \lambda_3 e^{-\lambda_3 x_3} \left[\frac{\lambda_1\lambda_2}{\lambda_2-\lambda_1} e^{-\lambda_1(z-x_3)} + \frac{\lambda_1\lambda_2}{\lambda_1-\lambda_2} e^{-\lambda_2(z-x_3)} \right] dx_3 \\ &= \frac{\lambda_1\lambda_2\lambda_3}{\lambda_2-\lambda_1} e^{-\lambda_1 z} \int_0^z e^{(\lambda_1-\lambda_3)x_3} dx_3 + \frac{\lambda_1\lambda_2\lambda_3}{\lambda_1-\lambda_2} e^{-\lambda_2 z} \int_0^z e^{(\lambda_2-\lambda_3)x_3} dx_3 \\ &= \frac{\lambda_1\lambda_2\lambda_3}{(\lambda_2-\lambda_1)(\lambda_1-\lambda_3)} e^{-\lambda_1 z} \left[e^{(\lambda_1-\lambda_3)z} - 1 \right] + \frac{\lambda_1\lambda_2\lambda_3}{(\lambda_1-\lambda_2)(\lambda_2-\lambda_3)} e^{-\lambda_2 z} \left[e^{(\lambda_2-\lambda_3)z} - 1 \right] \\ &= \frac{\lambda_1\lambda_2\lambda_3}{(\lambda_2-\lambda_1)(\lambda_3-\lambda_1)} e^{-\lambda_1 z} + \frac{\lambda_1\lambda_2\lambda_3}{(\lambda_1-\lambda_2)(\lambda_3-\lambda_2)} e^{-\lambda_2 z} + \frac{\lambda_1\lambda_2\lambda_3}{(\lambda_1-\lambda_3)(\lambda_2-\lambda_3)} e^{-\lambda_3 z} \quad \blacktriangleleft \end{aligned}$$

Inferring from the patters emerging from (5.12) and (5.13), one can state the corollary for the sum of N independent exponential random variables.

Corollary 2. *The pdf of $Z = X_1 + X_2 + \ldots + X_N$, where X_i $(i = 1, \ldots, N)$ are independent exponential random variables is*

$$f_Z(z) = \begin{cases} \displaystyle\prod_{k=1}^{N} \lambda_k \sum_{i=1}^{N} \frac{e^{-\lambda_i z}}{\displaystyle\prod_{\substack{j=1 \\ j\neq i}}^{N} (\lambda_j - \lambda_i)}, & z \geq 0; \\ 0, & \textit{otherwise.} \end{cases} \tag{5.14}$$

Prove. The theorem will be proved using mathematical induction.
The equation is true for $i = 2$, viz.,

$$\begin{aligned} f_Z(z) &= \prod_{k=1}^{2} \lambda_k \sum_{i=1}^{2} \frac{e^{-\lambda_i z}}{\displaystyle\prod_{\substack{j=1 \\ j\neq i}}^{2} (\lambda_j - \lambda_i)} \\ &= \lambda_1\lambda_2 \left[\frac{1}{\lambda_2-\lambda_1} e^{-\lambda_1 z} + \frac{1}{\lambda_1-\lambda_2} e^{-\lambda_2 z} \right] \quad \blacktriangleleft \end{aligned}$$

Assume (5.14) is true for $i = n$. One should show that it is true for $i = n + 1$.

Let $Z = Y + X_{n+1}$ where Y's pdf is (5.14). Then,

$$\begin{aligned}
f_Z(z) &= \int_0^z f_{X_{n+1}}(x_{n+1}) f_Y(z - x_{n+1})\, dx_{n+1} \\
&= \int_0^z \lambda_{n+1} e^{-\lambda_{n+1}x_{n+1}} \left[\prod_{k=1}^{n} \lambda_k \sum_{i=1}^{n} \frac{e^{-\lambda_i(z-x_{n+1})}}{\prod_{\substack{j=1\\ j\neq i}}^{n}(\lambda_j - \lambda_i)} \right] dx_{n+1} \\
&= \left(\lambda_{n+1} \prod_{k=1}^{n} \lambda_k \right) \sum_{i=1}^{n} \frac{1}{\prod_{\substack{j=1\\ j\neq i}}^{n}(\lambda_j - \lambda_i)} \int_0^z e^{-\lambda_{n+1}x_{n+1}} e^{-\lambda_i(z-x_{n+1})} dx_{n+1} \\
&= \left(\prod_{k=1}^{n+1} \lambda_k \right) \sum_{i=1}^{n} \frac{e^{-\lambda_i z}}{\prod_{\substack{j=1\\ j\neq i}}^{n}(\lambda_j - \lambda_i)} \int_0^z e^{(\lambda_i - \lambda_{n+1})x_{n+1}} dx_{n+1} \\
&= \left(\prod_{k=1}^{n+1} \lambda_k \right) \sum_{i=1}^{n} \frac{e^{-\lambda_i z}}{\prod_{\substack{j=1\\ j\neq i}}^{n}(\lambda_j - \lambda_i)} \left[\frac{e^{(\lambda_i - \lambda_{n+1})z} - 1}{\lambda_i - \lambda_{n+1}} \right] \\
&= \left(\prod_{k=1}^{n+1} \lambda_k \right) \sum_{i=1}^{n} \frac{1}{\prod_{\substack{j=1\\ j\neq i}}^{n}(\lambda_j - \lambda_i)} \left[\frac{e^{-\lambda_{n+1} z} - e^{-\lambda_i z}}{\lambda_i - \lambda_{n+1}} \right] \\
&= \left(\prod_{k=1}^{n+1} \lambda_k \right) \left[\sum_{i=1}^{n} \frac{e^{-\lambda_i z}}{\prod_{\substack{j=1\\ j\neq i}}^{n}(\lambda_j - \lambda_i)(\lambda_{n+1} - \lambda_i)} + \sum_{i=1}^{n} \frac{e^{-\lambda_{n+1} z}}{\prod_{\substack{j=1\\ j\neq i}}^{n}(\lambda_j - \lambda_i)(\lambda_i - \lambda_{n+1})} \right]
\end{aligned}$$

Consider the first and the second terms inside the bracket. The expression in the denominator of the first term can be simplified as

$$\begin{aligned}
\prod_{\substack{j=1\\ j\neq i}}^{n} (\lambda_j - \lambda_i)(\lambda_{n+1} - \lambda_i) &= (\lambda_1 - \lambda_i) \underbrace{\ldots}_{j\neq i} (\lambda_n - \lambda_i)(\lambda_{n+1} - \lambda_i) \\
&= \prod_{\substack{j=1\\ j\neq i}}^{n+1} (\lambda_j - \lambda_i)
\end{aligned}$$

The second term can further be simplified as

$$\begin{aligned}
\sum_{i=1}^{n} \frac{e^{-\lambda_{n+1} z}}{\prod_{\substack{j=1\\ j\neq i}}^{n}(\lambda_j - \lambda_i)(\lambda_i - \lambda_{n+1})} &= e^{-\lambda_{n+1} z} \left\{ \frac{1}{(\lambda_2 - \lambda_1)(\lambda_3 - \lambda_1)\cdots(\lambda_n - \lambda_1)(\lambda_1 - \lambda_{n+1})} \right. \\
&\quad + \frac{1}{(\lambda_1 - \lambda_2)(\lambda_3 - \lambda_2)\cdots(\lambda_n - \lambda_2)(\lambda_2 - \lambda_{n+1})} + \ldots \\
&\quad \left. \ldots + \frac{1}{(\lambda_n - \lambda_1)(\lambda_n - \lambda_1)\cdots(\lambda_n - \lambda_{n-1})(\lambda_n - \lambda_{n+1})} \right\} \\
&= e^{-\lambda_{n+1} z} \left\{ \frac{1}{(\lambda_{n+1} - \lambda_1)(\lambda_{n+1} - \lambda_2)\cdots(\lambda_{n+1} - \lambda_n)} \right\} \\
&= e^{-\lambda_{n+1} z} \frac{1}{\prod_{\substack{j=1\\ j\neq i}}^{n+1}(\lambda_j - \lambda_i)}
\end{aligned}$$

Thus, putting the results

$$
\begin{aligned}
f_Z(z) &= \left(\prod_{k=1}^{n+1} \lambda_k\right) \left[\sum_{i=1}^{n} \frac{e^{-\lambda_i z}}{\prod_{\substack{j=1\\ j\neq i}}^{n+1}(\lambda_j - \lambda_i)} + \frac{e^{-\lambda_{n+1} z}}{\prod_{\substack{j=1\\ j\neq i}}^{n+1}(\lambda_j - \lambda_i)}\right] \\
&= \left(\prod_{k=1}^{n+1} \lambda_k\right) \sum_{i=1}^{n+1} \frac{e^{-\lambda_i z}}{\prod\limits_{\substack{j=1\\ j\neq i}}^{n+1}(\lambda_j - \lambda_i)} \quad \blacktriangleleft
\end{aligned}
$$

which proves the theorem.

5.4 Distribution of SIR in Rayleigh Fading Channel

The SIR is defined as

$$
SIR = \frac{X_0}{X_1 + X_2 + \ldots + X_N} \tag{5.15}
$$

where X_0 is power of the desired signal while X_i $(i = 1, \ldots, N)$ are the powers of the interferer signals.

In a Rayleigh channel, the X_i's follow the exponential distribution as shown in the previous section (5.10).

Theorem 2. *The pdf of SIR is given by*

$$
\boxed{f_Z(z) = \begin{cases} \prod\limits_{k=0}^{N} \lambda_k \sum\limits_{i=1}^{N} \dfrac{1}{\prod\limits_{\substack{j=1\\ j\neq i}}^{N}(\lambda_j - \lambda_i)(\lambda_i + \lambda_0 z)^2}, & z \geq 0; \\ 0, & \textit{otherwise}. \end{cases}} \tag{5.16}
$$

Proof. Let

$$
W = X_1 + X_2 + \ldots + X_N
$$

W's pdf is given by (5.14). Then the pdf of $SIR \equiv Z = X_0/W$ using (5.7) is

$$
\begin{aligned}
f_Z(z) &= \int_{-\infty}^{\infty} |w| f_{X_0}(zw) f_Y(w)\, dw \\
&= \int_{0}^{\infty} w f_{X_0}(zw) f_Y(w)\, dw \\
&= \int_{0}^{\infty} w \lambda_0 e^{-\lambda_0 z w} \left[\prod_{k=1}^{N} \lambda_k \sum_{i=1}^{N} \frac{e^{-\lambda_i z}}{\prod_{\substack{j=1\\ j\neq i}}^{N}(\lambda_j - \lambda_i)}\right] dw \\
&= \lambda_0 \prod_{k=1}^{N} \lambda_k \sum_{i=1}^{N} \frac{1}{\prod_{\substack{j=1\\ j\neq i}}^{N}(\lambda_j - \lambda_i)} \int_{0}^{\infty} w e^{-(\lambda_0 z + \lambda_i) w}\, dw \\
&= \prod_{k=0}^{N} \lambda_k \sum_{i=1}^{N} \frac{1}{\prod_{\substack{j=1\\ j\neq i}}^{N}(\lambda_j - \lambda_i)} \frac{1}{(\lambda_i + \lambda_0 z)^2} \quad \blacktriangleleft
\end{aligned}
$$

In terms of the average signal power $\Omega_i = 1/\lambda_i$ ($i = 0, \ldots, N$), the pdf of SIR (5.16) can be expressed as,

$$\boxed{f_Z(z) = \begin{cases} \displaystyle\prod_{k=0}^{N} \frac{1}{\Omega_k} \sum_{i=1}^{N} \frac{1}{\displaystyle\prod_{\substack{j=1\\ j\neq i}}^{N} \left(\frac{1}{\Omega_j} - \frac{1}{\Omega_i}\right) \left(\frac{1}{\Omega_i} + \frac{1}{\Omega_0} z\right)^2}, & z \geq 0; \\ 0, & \text{otherwise.} \end{cases}} \tag{5.17}$$

Theorem 3. *The cumulative distribution function of SIR is*

$$F_Z(z) = \begin{cases} \displaystyle\prod_{k=0}^{N} \frac{1}{\Omega_k} \sum_{i=1}^{N} \frac{1}{\displaystyle\prod_{\substack{j=1\\ j\neq i}}^{N} \left(\frac{1}{\Omega_j} - \frac{1}{\Omega_i}\right)} \frac{z}{\frac{1}{\Omega_i^2} + \frac{1}{\Omega_0 \Omega_i} z}, & z \geq 0; \\ 0, & \textit{otherwise.} \end{cases} \tag{5.18}$$

Proof. The cumulative distribution is

$$\begin{aligned} F_Z(z) = Pr(Z \leq z) &= \int_{-\infty}^{z} f_Z(z)\, dz \\ &= \prod_{k=0}^{N} \frac{1}{\Omega_k} \sum_{i=1}^{N} \frac{1}{\displaystyle\prod_{\substack{j=1\\ j\neq i}}^{N} \left(\frac{1}{\Omega_j} - \frac{1}{\Omega_i}\right)} \int_0^z \frac{dz}{\left(\frac{1}{\Omega_i} + \frac{1}{\Omega_0} z\right)^2} \\ &= \prod_{k=0}^{N} \frac{1}{\Omega_k} \sum_{i=1}^{N} \frac{1}{\displaystyle\prod_{\substack{j=1\\ j\neq i}}^{N} \left(\frac{1}{\Omega_j} - \frac{1}{\Omega_i}\right)} \frac{z}{\frac{1}{\Omega_i^2} + \frac{1}{\Omega_0 \Omega_i} z} \qquad \blacktriangleleft \end{aligned}$$

An outage occurs if the instantaneous SIR falls below some acceptable $SIR_{\min}$. Thus the *outage probability* can be given as

$$\boxed{p_{\text{out}} = F_Z(SIR_{\min}) = \prod_{k=0}^{N} \frac{1}{\Omega_k} \sum_{i=1}^{N} \frac{1}{\displaystyle\prod_{\substack{j=1\\ j\neq i}}^{N} \left(\frac{1}{\Omega_j} - \frac{1}{\Omega_i}\right)} \frac{SIR_{\min}}{\frac{1}{\Omega_i^2} + \frac{1}{\Omega_0 \Omega_i} SIR_{\min}}} \tag{5.19}$$

5.5 Conclusion and Recommendations

In fading channels the SINR and SIR are random variables and their distributions have to be known for a correct description of the receiver.

In this chapter the distributions of SIR in Rayleigh fading channel have been derived in a closed form expression. Results for the probability density function, cumulative distribution and outage probabilities have been shown. Other fading channels can be similarly studied.

Chapter 6

Conclusions and Recommendations

The main contributions of this dissertation are contained in Chapters 3, 4 and 5. The findings reached at and the conclusions drawn have been stated in the respective chapters. For easy of reference, the conclusions and the corresponding recommendations are summarized below.

- Genetic algorithm was used to design a non-uniform linear antenna array such that the array is to approximate the beamwidth of a uniform array with the same number of elements and element spacing while keeping its sidelobe level smaller than that of Dolph-Chebyshev array. The designed array generally exhibits the largest directivity as compared to the uniform, Binomial and Dolph-Chebyshev arrays. It is to be noted that a uniform array yields the smallest beamwidth and hence the highest directivity. It is followed, in order, by the Dolph-Chebyshev and Binomial arrays. In contrast, Binomial arrays usually possess the smallest sidelobes followed, in order, by the Dolph-Chebyshev and uniform arrays.

  As shown in section 3.4, genetic algorithm was used to generate the excitation coefficients of a non-uniform linear array and its performance, in terms of beamwidth and sidelobe level, was compared with uniform, binomial and Dolph-Chebyshev arrays having equal number of array elements and inter-element spacing. It was shown that for $N = 10$ and $d = 0.25\lambda$, the array designed using GA exhibits the largest directivity while keeping its beamwidth as narrow as the uniform array. For $N = 20$ and $d = 0.25\lambda$, the GA still produced a better array but the improvement in directivity is less as compared with the case $N = 10$.

  When the inter-element spacing d becomes larger, the number of sidelobes proportionally increases. This means the fluctuations between nulls and sidelobe peaks increases and the efficiency of the genetic algorithm decreases. This effect was illustrated by taking $N = 10$ and $d = 0.5\lambda$. This is not a problem in practical terms since real arrays usually will have inter-element spacing less than or equal to 0.5λ to avoid large number of sidelobes and perhaps grating lobes.

  The method can be used in applications where beams exhibiting narrow beamwidth and lower sidelobes levels are preferred such as in switched-beam smart antennas.

  For future work, the excitation amplitude and excitation phases can be simultaneously used to design the non-uniform array using GA. Since the optimization parameters are doubled, a better performance can be expected than the results presented here.

- It has been shown that the angle spectrum in cognitive radio system can be greatly exploited using smart antennas and thus leading to multiplexing of multiple users in the same channel at the same time in the same geographical area. The resulting efficiency in spectrum utilization greatly relieves the already congested radio spectrum. The region where the cognitive radios are to be deployed and the achieved angle spectral efficiency for a given primary transmitter, primary receiver and cognitive transmitter locations was determined for Rayleigh fading channel and compared with the non-fading channel. It was shown that the angle spectral efficiency for Rayleigh channel is lower as compared to a non-fading channel with the same power levels and radio terminal locations. Moreover it has been shown that increasing the cognitive transmitter power beyond a certain level has negligible effect on the angle spectral efficiency.

As shown in section 4.4, simulations were conducted where the CT was equipped with a beamforming smart antenna while the PT, PR, and CR are equipped with omnidirectional antennas. The smart antenna uses a circular array of 8 elements with array radius equal to λ. The CT should keep the interference to the primary receiver below a given threshold I_0 while at the same time ensuring high enough signal-to-interference-plus-noise ratio $\bar{\gamma}_c$ at the cognitive receiver. The allowable region where the cognitive receivers are to be deployed and the achieved angle spectral efficiency η_a for a given PT, PR and CT locations were simulated using the Monte-Carlo simulation for Rayleigh fading channel and compared with the non-fading channel. Accordingly, for $\bar{\gamma}_c = 20$ dB, $\bar{\gamma}_p = 10$ dB, $T = 6$ dB, and $p = 0.70$, the allowable region, both for non-fading and Rayleigh fading channels, was simulated in Figure 4.2. The angle spectrum efficiencies, respectively, for the non-fading and Rayleigh channels are 80.89% and 71.80%. This mean that CRs can be deployed in approximately 72% (for Rayleigh) of the region around the CT and allowed to use the channel which was otherwise dedicated to the primary licensed users (PT and PR). Thus a new spectrum opportunity was obtained and a 72% improvement on angle spectral usage was achieved due to the beamforming capability of the CT. Obviously, it is to be expected that the angle spectral efficiency for non-fading channel is greater that that of Rayleigh fading.

Decreasing the transmit power of CT obviously decreases the allowable area where the CR can be deployed and hence results in a decreased angle spectral efficiency. This was illustrated for $\bar{\gamma}_c = 15$ dB and keeping the other parameters as in the above case. The resulting allowable region was simulated in Figure 4.3 and the achieved angle spectrum efficiencies were respectively 64.27% and 10.38% for the non-fading and Rayleigh fading channels.

Increasing the probability of cognitive communication p (4.22) in Rayleigh channel decreases the allowable region and hence lowers the angle spectral efficiency. This was illustrated for the cases $p = 0.85$ and $p = 0.90$. In both cases, $\bar{\gamma}_c = 20$ dB, $\bar{\gamma}_p = 10$ dB, and $T = 6$ dB were taken and the allowable regions were simulated in Figure 4.4. The resulting angle spectrum efficiencies were $\eta_a|_{p=0.85} = 34.22\%$, and $\eta_a|_{p=0.90} = 2.0\%$

The effect of variation of the spectral efficiency η_a as a function of the average SINR at the CR, $\bar{\gamma}_c$, for non-fading and Rayleigh fading was investigated. The Rayleigh channel was parameterized against different values of p. The effect was simulated in Figure 4.5. From the figure, it can be inferred that the angle spectral efficiency jumps from zero to approximately 70% in almost 5 dB $\bar{\gamma}_c$ interval and then saturates. This implies that indefinitely increasing the CT power beyond a certain value has negligible effect on the angle spectral efficiency and hence an optimal CT power can be set for a given communication scenario.

Future work might extend the present model to scenarios where multiple primary and cognitive users are present. Other types of fading channels such as Rician and Nakagami can be considered. Fast fading and frequency selective Rayleigh channels can also be considered. Real world 3D scenarios can also be considered for future work.

- In fading channels the SINR and SIR are random variables and their distributions have to be known for a correct description of the receiver. In Chapter 4, the distributions of SINR was derived in closed form when only a single interfere is present. The concept was extended in Chapter 5 to the determination of the distributions of SIR in closed form when N Rayleigh distributed interferes are present. Unlike approximate solutions, closed form mathematical equations have the advantage of displaying the full behaviour of the function over the domain of definition.

  The probability distributions of the SIR in Rayleigh fading have been rigourously derived in a closed form expression. The results for the probability density function, cumulative distribution and outage probabilities have been shown.

  Future works can extend the problem to other types of distributions.

Appendix A

Monte Carlo Method

The Monte Carlo method was used in Chapter 4 to simulate the region where cognitive radios are to be successfully deployed. On each simulation, random positions of cognitive radio are generated while keeping the positions of PT, PR, and CT fixed. For each randomly generated position of CR, P_T (4.22) is computed for a prescribed values of $\bar{\gamma}_c, \bar{\gamma}_p, T$, and p. If $P_T \geq p$, that particular physical position is allowed to be occupied by a CR and establish communication with the CT without disrupting the communication between the primary users.

This chapter gives an overview of the Monte Carlo method. Monte Carlo methods are a class of computational algorithm techniques that involve using random numbers and probability to solve problems. These methods are most suited to calculation by a computer and tend to be used when it is infeasible to compute an exact result with a deterministic algorithm. This method is also used to complement theoretical derivations.

Monte Carlo methods are especially useful for simulating systems with many coupled degrees of freedom, such as fluids, disordered materials, strongly coupled solids, and cellular structures. They are used to model phenomena with significant uncertainty in inputs, such as the calculation of risk in business. They are widely used in mathematics, for example to evaluate multidimensional definite integrals with complicated boundary conditions, in VLSI design, nuclear reactor design, quantum chromodynamics, radiation cancer therapy, traffic flow, stellar evolution, econometrics and oil well exploration.

The Monte Carlo method was coined in the 1940s by John von Neumann, Stanislaw Ulam and Nicholas Metropolis, while they were working on nuclear weapon projects (Manhattan Project) in the Los Alamos National Laboratory. It was named after the Monte Carlo Casino, a famous casino where Ulam's uncle often gambled away his money [229].

The Monte Carlo method iteratively evaluates a *deterministic model* using sets of random numbers as inputs. By using random inputs, one is essentially turning the deterministic model into a *stochastic model*. A block diagram representation of the Monte Carlo model is shown in Figure A.1. In the model, the inputs $\mathbf{x} = [x_1, \ldots, x_N]$ are random numbers while the model $\mathbf{y} = f(\mathbf{x})$ is deterministic.

Generally, Monte Carlo methods vary but tend to follow similar pattern:

1. Define a model and domain of possible inputs, $\mathbf{y} = f(\mathbf{x})$

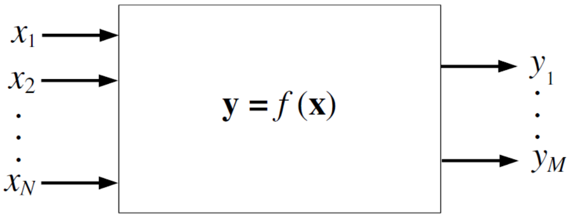

Figure A.1: A deterministic model maps a set of random input variables to a set of output variables.

2. Generate inputs randomly from a probability distribution over the domain, $\mathbf{x} = [x_1, x_2, \ldots, x_N]$
3. Perform a deterministic computation on the inputs and store the results, $y_i, i = 1, \ldots, M$
4. Aggregate the results.

The most common use of Monte Carlo methods is the evaluation of numerical integrals. To approximate the integral (Figure A.2)

$$I = \int_a^b f(x)dx \tag{A.1}$$

follow the following simple steps:

1. Generate uniformly distributed sample points within A
2. Calculate the proportion ρ of points in region of interest
3. Area under the curve $\approx \rho$.

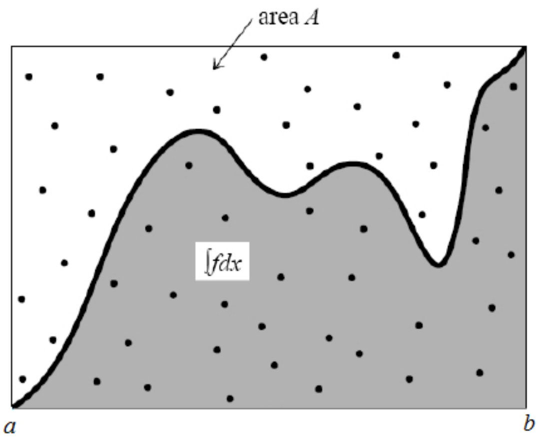

Figure A.2: Area under a curve.

Consider an example, called the *raindrop experiment for computing* π. Assume that one could produce 'uniform rain' on the square $[-1,1] \times [-1,1]$, such that the probability of a raindrop falling into a region $R \subset [-1,1] \times [-1,1]$ is proportional to the area of R.

The two coordinates are independent and identically distributed (i.i.d) uniform random variables, i.e.,

$$X, Y \overset{i.i.d}{\sim} U(-1, 1) \tag{A.2}$$

Now consider the probability that a raindrop falls into the unit circle inscribed in the square. It is

$$\begin{aligned} Pr(\text{drop within circle}) &= \frac{\text{area of the unit circle}}{\text{area of the square}} \\ &= \frac{\iint_{x^2+y^2\le 1} 1dxdy}{\iint_{-1\le x,y\le 1} 1dxdy} \\ &= \frac{\pi}{4} \end{aligned} \tag{A.3}$$

hence,

$$\pi = 4 \times Pr(\text{drop within circle}), \tag{A.4}$$

Thus one can estimate π by

$$\hat{\pi}_n = 4 \times \frac{\text{no. of points inside circle}}{\text{total no. of point in trial}} \tag{A.5}$$

A trial for $n = 1000$ is shown in Figure A.3. As can be seen in the simulation Figure A.4, $\hat{\pi}_n$ converging to π as the number of random points keeps on increasing.

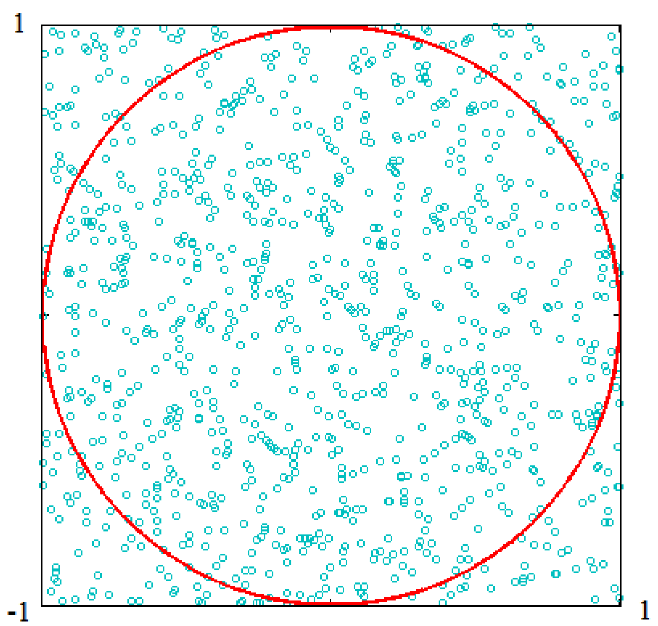

Figure A.3: The rain drop experiment, $\hat{\pi}_n = 4 \times \frac{785}{1000} = 3.14$.

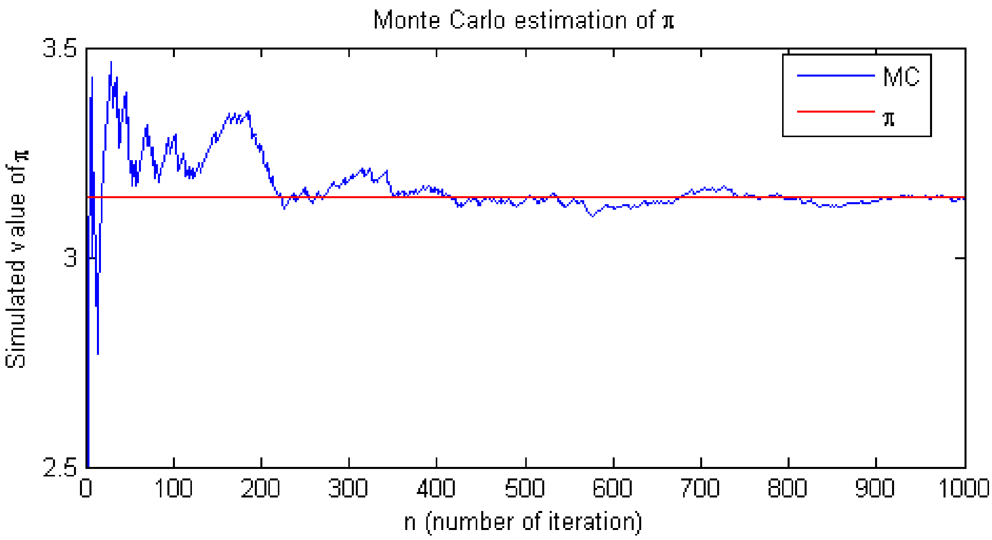

Figure A.4: Simulated values of π in the rain drop experiment.

Declaration

I, the undersigned, hereby declare that this dissertation work is my original work performed under the supervision of Dr.-Ing. Mohammad Abdo, has not been presented for a degree program in this or any other university. All sources of materials used for this dissertation work have been duly acknowledged.

Name: Murad Ridwan Hassen

Signature: ______________________________

Place: Addis Ababa, Ethiopia

Date: Aug 22, 2012.

This dissertation has been submitted for examination with my approval as a university advisor.

Name: Dr.-Ing. Mohammad Abdo

Signature: ______________________________

Place: Addis Ababa, Ethiopia

Date: ______________________________

References

[1] Frank B. Gross, *Smart Antennas for Wireless Communications With MATLAB*, McGraw-Hill, NY, 2005.

[2] Haykin, S., Ed., *Array Signal Processing*, Prentice Hall, New York, 1985.

[3] Johnson, D., and D. Dudgeon, *Array Signal Processing-Concepts and Techniques*, Prentice Hall, New Jersey, 1993.

[4] Trees, H.V., *Optimum Array Processing-Part IV of Detection, Estimation, and Modulation Theory*, Wiley Interscience, New York, 2002.

[5] Brookner, E., *Practical Phased-Array Antenna Systems*, Artech House, Boston, MA, 1991.

[6] Dudgeon, D.E., "Fundamentals of Digital Array Processing," *Proceedings of IEEE*, Vol. 65, pp. 898-904, June 1977.

[7] C. A. Balanis, *Antenna Theory: Analysis and Design*, 3rd ed. New York: Wiley, 2005.

[8] Kraus, J.D., and R.J. Marhefka, *Antennas for All Applications*, 3d ed., McGraw-Hill, New York, 2002.

[9] Lal Chand Godara, *Smart Antennas,* CRC Press, Boca Raton, New York, 2004.

[10] IEEE, "Special issue on active and adaptive antennas," *IEEE Trans. Antennas Propagat.*, 12, 1964.

[11] IEEE, "Special issue on adaptive antennas," *IEEE Trans. Antennas Propagat.*, 24, 1976.

[12] IEEE, "Special issue on beamforming," *IEEE J. Oceanic Eng.*, 10, 1985.

[13] IEEE, "Special issue on adaptive processing antenna systems," *IEEE Trans. Antennas Propagat.*, 34, 1986.

[14] IEEE, "Special issue on adaptive systems and applications," *IEEE Trans. Circuits Syst.*, 34, 1987.

[15] IEEE, "Special issue on underwater acoustic signal processing", *IEEE J. Oceanic Eng.*, 12, 1987.

[16] Hudson, J.E., *Adaptive Array Principles*, Peter Peregrins, New York, 1981.

[17] Monzingo, R. A. and Miller, T. W., *Introduction to Adaptive Arrays*, Wiley, New York, 1980.

[18] Widrow, B. et al., "Adaptive antenna systems", *IEEE Proc.*, 55, 2143-2158, 1967.

[19] Widrow, B. and Stearns, S.D., *Adaptive Signal Processing*, Prentice Hall, New York, 1985.

[20] Compton Jr., R.T., *Adaptive Antennas: Concepts and Performances*, Prentice Hall, New York, 1988.

[21] Godara, L.C., Ed., *Handbook of Antennas in Wireless Communications*, CRC Press, Boca Raton, FL, 2002.

[22] Marr, J.D., "A selected bibliography on adaptive antenna arrays," *IEEE Trans. Aerosp. Electron. Syst.*, 22, 781-788, 1986.

[23] M. Chryssomallis, "Smart Antennas," *IEEE Antennas and Propagation Magazine*, Vol. 42, No. 3, June 2000.

[24] Paulraj, A. J., et al., "Smart Antennas for Mobile Communications," in *Encyclopedia for Electrical Engineering*, John Wiley Publishing Co., 2000.

[25] Applebaum, S.P., "Adaptive arrays," *IEEE Trans. Antennas Propagat.*, 24, 585-598, 1976.

[26] dAssumpcao, H.A., "Some new signal processors for array of sensors," *IEEE Trans. Inf. Theory*, 26, 441-453, 1980.

[27] dAssumpcao, H.A. and Mountford, G.E., "An overview of signal processing for arrays of receivers," *J. Inst. Eng. Aust. IREE Aust.*, 4, 6-19, 1984.

[28] Gabriel, W.F., "Adaptive arrays: An introduction," *IEEE Proc.*, 64, 239-272, 1976.

[29] Haykin, S. et al., "Some aspects of array signal processing," *IEEE Proc.*, 139, Part F, 1-19, 1992.

[30] Krim, H. and Viberg, M., "Two decades of array signal processing: the parametric approach", *IEEE Signal Process. Mag.*, 13(4), 67-94, 1996.

[31] Maillous, R.J., "Phased array theory and technology," *IEEE Proc.*, 70, 246-291, 1982.

[32] Schultheiss, P.M., *Some lessons from array processing theory, in Aspects of Signal Processing, Part 1*, Tacconi, G., Ed., D. Reidel, Dordrecht, 309-331, 1977.

[33] Stark, L., "Microwave theory of phased-array antennas: a review," *IEEE Proc.*, 62, 1661-1701, 1974.

[34] Van Veen, B.D. and Buckley, K.M., "Beamforming: a versatile approach to spatial filtering," *IEEE ASSP Mag.*, 5, 4-24, 1988.

[35] Angeliki Alexiou and Martin Haardt, "Smart Antenna Technologies for Future Wireless Systems: Trends and Challenges," *IEEE Communications Magazine*, Sep., 2004.

[36] Mathieu Boutin, et al., "A Novel Interference Safety Margin for Cognitive Radio MANET using Smart Antennas," *Journal of Communications*, Vol. 4, No. 4, 257-265, May 2009.

[37] I. H. Winters, J. Salz, and R. D. Gitlin, "The Impact of Antenna Diversity on the Capacity of Wireless Communications Systems," *IEEE Transactions on Communications*, COM-42, 1740-1751, 1994.

[38] L. C. Godara, "Application of Antenna Arrays to Mobile Communications, Part II: Beam-Forming and Direction-of-Arrival Considerations," *Proceedings of the IEEE*, 85, 8, 1195-1245, August 1997.

[39] ArrayComm, *Smart Antenna Systems*, http://www.webproforum.com/smar_ant and www.arraycomm.com, IntelliCell®technology, May 2002.

[40] Widrow, B., McCool, J.M. and Ball, M., "The complex LMS algorithm," *IEEE Proc.*, 63, 719-720, 1975.

[41] Widrow, B. and McCool, J.M., "A comparison of adaptive algorithms based on the methods of steepest descent and random search," *IEEE Trans. Antennas Propagat.*, 24, 615-637, 1976.

[42] Griffiths, L.J., "A simple adaptive algorithm for real-time processing in antenna arrays," *IEEE Proc.*, 57, 1696-1704, 1969.

[43] Horowitz, L.L. and Senne, K.D., "Performance advantage of complex LMS for controlling narrowband adaptive arrays," *IEEE Trans. Circuits Syst.*, 28, 562-576, 1981.

[44] Iltis, R.A. and Milstein, L.B., "An approximate statistical analysis of the Widrow LMS algorithm with application to narrowband interference rejection," *IEEE Trans. Commn.*, 33, 121-130, 1985.

[45] Clarkson, P.M. and White, P.R., "Simplified analysis of the LMS adaptive filter using a transfer function approximation," *IEEE Trans. Acoust. Speech Signal Process.*, 35, 987-993, 1987.

[46] Feuer, A. and Weinstein, E., "Convergence analysis of LMS filters with uncorrelated Gaussian data," *IEEE Trans. Acoust. Speech Signal Process.*, 33, 222-229, 1985.

[47] Gardner, W.A., "Comments on convergence analysis of LMS filters with uncorrelated data," *IEEE Trans. Acoust. Speech Signal Process.*, 34, 378-379, 1986.

[48] Boland, F.B. and Foley, J.B., *Stochastic convergence of the LMS algorithm in adaptive systems*, Signal Process., 13, 339-352, 1987.

[49] Foley, J.B. and Boland, F.M., "A note on the convergence analysis of LMS adaptive filters with Gaussian data," *IEEE Trans. Acoust. Speech Signal Process.*, 36, 1087-1089, 1988.

[50] Solo, V., "The limiting behavior of LMS," *IEEE Trans. Acoust. Speech Signal Process.*, 37, 1909-1922, 1989.

[51] Jaggi, S. and Martinez, A.B., "Upper and lower bounds of the misadjustment in the LMS algorithm" *IEEE Trans. Acoust. Speech Signal Process.*, 38, 164-166, 1990.

[52] Solo, V., "The error variance of LMS with time-varying weights," *IEEE Trans. Signal Process.*, 40, 803-813, 1992.

[53] Reed, I.S., Mallett, J.D. and Brennan, L.E., "Rapid convergence rate in adaptive arrays," *IEEE Trans. Aerosp. Electron. Syst.*, 10, 853-863, 1974.

[54] Van Veen, B.D., "Adaptive convergence of linearly constrained beamformers based on the sample covariance matrix," *IEEE Trans. Signal Process.*, 39, 1470-1473, 1991.

[55] Horowitz, L.L., et al., "Controlling adaptive antenna arrays with the sample matrix inversion algorithm," *IEEE Trans. Aerosp. Electron. Syst.*, 15, 840-847, 1979.

[56] Haykin, S., *Adaptive Filter Theory*, 4th ed., Prentice Hall, New York, 2002.

[57] Golub,G.H., and C.H.Van Loan, *Matrix Computations*, The Johns Hopkins University Press, 3d ed., 1996.

[58] Gebauer, T. and Gockler, H.G., "Channel-individual adaptive beamforming for mobile satellite communications," *IEEE J. Selected Areas Commn.*, 13, 439-48, 1995.

[59] Lindskog, E., "Making SMI-beamforming insensitive to the sampling timing for GSM signals," *Proceedings of IEEE International Symposium on Personal, Indoor and Mobile Radio Communications*, 664-668, 1995.

[60] Vaughan, R.G., "On optimum combining at the mobile," *IEEE Trans. Vehicular Technol.*, 37, 181-188, 1988.

[61] Hashemi, H., "The indoor radio propagation channels," *IEEE Proc.*, 81, 943-968, 1993.

[62] Passerini, C., et al., "Adaptive antenna arrays for reducing the delay spread in indoor radio channels," *IEE Electron. Lett.*, 32, 280-281, 1996.

[63] D. N. Goddard, "Self-Recovering Equalization and Carrier Tracking in a Two-Dimensional Data Communication System," *IEEE Trans. Comm.*, vol. 28, pp. 1867-1875, 1980.

[64] J. R. Treichler and B. Agee, "A New Approach to Multipath Correction of Constant Modulus Signals," *IEEE Trans. Acoustic, Speech, and Signal Processing*, vol. ASSP-31, pp. 459-472, Apr. 1983.

[65] J. Litva and T. K.Y. Lo, *Digital Beamforming in Wireless Communications*, Artech House, Boston, 1996.

[66] Ohgane, T., "Characteristics of CMA adaptive array for selective fading compensation in digital land mobile radio communications," *Electron. Commn. (Jpn.)*, 74, 43-53, 1991.

[67] Ohgane, T., et al., "An implementation of a CMA adaptive array for high speed GMSK transmission in mobile communications," *IEEE Trans. Vehicular Technol.*, 42, 282-288, 1993.

[68] Ohgane, T., et al., "BER performance of CMA adaptive array for high-speed GMSK mobile communication: a description of measurements in central Tokyo," *IEEE Trans. Vehicular Technol.*, VT-42, 484-490, 1993.

[69] Tanaka, T., et al., "An ASIC implementation scheme to realize a beam space CMA adaptive array antenna," *IEICE Trans. Commn.*, E78-B, 1467-1473, Nov. 1995.

[70] Chiba, I., Chujo, W. and Fujise, M., "Beamspace constant modulus algorithm adaptive array antennas," *IEEE 8th Int. Conf. Antennas Propagat.*, 975-978, 1993.

[71] Wang, Y. and Cruz, J.R., "Adaptive antenna arrays for the reverse link of CDMA cellular communication systems," *IEE Electron. Lett.*, 30, 1017-1018, 1994.

[72] Larimore, M., and J. Treichler, "Convergence Behavior of the Constant Modulus Algorithm, Acoustics," *IEEE International Conference on ICASSP'83*, Vol. 8, pp. 13-16, April 1983.

[73] Parra, I., Xu, G. and Liu, H., "Least squares projective constant modulus approach," *Proceedings of IEEE International Symposium on Personal, Indoor and Mobile Radio Communications*, 673-676, 1995.

[74] Nishimori, K., Kikuma, N. and Inagaki, N., "The differential CMA adaptive array antenna using an eigen-beamspace system," *IEICE Trans. Commn.*, E78-B, 1480-1488, 1995.

[75] Capon, J., "High-Resolution Frequency-Wavenumber Spectrum Analysis," *Proceedings of the IEEE*, Vol. 57, No. 8, pp. 1408-1418, Aug. 1969.

[76] Johnson, D., "The Application of Spectral Estimation Methods to Bearing Estimation Probems," *Proceedings of the IEEE*, Vol. 70, No. 9, pp. 1018-1028, Sept. 1982.

[77] Van Trees, H., *Optimum Array Processing: Part IV of Detection, Estimation, and Modulation Theory*, Wiley Interscience, New York, 2002.

[78] Stoica, P., and R. Moses, *Introduction to Spectral Analysis*, Prentice Hall, New York, 1997.

[79] R. Kohno, C. Yim and H. Imai, "Array Antenna Beamforming Based on Estimation on Arrival Angles Using DFT on Spatial Domain," *Proceedings of PIMRC*, London, UK, September 1991,pp. 38-43.

[80] M. Nagatsuka, N. Ishii, R. Kohno and H. Imai, "Adaptive Array Antenna Based on Spatial Spcetral Estimation Using Maximum Entropy Method," *IEEE Transactions on Communications*, E77-B, 5, 1994, pp. 624-633.

[81] R.O. Schmidt, "Multiple Emitter Location and Signal Parameter Estimation," *IEEE Transactions on Antennas and Propagation*, AP-34, 3, March 1986, pp. 276-280.

[82] A. El Zooghhy, C. G. Christodoulou, and M. Georgiopoulos, "Performance of Radial Basis Function Networks for Direction of Arrival Estimation with Antenna Arrays," *IEEE Transactions on Antennas and Propagation*, AP-45, 11, November 1997, pp. 1611-1617.

[83] Fabre, P. and Gueguen, C., "Improvement of the fast recursive least-squares algorithms via normalization: a comparative study," *IEEE Trans. Acoust. Speech Signal Process.*, 34, 296-308, 1986.

[84] Gardner, W.A. and Brown III, W.A., "A new algorithm for adaptive arrays," *IEEE Trans. Acoust. Speech Signal Process.*, 35, 1314-1319, 1987.

[85] Fernandez, J., Corden, I.R. and Barrett, M., "Adaptive array algorithms for optimal combining in digital mobile communication systems," *Proceedings of IEEE International Conference on Antennas and Propagation,* 983-986, 1993.

[86] Cioffi, J.M. and Kailath, T., "Fast recursive-least-square, transversal filters for adaptive filtering," *IEEE Trans. Acoust. Speech Signal Process.*, 32, 998-1005, 1984.

[87] Roy, R., and T. Kailath, "ESPRIT-Estimation of Signal Parameters Via Rotational Invariance Techniques," *IEEE Transactions on ASSP*, Vol. 37, No. 7, pp. 984-995, July 1989.

[88] FCC, *Spectrum Policy Task Force*, ET Docket 02-135, Nov. 2002.

[89] QinetiQ Proprietary, *Cognitive Radio Technology - A Study for Ofcom*, Feb. 2007.

[90] Federal Communications Commission, *Facilitating opportunities for flexible, efficient, and reliable spectrum use employing cognitive radio technologies, notice of proposed rule making and order, FCC 03-322,* Dec. 2003.

[91] M. M. Buddhikot, "Understanding dynamic spectrum access: models, taxonomy and challenges," *Proceedings of IEEE International Symposium on New Frontiers in Dynamic Spectrum Access Networks (DySPAN)*, April 2007, pp. 649-663.

[92] Ekram Hossain, Dusit Niyato and Zhu Han, *Dynamic Spectrum Access and Management in Cognitive Radio Networks,* Cambridge University Press, 2009.

[93] Bruce A. Fette (ed.), *Cognitive Radio Technology*, Elsevier Inc., 2006.

[94] F. K. Jondral, "Software-defined radio: basics and evolution to cognitive radio," *EURASIP Journal on Wireless Communications and Networking*, vol. 5, no. 3, pp. 275-283, 2005.

[95] Hüseyin Arslan (ed.),*Cognitive Radio, Software Defined Radio, and Adaptive Wireless Systems*, Springer, 2007.

[96] I. Mitola, J. and J. Maguire, G. Q., "Cognitive radio: making software radios more personal," *IEEE Personal Commun. Mag.*, vol. 6, no. 4, pp. 1318, Aug. 1999.

[97] S. Haykin, "Cognitive radio: Brain-empowered wireless communications," *IEEE J. Sel. Areas Commun.*, vol 23, pp. 201-220, Feb. 2005.

[98] M. Marcus, "Real time spectrum markets and interruptible spectrum: new concepts of spectrum use enabled by cognitive radio," *First IEEE International Symposium on Dynamic Spectrum Access Networks, DySPAN*, 2005, pp. 512-517.

[99] S. Haykin, David J. Thomson and Jeffrey H. Reed, "Spectrum Sensing for Cognitive Radio," *IEEE Proc.*, vol. 97, N0. 5, May 2009.

[100] Tevfik Yücek and Hüseyin Arslan, "A Survey of Spectrum Sensing Algorithms for Cognitive Radio Applications," *IEEE Communications Surveys & Tutorials*, vol. 11, no. 1, first quarter 2009.

[101] P. Kolodzy et al., "Next generation communications: Kickoff meeting," *Proc. DARPA*, Oct. 2001.

[102] S. Shankar, C. Cordeiro, and K. Challapali, "Spectrum agile radios: utilization and sensing architectures," *Proc. IEEE Int. Symposium on New Frontiers in Dynamic Spectrum Access Networks*, Baltimore, Maryland, USA, Nov. 2005, pp. 160-169.

[103] Y. Yuan, P. Bahl, R. Chandra, P. A. Chou, J. I. Ferrell, T. Moscibroda, S. Narlanka, and Y. Wu, "KNOWS: Cognitive radio networks over white spaces," *Proc. IEEE Int. Symposium on New Frontiers in Dynamic Spectrum Access Networks*, Dublin, Ireland, Apr. 2007, pp. 416-427.

[104] J. Lehtomaki, J. Vartiainen, M. Juntti, and H. Saarnisaari, "Spectrum sensing with forward methods," *Proc. IEEE Military Commun. Conf.*, Washington, D.C., USA, Oct. 2006, pp. 1-7.

[105] J. Lehtomaki, M. Juntti, H. Saarnisaari, and S. Koivu, "Threshold setting strategies for a quantized total power radiometer," *IEEE Signal Processing Lett.*, vol. 12, no. 11, pp. 796-799, Nov. 2005.

[106] G. Ganesan and Y. Li, "Agility improvement through cooperative diversity in cognitive radio," *Proc. IEEE Global Telecomm. Conf. (Globecom)*, vol. 5, St. Louis, Missouri, USA, Nov./Dec. 2005, pp. 2505-2509.

[107] P. Wang, L. Xiao, S. Zhou, and J. Wang, "Optimization of detection time for channel efficiency in cognitive radio systems," *Proc. IEEE Wireless Commun. and Networking Conf.*, Hong Kong, Mar. 2007, pp. 111-115.

[108] D. Cabric, A. Tkachenko, and R. Brodersen, "Spectrum sensing measurements of pilot, energy, and collaborative detection," *Proc. IEEE Military Commun. Conf.*, Washington, D.C., USA, Oct. 2006, pp. 1-7.

[109] Y. Yuan, P. Bahl, R. Chandra, P. A. Chou, J. I. Ferrell, T. Moscibroda, S. Narlanka, and Y. Wu, "KNOWS: Cognitive radio networks over white spaces," *Proc. IEEE Int. Symposium on New Frontiers in Dynamic Spectrum Access Networks*, Dublin, Ireland, Apr. 2007, pp. 416-427.

[110] F. Weidling, D. Datla, V. Petty, P. Krishnan, and G. Minden, "A framework for RF spectrum measurements and analysis," *Proc. IEEE Int. Symposium on New Frontiers in Dynamic Spectrum Access Networks*, vol. 1, Baltimore, Maryland, USA, Nov. 2005, pp. 573-576.

[111] A. Ghasemi and E. Sousa, "Optimization of spectrum sensing for opportunistic spectrum access in cognitive radio networks," *Proc. IEEE Consumer Commun. and Networking Conf.*, Las Vegas, Nevada, USA, Jan. 2007, pp. 1022-1026.

[112] D. Datla, R. Rajbanshi, A. M. Wyglinski, and G. J. Minden, "Parametric adaptive spectrum sensing framework for dynamic spectrum access networks," *Proc. IEEE Int. Symposium on New Frontiers in Dynamic Spectrum Access Networks*, Dublin, Ireland, Apr. 2007, pp. 482-485.

[113] S. Geirhofer, L. Tong, and B. Sadler, "Dynamic spectrum access in the time domain: Modeling and exploiting white space," *IEEE Commun.Mag.*, vol. 45, no. 5, pp. 66-72, May 2007.

[114] F. Digham, M. Alouini, and M. Simon, "On the energy detection of unknown signals over fading channels," *Proc. IEEE Int. Conf. Commun.*, vol. 5, Seattle, Washington, USA, May 2003, pp. 3575-3579.

[115] P. Qihang, Z. Kun, W. Jun, and L. Shaoqian, "A distributed spectrum sensing scheme based on credibility and evidence theory in cognitive radio context," *Proc. IEEE Int. Symposium on Personal, Indoor and Mobile Radio Commun.*, Helsinki, Finland, Sept. 2006, pp. 1-5.

[116] M. Wylie-Green, "Dynamic spectrum sensing by multiband OFDM radio for interference mitigation," *Proc. IEEE Int. Symposium on New Frontiers in Dynamic Spectrum Access Networks*, Baltimore, Maryland, USA, Nov. 2005, pp. 619-625.

[117] P. Papadimitratos, S. Sankaranarayanan, and A. Mishra, "A bandwidth sharing approach to improve licensed spectrum utilization," *IEEE Commun. Mag.*, vol. 43, no. 12, pp. 10-14, Dec. 2005.

[118] T. Yücek and H. Arslan, "Spectrum characterization for opportunistic cognitive radio systems," *Proc. IEEE Military Commun. Conf.*, Washington, D.C., USA, Oct. 2006, pp. 1-6.

[119] H. Tang, "Some physical layer issues of wide-band cognitive radio systems," *Proc. IEEE Int. Symposium on New Frontiers in Dynamic Spectrum Access Networks*, Baltimore, Maryland, USA, Nov. 2005, pp. 151-159.

[120] H. Urkowitz, "Energy detection of unknown deterministic signals," *Proc. IEEE*, vol. 55, pp. 523-531, Apr. 1967.

[121] A. Sahai, R. Tandra, S. M. Mishra, and N. Hoven, "Fundamental design tradeoffs in cognitive radio systems," *Proc. of Int. Workshop on Technology and Policy for Accessing Spectrum*, Aug. 2006.

[122] S. t. B. S. M. Mishra, R. Mahadevappa, and R. W. Brodersen, "Cognitive technology for ultra-wideband/WiMax coexistence," *Proc. IEEE Int. Symposium on New Frontiers in Dynamic Spectrum Access Networks*, Dublin, Ireland, Apr. 2007, pp. 179-186.

[123] N. Khambekar, L. Dong, and V. Chaudhary, "Utilizing OFDM guard interval for spectrum sensing," *in Proc. IEEE Wireless Commun. and Networking Conf.*, Hong Kong, Mar. 2007, pp. 38-42.

[124] M. Oner and F. Jondral, "Cyclostationarity based air interface recognition for software radio systems," *in Proc. IEEE Radio and Wireless Conf.*, Atlanta, Georgia, USA, Sept. 2004, pp. 263-266.

[125] ___, "Cyclostationarity-based methods for the extraction of the channel allocation information in a spectrum pooling system," *in Proc. IEEE Radio and Wireless Conf.*, Atlanta, Georgia, USA, Sept. 2004, pp. 279-282.

[126] M. Ghozzi, F. Marx, M. Dohler, and J. Palicot, "Cyclostationarity based test for detection of vacant frequency bands," *in Proc. IEEE Int. Conf. Cognitive Radio Oriented Wireless Networks and Commun. (Crowncom)*, Mykonos Island, Greece, June 2006.

[127] N. Han, S. H. Shon, J. H. Chung, and J. M. Kim, "Spectral correlation based signal detection method for spectrum sensing in IEEE 802.22 WRAN systems," *in Proc. IEEE Int. Conf. Advanced Communication Technology,* vol. 3, Feb. 2006.

[128] J. Lundén, V. Koivunen, A. Huttunen, and H. V. Poor, "Spectrum sensing in cognitive radios based on multiple cyclic frequencies," *in Proc. IEEE Int. Conf. Cognitive Radio Oriented Wireless Networks and Commun. (Crowncom)*, Orlando, Florida, USA, July/Aug. 2007.

[129] K. Kim, I. A. Akbar, K. K. Bae, J.-S. Um, C. M. Spooner, and J. H. Reed, "Cyclostationary approaches to signal detection and classification in cognitive radio," *in Proc. IEEE Int. Symposium on New Frontiers in Dynamic Spectrum Access Networks*, Dublin, Ireland, Apr. 2007, pp. 212-215.

[130] M. Gandetto and C. Regazzoni, "Spectrum sensing: A distributed approach for cognitive terminals," *IEEE J. Select. Areas Commun.*, vol. 25, no. 3, pp. 546-557, Apr. 2007.

[131] Z. Tian and G. B. Giannakis, "A wavelet approach to wideband spectrum sensing for cognitive radios," *in Proc. IEEE Int. Conf. Cognitive Radio Oriented Wireless Networks and Commun. (Crowncom)*, Mykonos Island, Greece, June 2006.

[132] Z. Tian and G. Giannakis, "Compressed sensing for wideband cognitive radios," *in Proc. IEEE Int. Conf. on Acoustics, Speech, and Signal Processing*, vol. 4, Honolulu, Hawaii, USA, Apr. 2007, pp. 1357-1360.

[133] M. P. Olivieri, G. Barnett, A. Lackpour, and A. Davis, "A scalable dynamic spectrum allocation system with interference mitigation for teams of spectrally agile software defined radios," *in Proc. IEEE Int. Symposium on New Frontiers in Dynamic Spectrum Access Networks*, Baltimore, Maryland, USA, Nov. 2005, pp. 170-179.

[134] K. Challapali, S. Mangold, and Z. Zhong, "Spectrum agile radio: Detecting spectrum opportunities," *in Proc. Int. Symposium on Advanced Radio Technologies*, Boulder, Colorado, USA, Mar. 2004.

[135] S. Geirhofer, L. Tong, and B. Sadler, "A measurement-based model for dynamic spectrum access in WLAN channels," *in Proc. IEEE Military Commun. Conf.*, Washington, D.C., USA, Oct. 2006.

[136] S. Lal and A. Mishra, "A look ahead scheme for adaptive spectrum utilization," *in Proc. IEEE Radio and Wireless Conf.*, Boston, Massachusetts, USA, Aug. 2003, pp. 83-86.

[137] S. Geirhofer, B. Sadler, and L. Tong, "Dynamic spectrum access in WLAN channels: Empirical model and its stochastic analysis," *in Proc. of Int. Workshop on Technology and Policy for Accessing Spectrum*, Boston, Massachusetts, USA, Aug. 2006.

[138] A. Ghasemi and E. Sousa, "Collaborative spectrum sensing for opportunistic access in fading environments," *in Proc. IEEE Int. Symposium on New Frontiers in Dynamic Spectrum Access Networks*, Baltimore, Maryland, USA, Nov. 2005, pp. 131-136.

[139] U. Gardner, WA, "Exploitation of spectral redundancy in cyclostationary signals," *IEEE Signal Processing Mag.*, vol. 8, no. 2, pp. 14-36, 1991.

[140] K. Maeda, A. Benjebbour, T. Asai, T. Furuno, and T. Ohya, "Recognition among OFDM-based systems utilizing cyclostationarity-inducing transmission," *in Proc. IEEE Int. Symposium on New Frontiers in Dynamic Spectrum Access Networks*, Dublin, Ireland, Apr. 2007, pp. 516-523.

[141] P. D. Sutton, K. E. Nolan, and L. E. Doyle, "Cyclostationary signatures for rendezvous in OFDM-based dynamic spectrum access networks," *in Proc. IEEE Int. Symposium on New Frontiers in Dynamic Spectrum Access Networks*, Dublin, Ireland, Apr. 2007, pp. 220-231.

[142] P. D. Sutton, J. Lotze, K. E. Nolan, and L. E. Doyle, "Cyclostationary signature detection in multipath rayleigh fading environments," *in Proc. IEEE Int. Conf. Cognitive Radio Oriented Wireless Networks and Commun. (Crowncom)*, Orlando, Florida, USA, Aug. 2007.

[143] A. Fehske, J. Gaeddert, and J. Reed, "A new approach to signal classification using spectral correlation and neural networks," *in Proc. IEEE Int. Symposium on New Frontiers in Dynamic Spectrum Access Networks*, Baltimore, Maryland, USA, Nov. 2005, pp. 144-150.

[144] M. K. Tsatsanis and G. B. Giannakis, "Transmitter induced cyclostationarity for blind channel equalization," *IEEE Trans. Signal Processing*, vol. 45, no. 7, pp. 1785-1794, July 1997.

[145] A. Tkachenko, D. Cabric, and R. W. Brodersen, "Cyclostationary feature detector experiments using reconfigurable BEE2," *in Proc. IEEE Int. Symposium on New Frontiers in Dynamic Spectrum Access Networks*, Dublin, Ireland, Apr. 2007, pp. 216-219.

[146] M. Mehta, N. Drew, G. Vardoulias, N. Greco, and C. Niedermeier, "Reconfigurable terminals: an overview of architectural solutions," *IEEE Commun. Mag.*, vol. 39, no. 8, pp. 82-89, 2001.

[147] J. Palicot and C. Roland, "A new concept for wireless reconfigurable receivers," *IEEE Commun. Mag.*, vol. 41, no. 7, pp. 124-132, 2003.

[148] J. G. Proakis, *Digital Communications*, 4th ed. McGraw-Hill, 2001.

[149] R. Tandra and A. Sahai, "Fundamental limits on detection in low SNR under noise uncertainty," *in Proc. IEEE Int. Conf. Wireless Networks, Commun. and Mobile Computing*, vol. 1, Maui, HI, June 2005, pp.464-469.

[150] Y. Zeng and Y.-C. Liang, "Covariance based signal detections for cognitive radio," *in Proc. IEEE Int. Symposium on New Frontiers in Dynamic Spectrum Access Networks*, Dublin, Ireland, Apr. 2007, pp. 202-207.

[151] Y. Hur, J. Park, W. Woo, K. Lim, C. Lee, H. Kim, and J. Laskar, "A wideband analog multi-resolution spectrum sensing (MRSS) technique for cognitive radio (CR) systems," *in Proc. IEEE Int. Symp. Circuits and Systems*, Island of Kos, Greece, May 2006, pp. 4090-4093.

[152] Y. Youn, H. Jeon, J. Choi, and H. Lee, "Fast spectrum sensing algorithm for 802.22 WRAN systems," *in Proc. IEEE Int. Symp. Commun. and Information Techn.*, Bangkok, Thailand, Oct. 2006, pp. 960-964.

[153] Y. Hur, J. Park, K. Kim, J. Lee, K. Lim, C. Lee, H. Kim, and J. Laskar, "A cognitive radio (CR) testbed system employing a wideband multiresolution spectrum sensing (MRSS) technique," *in Proc. IEEE Veh. Technol. Conf.*, Montreal, Quebec French, Canada, Sept. 2006, pp. 1-5.

[154] A. Goldsmith, S. Jafar, I. Maric, and S. Srinivasa, "Breaking Spectrum Gridlock With Cognitive Radios: An Information Theoretic Perspective," *Invited Paper, Proceedings of the IEEE*, Vol. 97, No. 5, pp. 894-914, May 2009.

[155] Jing Lv and Eduard Jorswieck (editors), *Advanced coexistence technologies for radio optimisation in licensed and unlicensed spectrum (ACROPOLIS)*, Document Number D13.1, Technical University of Dresden (TUD), March 2012.

[156] G. Scutari, D. Palomar, J.-S. Pang, and F. Facchinei, "Flexible design of cognitive radio wireless systems," *IEEE Signal Process. Mag.*, vol. 26, no. 5, pp. 107-123, Sep. 2009.

[157] R. Zhang and Y.-C. Liang, "Exploiting multi-antennas for opportunistic spectrum sharing in cognitive radio networks," *IEEE J. Sel. Topics in Signal Process.*, vol. 2, no. 1, pp. 88-102, Feb. 2008.

[158] R. Zhang and S. Cui, "Cooperative interference management with MISO beamforming," *IEEE Trans. on Signal Processing*, vol. 58, no. 10, pp. 5450-5458, Oct. 2010.

[159] R. Zhang, Y.-C. Liang, and S. Cui, "Dynamic resource allocation in cognitive radio networks," *IEEE Signal Process. Mag.*, vol. 27, no. 3, pp. 102-114, May 2010.

[160] J. Lv and E. A. Jorswieck, "Spatial shaping in cognitive system with coded legacy transmission," *in Proc. of International ITG Workshop on Smart Antennas (WSA)*, Feb. 2011.

[161] J. R. Hoffman, M. G. Cotton, R. J. Achatz, R. N. Statz, and R. A. Dalkejnm, "Measurements to Determine Potential Interference to GPS Receivers from Ultra-wideband Transmission Systems," *NTIA Report TR-01-384*, February 2001.

[162] M. Hamalainen, V. Hovinen, R. Tesi, J. H. J. Iinatti, and M. Latva-aho, "On the UWB system coexistence with GSM900, UMTS/WCDMA, and GPS," *IEEE Journal on Selected Areas in Communications*, vol. 20, no. 9, pp. 1712-1721, September 2002.

[163] M. G. Di Benedetto and G. Giancola, *Understanding Ultra Wide Band Radio Fundamentals,* Prentice Hall, 2004.

[164] Y. Wang, X. Dong, and I. J. Fair, "Spectrum Shaping and NBI Suppression in UWB Communications," *IEEE Transactions on Wireless Communications*, vol. 6, no. 5, pp. 1944-1952, May 2007.

[165] J. A. Ney da Silva and M. L. R. de Campos, "Spectrally Efficient UWB Pulse Shaping With Application in Orthogonal PSM," *IEEE Transactions on Communications*, vol. 55, no. 2, pp. 313-322, February 2007.

[166] M. Abtahi, J. Magne, M. Mirshafiei, L.A. Rusch, and S. LaRochelle, "Generation of Power-Efficient FCC-Compliant UWB Waveforms Using FBGs: Analysis and Experiment," *Journal of Lightwave Technology*, vo. 26, no.5, pp. 628-635, March 2008.

[167] M.-G. Di Benedetto and L. De Nardis, "Tuning UWB Signals by Pulse Shaping: Towards context-aware wireless networks," *Special Issue on Signal Processing in UWB Communications, Signal processing*, Elsevier Publishers, vo. 86, no. 9, pp. 2172-2184, September 2006.

[168] M. Biagi and V. Polli, "Ultra Wide Band Cognitive Pulse Shaping under Physical-Layer QoS Constraints," *IEEE Transactions on Communications*, vol. 59, no. 11, pp. 3167-3176, November 2011.

[169] S. Gambini, L. De Nardis, E. Alon, and J. Rabaey, "Interference robust self-mixing UWB systems using phase-domain spreading," *IEEE International Conference on UWB 2011 (ICUWB2011)*, Bologna, Italy, September 2011.

[170] D. Leenaerts, R. van de Beek, J. Bergervoet, H. Kundur, and G. van der Weide, "WiMedia UWB technology: 480Mb/s wireless USB," *IEEE International Workshop on Radio-Frequency Integration Technology (RFIT)*, 2007.

[171] B. Fa, F.-J. Han, A.-M. Zhang, and F.-J. Han, "Spectrum sensing in MB-OFDM based cognitive UWB systems coexistence with WiMax," *11th IEEE Singapore International Conference on Communication Systems (ICCS)*, pp. 203-207, Nov. 2008.

[172] L. Feng, B. Li, W.-X. Zou, Z. Zhou, and X.-J. Huang, "Interference analysis for UWB coexistence with 3.5GHz WiMAX system," *International Symposium on Communications and Information Technologies (ISCIT)*, Oct. 2010.

[173] M. Li, D.-Q. Wang, Y.-X. Song, and Y.-Y. Yang, "Cognitive radio-based interference avoidance schemes for MB-OFDM UWB," *IEEE International Conference on Information Theory and Information Security (ICITIS)*, Dec. 2010.

[174] N. Devroye, P. Mitran, and V. Tarokh, "Achievable rates in cognitive radio channels," *IEEE Trans. on Information Theory*, vol. 52, no. 5, pp. 1813-1827, May 2006.

[175] W. Wu, S. Vishwanath, and A. Arapostathis, "Capacity of a class of cognitive radio channels: Interference channels with degraded message sets," *IEEE Trans. on Information Theory*, vol. 53, no. 11, pp. 4391-4399, Nov. 2007.

[176] A. Jovicic and P. Viswanath, "Cognitive radio: An information-theoretic perspective," *IEEE Trans. on Information Theory*, vol. 55, no. 9, pp. 3945-3958, Sept. 2009.

[177] I. Maric, R. Yates, and G. Kramer, "Capacity of interference channels with partial transmitter cooperation," *IEEE Trans. on Information Theory*, vol. 53, no. 10, pp. 3536-3548, Oct. 2007.

[178] E. Hossain, L. Le, N. Devroye, and M. Vu, "Cognitive Radio: From Theory to Practical Network Engineering," *in New Directions in Wireless Communications Research*. Springer, 2009, ch. 10, pp. 251-289.

[179] M. Costa, "Writing on dirty paper," *IEEE Trans. Inf. Theory*, vol. 29, no. 3, pp. 439-441, May 1983.

[180] N. Michelusi, O. Simeone, M. Levorato, P. Popovski, and M. Zorzi, "Optimal cognitive transmission exploiting redundancy in primary ARQ process," *in Proc. Workshop on Inf. Theory and Applications (ITA)*.

[181] R. A. Tannious and A. Nosratinia, "Cognitive radio protocols based on exploiting hybrid ARQ retransmissions," *IEEE Transactions on Wireless Communications*, vol. 9, no. 9, Sept. 2012.

[182] Y. Han, A. Pandharipande, and S. Ting, "Cooperative decode-and-forward relaying for secondary spectrum access," *IEEE Transactions on Wireless Communications*, vol. 8, no. 10, pp. 4945-4950, Oct. 2009.

[183] Y. Li, P. Wang, and D. Niyato, "Optimal power allocation for secondary users in cognitive relay networks," *in Proc. IEEE Wireless Communications and Networking Conf. (WCNC)*, Mar. 2011, pp. 862-867.

[184] A. Ghasemi, et al., "Opportunistic Spectrum Access in Fading Channels through Collaborative Sensing," *IEEE Journal of Communications*, vol. 2, no. 2, pp. 71-81, March 2007.

[185] Federal Communications Commision, Tech. Rep. 08-260, Nov. 2008. Available: hraunfoss.fcc.gov/edocs public/attachmatch/FCC-08-260A1.pdf

[186] Federal Communications Commision, *Memorandam Opinion and Order on Reconstruction of the Seventh Report and Order and Eighth report and Order*, Tech. Rep. 08-72, Mar. 2008. Available: hraunfoss.fcc.gov/edocs_public/attachmatch/FCC-08-72A1.pdf

[187] Federal Communications Commission, *List of All Class A, LPTV, and TV Translator Stations,* Tech. Rep., 2008. Available: www.dtv.gov/MasterLowPowerList.xls

[188] *Report C from CEPT to the European Commission in response to the mandate on Technical considerations regarding harmonisation options for the digital dividend,* CEPT-ECC, Tech. Rep., Jun 2008.

[189] V. R. Petty, R. Rajbanshi, D. Datla et al., "Feasibility of dynamic spectrum access in underutilized television bands," *in Proceedings of IEEE International Symposium on New Frontiers in Dynamic Spectrum Access Networks (DySPAN)*, April 2007, pp. 331-339.

[190] J. F. Hauris, "Genetic algorithm optimization in a cognitive radio for autonomous vehicle communications," *in Proceedings of IEEE International Symposium on Computational Intelligence in Robotics and Automation (CIRA)*, June 2007, pp. 427-431.

[191] R.D. Hinman, "Application of cognitive radio technology to legacy military waveforms in a JTRS (joint tactical radio system) radio," *in Proceedings of IEEE Military Communications Conference (MILCOM)*, October 2006.

[192] H. Kim and K. G. Shin, "Efficient discovery of spectrum opportunities with MAC-layer sensing in cognitive radio networks," *IEEE Transactions on Mobile Computing*, vol. 7, no. 5, pp. 533-545, 2008.

[193] Q.Wang and H. Zheng, "Route and spectrum selection in dynamic spectrum networks," *in Proceedings of 3rd IEEE Consumer Communications and Networking Conference (CCNC)*, vol. 1, January 2006, pp. 625-629.

[194] C. Xin, "A novel layered graph model for topology formation and routing in dynamic spectrum access networks," *in Proceedings of IEEE International Symposium on New Frontiers in Dynamic Spectrum Access Networks (DySPAN)*, November 2005, pp. 308-317.

[195] J. Zhao, H. Zheng, and G.-H. Yang, "Distributed coordination in dynamic spectrum allocation networks," *in Proceedings of IEEE International Symposium on New Frontiers in Dynamic Spectrum Access Networks (DySPAN)*, November 2005, pp. 259-268.

[196] A. M. R. Slingerland, P. Pawelczak, R.V. Prasad, A. Lo, and R. Hekmat, "Performance of transport control protocol over dynamic spectrum access links," *in Proceedings of IEEE International Symposium on New Frontiers in Dynamic Spectrum Access Networks (DySPAN)*, April 2007, pp. 486-495.

[197] A. Maharshi, L. Tong, and A. Swami, "Cross-layer designs of multichannel reservation MAC under Rayleigh fading," *IEEE Transactions on Signal Processing*, vol. 51, no. 8, pp. 2054-2067, 2003.

[198] J.Wang, L. Li, S. H. Low, and J. C. Doyle, "Cross-layer optimization in TCP/IP networks," *IEEE/ACM Transactions on Networking*, vol. 13, no. 3, pp. 582-595, 2005.

[199] N. Baldo and M. Zorzi, "Fuzzy logic for cross-layer optimization in cognitive radio networks," *in Proceedings of Consumer Communications and Networking Conference (CCNC)*, January 2007, pp. 1128-1133.

[200] C. Clancy, J. Hecker, E. Stuntebeck, and T. O'Shea, "Applications of machine learning to cognitive radio networks," *IEEE Wireless Communications*, vol. 14, no. 4, pp. 47-52, 2007.

[201] G. Xu and Y. Lu, "Channel and modulation selection based on support vector machines for cognitive radio," *in Proceedings of IEEE International Conference on Wireless Communications, Networking and Mobile Computing (WiCOM)*, September 2006.

[202] A. Ginsberg, J.D. Poston, andW.D. Horne, "Toward a cognitive radio architecture: integrating knowledge representation with software defined radio technologies," *in Proceedings of IEEE Military Communications Conference (MILCOM)*, October 2006.

[203] P. Jackson, *Introduction to Expert Systems.* Addison Wesley, 1998.

[204] L. R. Rabiner, "A tutorial on hidden Markov models and selected applications in speech recognition," *in Proceedings of the IEEE*, vol. 77, no. 2, February 1989, pp. 257-286.

[205] S. Haykin, *Neural Networks: A Comprehensive Foundation.* Prentice Hall, 1998.

[206] R. S. Sutton and A. G. Barto, *Reinforcement Learning: An Introduction.* MIT Press, 1998.

[207] D. E. Goldberg, *Genetic Algorithms in Search, Optimization, and Machine Learning.* Addison-Wesley, 1989.

[208] D. A. Levine, I. F. Akyildiz, and M. Naghshineh, "A resource estimation and call admission algorithm for wireless multimedia networks using the shadow cluster concept," *IEEE/ACM Transactions on Networking*, vol. 5, no. 1, pp. 1-12, 1997.

[209] A. Aljadhai and T. F. Znati, "Predictive mobility support for QoS provisioning in mobile wireless environments," *IEEE Journal on Selected Areas in Communications*, vol. 19, no. 10, pp. 1915-1930, 2001.

[210] H. Celebi and H. Arslan, "Adaptive positioning systems for cognitive radios," *in Proceedings of IEEE International Symposium on New Frontiers in Dynamic Spectrum Access Networks (DySPAN)*, April 2007, pp. 78-84.

[211] H. Celebi and H. Arslan, "Cognitive positioning systems," *IEEE Transactions on Wireless Communications*, vol. 6, no. 12, pp. 4475-4483, 2007.

[212] H. Celebi and H. Arslan, "Utilization of location information in cognitive wireless networks," *IEEE Wireless Communications*, vol. 14, no. 4, pp. 6-13, 2007.

[213] S. Yarkan and H. Arslan, "Exploiting location awareness toward improved wireless system design in cognitive radio," *IEEE Communications Magazine*, vol. 46, no. 1, pp. 128-136, 2008.

[214] M. J. Marcus, P.Kolodzy, and A. Lippman, "Reclaiming the vast wasteland: why unlicensed use of the white space in the TV bands will not cause interference to DTV viewers," *New America Foundation: Wireless Future Program, Report*, 2005.

[215] Y. Rahmat-Samii and E. Michielssen, eds., *Electromagnetic Optimization by Genetic Algorithms*, New York: Wiley, 1999.

[216] J. M. Johnson and Y. Rahmat-Samii, "Genetic Algorithms in Engineering Electromagnetic," *IEEE Antennas Propag. Mag.*, vol. 39, no. 4, pp. 7-25, 1997.

[217] D. E. Goldberg, *Genetic Algorithms in Search, Optimization and Machine Learning*, Reading, MA: Addison-Wesley, 1989.

[218] D. W. Boeringer, D. H.Werner, and D. W. Machuga, "A simultaneous parameter adaptation scheme for genetic algorithms with application to phased array synthesis," *IEEE Trans. Antennas Propag.*, vol. 53, pp. 356-371, Jan. 2005.

[219] W. P. Liao and F. L. Chu, "Array pattern synthesis with null steering using genetic algorithm by controlling only the current amplitudes," *Int. J. Elect.*, vol. 86, no. 4, pp. 445-457, 1999.

[220] B. K. Yeo and Y. Lu, "Array failure correction with a genetic algorithm," *IEEE Trans. Antennas Propag.*, vol. 47, no. 5, pp. 823-828, May 1999.

[221] K. K. and Y. Lu, "Side-lobe reduction in array-pattern synthesis using genetic algorithm," *IEEE Trans. Antennas Propag.*, vol. 45, no. 7, pp. 1117-1121, Jul. 1997

[222] W.L. Weeks, *Antenna Engineering*, McGraw-Hill, New York, 1968.

[223] Francisco J. Ares-Pena, Juan A. Rodriguez-Gonzalez, E. Villanueva-Lopez, and S. R. Rengarajan, "Genetic Algorithms in the Design and Optimization of Antenna Array Patterns," *IEEE Trans. Antennas Propagat.*, vol. 47, no. 3, March 1999.

[224] Ridwan, Murad; Abdo, Mohammed; Jorswieck, E.;, "Design of non-uniform antenna arrays using genetic algorithm," *The 13th International Conference on Advanced Communication Technology (ICACT)*, pp. 13-16 Feb. 2011.

[225] Ridwan, Murad; Abdo, Mohammed; Jorswieck, E.;, "Design of non-uniform antenna arrays using genetic algorithm," *Journal of Wireless Networking and Communications*, vol. 2, no. 2, pp.7-10, Apr. 2012.

[226] Senhu Huang, Zhi Ding, and Xin Liu, "Non-intrusive cognitive radio networks based on smart antenna technology," *in Proc. IEEE GLOBECOM*, pp. 4862-4867, 2007.

[227] Marsaglia, G.,"Ratios of normal variables," *Journal of Statistical Software*, 16(4), pp. 1-10, 2006.

[228] N. B. Khoolenjani, K. Khorshidian, "On the Ratio of Rice Random Variables," *JIRSS vol.* 8, Nos. 1-2, pp 61-71, 2009.

[229] N. Metropolis, *The Beginning of the Monte Carlo Method*, Los Alamos Science Special Issue 1987.